ABSTRACT

KUNTUKOVA, YEKATERINA. Storm-event Rainfall-runoff Response in Carolina Slate Belt and Triassic Basin Catchments. (Under the direction of Dr. April. L. James).

This Master's Thesis focuses on investigating storm-event runoff generation mechanisms at five headwater catchments in the Piedmont region of North Carolina. All catchments have similar climate and precipitation conditions but three of the catchments are located within the Carolina Slate Belt and two within Triassic Basin Ecoregions. The two Carolina Slate Belt catchments exhibit distinctly different runoff responses than the Triassic Basin ones. The two-component hydrograph separation indicates that event water contributes a larger percent to stromflow at Triassic Basin catchments than at Carolina Slate Belt catchments which is consistent with the higher contribution by overland flow. The examination of relationship between antecedent moisture conditions and storm response shows a clear threshold-based response of stormflow to the sum of antecedent soil index (ASI) and precipitation. This threshold influences the runoff response. The threshold behavior is hypothesized to represent a transition between runoff generated from the saturated near stream zone below threshold and increasing hillslope contributions above threshold. Isotope hydrograph separation confirms that event water contributions are significant below the threshold.

Storm-event Rainfall-runoff Response in Carolina Slate Belt and Triassic Basin Catchments

by
Yekaterina Kuntukova

A thesis submitted to the Graduate Faculty of
North Carolina State University
in partial fulfillment of the
requirements for the degree of
Master of Science

Natural Resources

Raleigh, North Carolina

March 16, 2011

APPROVED BY:

_____	_____
April L. James, Ph.D. Committee Chair	Ge Sun, Ph.D.
_____	
David Genereux, Ph.D	

BIOGRAPHY

Yekaterina Kuntukova was born and raised in the Republic of Kazakhstan. She found the love for nature and adventure in the beautiful mountains that surround her native city, Almaty. In 2001, Katya and her family moved to North Carolina, the state that became their new home. In 2006, Ms. Kuntukova completed her undergraduate degree at the University of North Carolina at Chapel Hill, where she acquired a Bachelor of Arts in Geological Sciences. After working for two years, she decided to go back to school to gain more knowledge of the subject that interested her most – hydrology. In 2008, she enrolled in North Carolina State University to receive a Masters in Natural Resources.

ACKNOWLEDGMENTS

This thesis would not have been possible without my adviser, Dr. April James, and all her positive encouragement, patience, motivation and knowledge. Her guidance helped me in the time of research as well as during the writing process. I also wish to thank the rest of my graduate committee: Dr. David Genereux and Dr. Ge Sun. Thanks are also due to Johnny Boggs and the stuff of U.S. Forrest Service for their data analysis and collaboration. I also would like to thank Chris Dreps for his assistance with the field equipment. A big hug to my family for their support throughout my life. Last by not least, special thanks to my friends who organized all the rock climbing trips and kept me in high spirits.

TABLE OF CONTENTS

LIST OF TABLES

LIST OF FIGURES

INTRODUCTION

Importance of Headwater Catchments

More than 70 percent of the area of watersheds in the United States is drained by headwater streams (Lowe and Likens, 2005). Headwater streams influence the supply, transport, and fate of water and nutrients throughout landscapes. Knowing the flowpaths of water to the streams, the time to discharge, and the relationship of rainfall to streamflow response are important for flood risk assessment, maintaining drinking water supply, and protecting habitat for aquatic biota (Lischeid, 2008).

The flowpath of water through soil controls the chemistry and nutrient dynamics of this water. Shallow pathways tend to have shorter residence times and less contact with soils, while deeper subsurface flow routes are more likely to have longer residence times and interaction with soil, resulting in chemical transformations (Monteith et al., 2006). Hence, headwater systems are critical areas for maintaining the water quality and overall ecological health, and providing habitat for macroinvertebrates, fish, and amphibians within watersheds (Meyer and Wallace, 2001). A study by Lyon et al. (2006) compared the effects of two modeled runoff generation processes on total phosphorus and soluble reactive phosphorus at mountainous catchments in Catskill, NY. They concluded that nutrient concentrations were directly influenced by the runoff delivery mechanisms. Identification of the primary runoff mechanisms and flowpaths is crucial in understanding changes in water quality and in implementing of management practices and development of nutrients transport models.

Headwater streams are characterized by strong and vital interactions with the systems that surround them (Lowe and Likens, 2005). Understanding how water moves through headwater catchments as well as understanding the interactions between groundwater and surface water is essential for effective management of water resources (Bishop et al., 2008). For example, planners require a comprehensive understanding of hydrological processes within watersheds to determine the most vulnerable areas to runoff and erosion. Small streams retain sediment eroded during storms and release it gradually downstream. If this storage is reduced, the amount of sediment transported downstream increases. Headwater catchments hold and store water during storms making them critical for mitigating flooding. Therefore, eliminating or degrading small streams affects frequency and intensity of flooding. Communities across North Carolina are finding that their water resources are degrading in response to growth and development (Mallin et al., 2000). Planners require a comprehensive understanding of hydrological processes within watersheds to determine the most vulnerable areas to runoff and erosion. Understanding the flowpaths and runoff generation mechanisms will improve our ability to effectively manage water resources.

Review of Water Flowpaths and Runoff Generation Mechanisms

Identifying flowpaths and mechanisms of runoff generation that are responsible for the observed runoff response are particular important to catchment hydrology. Determining which flowpath contribute most to streamflow and how the contributions change depending on antecedent moisture conditions and storm characteristics is important for prediction of

sediment and pollutant sources and implementation of effective water management strategies. Despite efforts to classify and organize hillslope behavior, there is still substantial uncertainty what flowpaths water travels to the stream. The flowpaths that are primarily responsible for producing the storm hydrograph include infiltration overland flow (also called Horton overland flow, HOLF), saturation excess overland flow (SOLF), and subsurface stormflow. Horton overland flow occurs when rainfall rate exceeds soil infiltration capacity and is most commonly encountered in arid and semi-arid regions or on impermeable and disturbed areas. Saturation excess overland flow occurs when soils become saturated and any additional precipitation produces surface runoff. It most often happens near stream channels. Source areas of overland flow are dynamic and may vary seasonally (Sidle et al., 2000). The large majority of the studies in the small forested catchments have identified subsurface flow as a major stormflow runoff component (Lischeid, 2008).

Research on runoff generation processes has produced a variety of runoff generation mechanisms that try to resolve the question of how subsurface flow is delivered so rapidly to the stream. Some of the mechanisms that can account for a large subsurface stormflow contribution include groundwater ridging (Abdul and Gillham, 1989; Sklash and Farvolden, 1979), transmissivity feedback (Bishop, 1991), preferential flow through macropores and pipes or due to development of perched water table at a conductivity barrier (Buttle et al, 1994; Brown et al, 1999; McDonnell, 1990).

The Variability and Role of Geology and Soils for Headwater Watersheds

The variable nature of how headwater catchments deliver water to the stream remains difficult to predict. Study catchments such as Hubbard Brook, NH, Panola Mountain, GA, Sleepers River, VT, and Maimai, New Zealand, provided a wealth of knowledge about hydrologic processes in headwaters (Bishop et al., 2008). However, the great spatial and temporal variability of soil characteristics, bedrock geology and landcover in headwater catchments makes it hard to extrapolate this knowledge to other regions. Recent literature demonstrates the need for a broad-scale classification of catchments to explain variation of hydrologic regimes across the landscape (Buttle, 2006). A few studies have examined the differences in runoff generation among several catchments (for example, Freeze, 1972; Onda et al., 2006). Onda et al. (2006) compared runoff generation processes in watersheds located in two areas in Ina region of central Japan. The bedrock in one area consists of granite and of shale in another one. The shale watersheds exhibited distinctly different runoff responses to the same storm event than the granite watersheds. The shale watersheds showed delayed runoff response to the rainfall peak while in granite watersheds high runoff peaks coincided with the rainfall peaks. Tensiometers located on hillslopes indicated that soil water percolated downward into the bedrock in the shale watersheds, while subsurface flow parallel to the slope was observed in the granite watersheds. They concluded that subsurface flow was the dominant contributor to stormflow in both type of watersheds. However, in shale watersheds the soil water percolated downward to bedrock and then moved along bedrock interface while in granite watersheds the flow through the soil mantle was observed parallel

to the slope. However, in shale watersheds the soil water percolated downward to bedrock and then moved along bedrock interface while in granite watersheds the flow through the soil mantle was observed parallel to the slope. Therefore, comparing flowpaths and runoff generation between catchments with different geology is important in order to generalize the runoff generation processes (Onda et al, 2006). Examination of catchment similarities and differences is especially relevant for the Piedmont region of North Carolina where significant differences in landscape characterization exist.

General Research Objectives

This study focuses on investigating storm-scale runoff generation mechanisms at five headwater catchments in the Piedmont region of North Carolina, three within the Carolina Slate Belt and two within Triassic Basin Ecoregions. This study complements ongoing USDA Forest Service research at these catchments (Boggs et al., 2008). The Forest Service study examines the effectiveness of buffer zones and stream crossings on water quality in North Carolina Piedmont forested watersheds. The findings will offer reference data for watersheds planning taking into account the dominant geologic features. The objectives of this study are: i) to quantify storm-event rainfall-runoff response and to investigate whether the water flowpaths vary within Carolina Slate Belt and Triassic Basin geologic regions, ii) to examine how flowpaths and runoff generation mechanisms vary as a function of antecedent moisture conditions and storm characteristics. Delivery flowpaths and dominant runoff mechanisms are interpreted from hydrometric and isotopic tracer evidence. In Chapter

1 runoff generation from five catchments is examined for individual storm events occurring under various antecedent moisture conditions and storm characteristics. Chapter 2 examines stable isotope separation for evidence of flowpath contributing to streamflow. Knowing the factors that contribute to runoff generation is essential in flood risk assessment, maintaining drinking supply, and understanding the watersheds ecosystems.

CHAPTER 1

INTRODUCTION

A review of Storm Hydrograph Analysis

Traditional hydrometric measurements of precipitation and streamflow can provide useful information on hydrologic functioning of a watershed. Studying rainfall-runoff relationship can be useful in narrowing the range of possible interpretation of runoff generation mechanisms and in comparisons of these mechanisms from catchment to catchment. The analysis of characteristics of the storm hydrograph such as lag times, recession parameters, peak discharge, and runoff ratios can provide some insight into the mechanisms involved in the generation of storm runoff (Dunne, 1978). Dunne (1978) showed that values for storm characteristics such as runoff ratios, peak discharge, lag time cluster in different ranges for different runoff generation mechanisms. Changes in total flow and runoff ratios can give first estimate of the runoff generation under different moisture conditions.

Storm hydrograph analysis continues to be used in contemporary studies often in combination with hydrochemical data (Brown et al., 1998; Gomi et al., 2010). Slattery et al. (2006) used hydrograph characteristics to investigate runoff processes that generate stormflow in NC coastal plain agricultural watershed. Their study suggested that the range in peak lag times and the magnitude of runoff coefficients were indicative of a basin dominated by surface flowpaths in the form of Hortonian overland flow and saturation overland flow despite the relatively permeable soils. Haga et al. (2005) investigated the effects of rainfall properties, antecedent moisture conditions, and flow paths on runoff response in a granitic forested catchment located in central Japan. The runoff response was characterized by two types of lag times: short and long. They concluded that lag times between peak rainfall and peak discharge were different depending on the dominant flow path during storm event. During events with short lag times, saturation excess overland flow was dominant, while during events with long lag times, saturated subsurface flow above the soil-bedrock interface was the dominant process. In their study Montgomety and Dietrich (2002) used the recession coefficient and lag times to investigate the role of slope and scale on hydrologic response in two steep-sloped, unchanneled catchments in the Oregon Coast Range. They observed that subsurface stormflow response on steep terrain was no faster than on lower gradient slopes of comparable size. Their finding supports the interpretation that differences in soil and geology as well as patterns of antecedent soil moisture control response time of runoff generation by subsurface stormflow. The storm-based stream hydrograph analysis can help in characterizing runoff generation mechanisms for this study as well as in investigating

whether these mechanisms vary across sites. Runoff ratios are useful for comparison with other catchments in order to understand how different factors (soil, landscape characteristics, moisture condition) influence runoff generation.

Antecedent Moisture Conditions and Threshold Changes in Runoff

The relative importance of different flowpaths may vary both spatially and temporally. Antecedent moisture conditions (AMCs) are important in activating dominant runoff generation processes by which a catchment responds to rainfall. James and Roulet (2009) examined spatial patterns of runoff generation as a function of AMC and geomorphology. Under drier conditions, high DOC values and transient perched water supported the interpretation that shallow subsurface flowpath and potentially SOLF from saturated riparian areas were major contributors to stormflow. During wet periods, hillslopes were more connected to the valley bottoms and subsurface flow contributed a large portion to the hydrograph through subsurface runoff.

Process-based field studies at hillslope and catchment scales have provided evidence of a non-linear threshold response in runoff generation based on storm size and/or AMCs (Tromp-van Meerveld and McDonnell, 2006, Buttle et al., 2001, Detty and McGuire, 2010). Rapid lateral flow through a network of macropores has been linked to nonlinear threshold type behavior in hillslope runoff response. Tromp-van Meerveld and McDonnell (2006) presented the fill and spill hypothesis to explain the threshold in trenchflow observed on the Panola hillslope as a function of storm size. Their results showed that while a water table

developed on parts of the hillslope during events smaller than a threshold size (55 mm), the bedrock depressions on the hillslope were not filled and subsurface saturated areas remained disconnected. With the increase of storm size, preferential flowpaths, macropores, and bedrock depressions became connected and subsurface stormflow increased drastically. The subsurface stormflow increased by almost two orders of magnitude for events above threshold.

Detty and McGuire (2010) investigated a threshold relationship in stormflow for a small headwater catchment located in the Hubbard Brook Experimental Forest, NH. They found that total quickflow above a threshold value was strongly correlated with a maximum water table height index (calculated by normalizing each shallow groundwater well to its seasonal range, then the maximum value for each event was used to compute arithmetic mean for all wells) as well as the sum of total precipitation and antecedent soil moisture index (defined by an integration of soil moisture in the top 1.5 m). They believe that transmissivity feedback and/or preferential flows through macropores can explain the observed threshold response

Investigating AMCs and threshold changes may offer insights into the complex interactions of runoff generation mechanisms by revealing predictable patterns arising from nonlinear controls (Detty and McGuire, 2010). In our study, AMCs are quantified in order to examine how flowpaths and runoff generation mechanisms vary as function of AMCs. The threshold response of stormflow with a combination of storm size and AMCs may be a useful tool for intercomparison of the catchments with different soils and geology.

While many studies have confirmed that soil moisture is a major control of catchment rainfall-runoff responses, data is not always available to determine actual catchment antecedent moisture conditions. Average groundwater levels at the start of the event, antecedent baseflow, and precipitation-based indices have all been used as surrogates for AMCS. Ali and Roy (2010) evaluated relations between actual soil moisture contents measured in the top 5, 15, 30, and 45 cm along a 15 by 15 m sampling grid and selected precipitation based surrogates for AMCs. Their results showed poor relationship between measured soil moisture and the precipitation-based indices such as the cumulative sum of rainfall and number of days elapsed since the last rainfall. In addition, the relationships between point-scale soil moisture measurements and proxies for AMCs were not spatially homogenous. While in this study we can't comment on the spatial distribution of soil moisture, the usefulness of a range of surrogate antecedent moisture indices for our particular catchments can be investigated.

RESEARCH QUESTIONS

In this chapter, the following specific research questions and objectives will be addressed in an examination of storm response for the Slate Belt (3) and Triassic basin (2) catchments:

- What are the storm-event hydrograph characteristics of the Slate Belt (3) and Triassic basin (2) catchments?
- Do the storm hydrograph characteristics infer any significant differences between sites in flowpaths and runoff generation mechanisms?

- How do storm hydrograph characteristics vary as a function of antecedent moisture conditions and storm characteristics such as rainfall size and intensity? Do changes in hydrograph characteristics provide evidence for changes in dominant runoff mechanisms as a function of AMCs and storm size/intensity?
- Do we see evidence of the threshold like change in runoff generation with AMC or storm size?
- How well are soil moisture conditions reflected by surrogate antecedent moisture indices for the study sites?

SITE DESCRIPTION

For this study, five headwater catchments were selected in Durham County in the Piedmont region of North Carolina. The catchments are a part of an ongoing USDA Forest Service study of best management practices effectiveness. The five catchments are located in the Falls Lake watershed which is a part of the Neuse River Basin. Three headwater catchments in Hill Demonstration Forest, Durham County and two in Umstead Research Farm, Granville County were compared in this study. The Hill Forest and Umstead Farm catchments are located within 5 miles of each other. Precipitation inputs and vegetation cover are not significantly different across the two areas. The US Forest Service's map of ecological subregions describers Hill Forest as being in Carolina Slate Belt and Umstead farm in Triassic Basin (Cleland et al., 2007).

Durham County of North Carolina has an average annual temperature of 15ºC with winter mean monthly temperatures of 4°C and summer mean monthly temperatures 21ºC. On average, Durham County receives 1220 mm of rain per year. The distribution of rainfall throughout the year is shown in Table 1. In the growing season much of the rain comes from convective summer thunderstorms. Precipitation during winter and spring occurs mostly in connection with migratory low pressure storms, which appear with greater regularity and in a more even distribution than summer showers (State Climate Office of NC, 2010). The average annual potential evapotranspiration (PET) is estimated to be approximately 900 mm (Dreps 2010), resulting in aridity index (AI=P/PET) of 1.33, indicating a humid climate class (AI>0.65).

Hill Forest Catchment

Catchments HF1 (12.4 ha), HF2 (10.6 ha), and HFW1 (29.1 ha) are located in the NCSU Hill Forest site within Carolina Slate Belt (Figure 1). Catchments HF1 and HF2 are nested within HFW1. The study sites are mostly forested with mixed hardwood. At the Hill Forest site, the dominant soil series is Tatum (55%) (Dreps 2010). The rest 45% belong to hydrologically similar soils of Appling, Cecil, and Georgeville series which are moderately permeable, well-drained sandy loams and silt loams (soil base map from Natural Resources Conservation Service). Soils are generated from the parent material of metamorphosed granitic bedrock of the Carolina Slate belt (Cleland 2007). For these soils, the depth to bedrock typically ranges from 1.8 to 3 meters. The values for saturated hydraulic

conductivity (K_{sat}) of the representative soil types at Hill Forest sites are presented in Table 2 (National Cooperative Soil Survey). For more details on soils and land use see Dreps 2010.

Umstead Farm Catchments

Catchments UF1 (19.2 ha) and UF2 (28.3 ha) are located in the NCDA Umstead Research Farm site within Triassic Basin Ecoregion (Figure 2). The UF1 study site is mostly forested with mixed hardwood while UF2 has about 11% of area covered by agricultural land with hardwood forest in the rest of the area. The Umstead Farm site is underlain by sedimentary rocks of the Triassic basin (Cleland 2007). The soils primarily consist of slowly permeable, moderately well drained sandy loam and clay loam of Helena series (55%) (Dreps 2010). The soils are generally less deep, more erodible, and contain more clay content that soils found in Carolina Slate Belt. According to National Cooperative Soil Survey, saturated hydraulic conductivity (K_{sat}) varies sharply among horizons in these soils (Table 2). Perched water tables can form due to the presence of a low-permeability layer at Bt horizon (25-96cm). The rest of the catchments is mostly covered by Vance soil series, which can have moderate shrink-swell potential but perched water table typically do not occur. For more information on soil properties and land use see Dreps 2010.

METHODS

GIS

GIS was used to support general characterization of catchments such as size, slope, soils, and land cover. Each catchment was delineated from a DEM using GRASS GIS. The DEM was interpolated from LIDAR bare earth points at a 2-m resolution (North Carolina Floodplain Mapping Program). Table 3 summarizes basic catchments physiographic characteristics generated from the DEMs. The Soil Survey Geospatial database provided by Natural Resources Conservation Service was then used to document the soil type distribution of the catchments. The landcover data was downloaded from the US EPA Landscape Characterization Branch.

Hydrometric Measurements

The streamflow, precipitation, and weather data were collected and archived by the USDA Forest Service as a part of their ongoing best management practices (BMP) research. Streamflow data were collected from one weir (HFW1) and four flumes (HF1, HF2, UF1, UF2). Stage was measured by a pressure transducer and recorded every 10 minutes. A record of continuous discharge is available from 18-Sept-2007 to 30-May-2010. Rainfall was measured with tipping buckets and bulk rain gauges (1 at Hill Forest location and 1 at Umstead Farm location) and throughfall was measured with manual throughfall collectors (5 at HF1 site and 5 at UF2 site). Within HF2 and UF2 catchments water table elevations were

monitored using a transect of streamside wells located from the flume gauging station location and moving upstream (4 wells at HF2 site and 3 wells at UF2 site). Six of the wells were equipped with a water level recorder (Odyssey Capacitance Water Level Logger) and one with a pressure transducer. Water levels at all wells were recorded at 15 minute intervals. The well data is available for the period of 7-July-2009 – 30-May-2010. Within the HF2 and UF2 catchments soil moisture dynamics were monitored with a profile of soil moisture probes installed at 4 different depths (12.5 cm, 25 cm, 50 cm, and 90 cm). The soil moisture profile was located at a mid-slope position within each catchment (Figures 1 and 2). Volumetric soil moisture was recorded hourly and covers the period from 18-June-2009 to 30-May-2010. The location of all field equipment is shown in Figures 1 and 2.

Storm Hydrograph Characteristics

Storm-event rainfall-runoff dynamics were characterized by analyzing the storm hydrograph. Storm hydrograph characteristics (total flow, runoff ratio, runoff coefficient, peak flow rate, event duration, lag times, and recession coefficient) were calculated using streamflow and rainfall data for each storm event (Table 4). A Matlab program was developed to automate storm hydrograph characterization. This program identified storms based on total precipitation amount - only storms greater than 5 mm and separated by at least five hours without precipitation were considered. The start of the storm hydrograph was defined by a change in streamflow over time (dQ/dt) of greater than 5%. The program then graphed each identified storm and allowed the user to i) evaluate the appropriateness of these

general criteria and ii) to eliminate storms without continuous flow data or with baseflow less than $3x10^{-3}$ mm/10 min (0.5 l/s) (the pressure difference below 0.5 l/s was too small to be captured by the pressure transducer). The resulting number of storms identified for analysis for each catchment is shown in Table 5. Once the selection of the storms was confirmed by the user, the Matlab Program automatically calculated individual storm hydrograph characteristics based on the following definitions,

Quickflow (QF): In all of the analyses presented, quickflow (stormflow) was determined using the constant slope separation method of Hewlett and Hibbert (HH) (1967) as shown in figure 3. Although this graphic approach for separation has been criticized as having little physical basis (Freeze 1972), the use of this method provides a qualitative way to evaluate rainfall-runoff relationships and dominant runoff flowpaths, and allows for consistent comparison of stormflow from different catchments in this study. After examining hydrographs from about 200 water-years collected on fifteen small forested watersheds in the Appalachian-Piedmont region, Hewlett and Hibbert (1967) proposed the use of a constant separation slope of 0.05 cfs/mi^2/hr. A preliminary analysis of data included in this study showed that the Hewlett's value of 0.05 cfs/mi^2/hr was not appropriate for all time scales and all the storms (e.g. it could not accommodate some multipeak storms). Therefore, an alternative, more gentle slope ($1.82*10^{-6}$ mm/10min) was used based on visual judgment in order to capture more complex storms in the analysis. The end of the storm was defined by the intersection of the slope and the recession limb of the hydrograph.

Runoff ratio: The runoff ratio was then calculated as the ratio of quickflow to precipitation (QF/P).

Total flow: Total flow is the total volume of streamflow generated by the storm (total area under the storm hydrograph).

Runoff coefficient: The runoff coefficient is defined as a ratio of total flow to precipitation (TF/P). All flows are expressed in mm (normalized by catchment area).

Recession coefficient: Recession coefficient is a measure of how quickly a basin releases water from storage and is calculated as

$$K = (\frac{Q_t}{Q_o})^{\frac{1}{2}} \quad (1)$$

where (t) corresponds to the number of hours from peak flow to the end of the hydrograph, peak flow rate (Q_o) refers to maximum discharge in the storm hydrograph, and Q_t is the discharge at time t.

Lag times: Two lag times were calculated: L_P is the lag time from the maximum rainfall to the hydrograph peak; L_C is the time from the center of mass of rainfall to the hydrograph peak.

Duration: Event duration corresponds to the time over which a storm event occurs (in days).

Peak flow rate: Peak flow rate refers to maximum flow rate in the storm hydrograph. A graphical representation of storm hydrograph characteristics for HF2 catchment is presented in Figure 3 for a storm event on days 30-Nov-2008-1-Dec-2008.

General descriptive statistics which include mean, standard deviation, and range were calculated for all storm hydrograph characteristics. Box-and-whisker plots were used to visualize and compare storm hydrograph characteristics. To provide information on the rainfall-runoff relationship, correlation matrix between pairs of variables was examined.

Antecedent Moisture Conditions (AMCs)

The volumetric soil moisture located at mid-slope position was measured at HF2 and UF2 sites at 4 different depths in the soil profile: 12.5 cm, 25 cm, 50 cm and 90 cm. The soil moisture data immediately preceding the start of rainfall as well as 12-hour average preceding the start of rainfall was used to determine soil water content at each depth. The antecedent soil moisture index (ASI) was determined by the sum of integrated volumetric water content over the depth interval of each soil moisture sensor to a total depth of 1m (Haga et al., 2005).

The soil moisture data was not available for the entire period of the study, therefore several surrogates or proxies for AMCs were quantified (Table 4) based on available data on precipitation, additional weather station data, baseflow, and groundwater levels. The antecedent precipitation indices used were 3,7,15, and 30 day AP and API. Antecedent Precipitation (AP_N) is defined as

$$AP_N = \sum_{i=1}^{N} P_i \quad (2)$$

where P_i is the precipitation (mm/day) on the i_{th} day prior to the event.

Antecedent Precipitation Index (API_N) is defined as

$$API_N = \sum_{i=1}^{N}(P_i - PET_i) \quad (3)$$

where P_i is the precipitation (mm/day) on the i_{th} day prior to the event, and PET_i is potential evapotranspiration on the i_{th} day prior to the event. Daily potential evapotranspiration was estimated by Dr. Ge Sun and Chris Dreps with a commonly-used reference evapotranspiration formula from the United Nations Food and Agriculture Organization method (Allen et al., 1994) adapted from the Penman-Monteith method (Dreps 2010).

Antecedent baseflows and groundwater levels immediately preceding the start of rainfall as well as averages over 12-hour period preceding the start of rainfall were also used for analysis. The growing season is defined as the period between April 2nd and November 2nd. The soil moisture and well data from HF2 site was used to characterize AMCs across all three HF catchments, similarly data from UF2 site was used for UF1 site as well.

RESULTS

Storm characteristics

The number of events included in this analysis is shown in Table 5. The UF1 catchment has the smallest number of storms available for analysis due to a malfunction of pressure transducer at this site. Problems with the pressure transducer at the UF1 flume happened mostly during dry periods, which could be contributing to higher average total flow (Figure 4), runoff ratio (Figure 5), and runoff coefficient (Figure 6) at UF1 catchment compared to UF2 catchment. The bottom and top of the box plot are 25th and 75th percentile

and the middle band is 50^{th} percentile of the dataset. The ends of the whiskers represent the lowest or highest datum within 1.5 of the inter-quartile range. Any outliers are plotted as dots.

Total flow for the events studied ranged from 0.06 to 37.2 mm with the mean value of 2.9 mm at HF1 catchment, 0.2 to 41.3 mm with the mean value of 3.8 mm at HF2, 0.03 to 25.4 mm with the mean value of 2.9 mm at HFW1 catchment (Figure 4). In comparison, the two UF catchments have higher average and maximum total flows: total flows ranged from 0.02 to 42.1 mm with the mean value of 10.2 mm at UF1 catchment, and 0.02 to 59.6 mm with the mean value of 8.0 mm at UF2 catchment (Figure 4). Mean values of total flow were two to three times higher at UF sites than at HF sites.

All HF sites have similar ranges of runoff ratios (QF/P) (Figure 5). The runoff ratios range from 0.003 to 0.3 with an average value of 0.05 for HF1 site, 0.004 to 0.4 with an average value of 0.06 for HF2 site, and 0.001 to 0.38 with an average value of 0.05 for HFW1 site. In comparison, UF catchments have higher average runoff ratios, higher maximum ratios and higher variability than HF sites: runoff ratios range from 0.0006 to 0.69 with a mean of 0.25 for UF1, and 0.0009 to 0.71 with a mean of 0.18 for UF2 site (Figure 5). The variance at UF sites is 0.4 compared to 0.0 to 0.1 at HF sites.

The runoff coefficients (TF/P) demonstrate similar trends to runoff ratios (QF/P) (Figure 6). Using total flow in the numerator generally results in higher values for runoff coefficient. The average values for HF1, HF2, and HFW1 are 0.08, 0.11, and 0.08

respectively. The two UF sites have higher maximum and average runoff coefficients. The average runoff coefficients are 0.28 and 0.22 for UF1 and UF2 catchments respectively.

Peak flow rates (Figure 7) range from 0.002 cm/hr to 0.73 cm/hr with a mean value of 0.032 cm/hr for HF1 site, 0.003 cm/hr to 0.75 cm/hr with a mean value of 0.045 cm/hr for HF2 site, and 0.001 cm/hr to 0.315 cm/hr with a mean value of 0.03 cm/hr for HFW1 site. The peak flow rates vary from 0.001 cm/hr to 0.48 cm/hr with a mean of 0.11 cm/hr for UF1 site and 0.001 cm/hr to 0.39 cm/hr with a mean of 0.08 cm/hr for UF2 site. The UF sites have higher average peak flow rates, higher variability, and higher maximum rates except for one event which was the largest in the study period (130 mm). This event was tropical storm Hanna which occurred on dry AMCs. The average rainfall intensity was 2 mm/10 min and the maximum rainfall intensity was 7 mm/10 min. During this event, peak flow rates expressed in cubic feet per second (cfs) were similar for both HF and UF sites (8.9, 7.8 and 9.0 cfs for HF1, HF2 and HFW1 respectively and 9.0, 10.8 cfs for UF1, UF2 sites respectively). As HF1 and HF2 areas are approximately two times smaller than UF sites, peak flow rates expressed in cm/hr (flow normalized by area) are higher. For this extreme storm, the HF sites are generating much more water per unit area.

Recession coefficients exhibited a relatively narrow distribution for each catchment. The recession coefficient estimates range from 0.81 to 0.99 with an average of 0.98 for the HF1 site, 0.77 to 0.99 with an average of 0.98 for the HF2 site, 0.84 to 0.99 for the HFW1 with an average of 0.98, 0.81 to 0.99 with an average of 0.97 for the UF1 site, and 0.94 to

0.99 with an average of 0.98 for the UF2 site (Figure 8). Recession coefficients indicate that response time from peak to end of storm is very similar for all catchments.

Table 6 summarizes the statistics on lag times and durations of storm events for each catchment. Mean L_P values are smaller for HF1, HF2, and HFW1 catchments (2.6 hours, 1.4 hours, and 2.8 hours respectively) than for UF1 catchment (3.1 hours) and UF2 catchment (4.1 hours). L_C values are also smaller for HF1, HF2, and HFW1 catchments (3.1, 2.6, and 3.2 hrs respectively) compared to UF sites: 5.5 hrs at UF1 and 5.9 hrs at UF2. Average event durations are also longer at UF sites: 1.7, 1.5, and 1.6 days at HF1, HF2, and HFW1 compared to 2.2 days at UF1 and UF2 sites, respectively.

There are substantial differences in stormflow characteristics between Carolina Slate Belt (HF) and Triassic Basin (UF) catchments. UF sites generate higher and more variable total flow, runoff ratios, runoff coefficients, peak flow rates, and longer lag times and storm durations than the HF sites.

Relationships between AMCs, rainfall characteristics and storm response

Correlation matrices between storm hydrograph characteristics, rainfall characteristics, and AMCs for catchments HF2 and UF2 are shown in Table 7. The Pearson correlation is 1 in the case of perfect linear relationship and some value between -1 and 1 indicates the degree of linear dependence between two variables. This table indicates that at the HF2 site there is strong relationship between storm size and total flow, peak flow, and event duration. Recession coefficients seem to be most strongly related (negatively) to

maximum and average rainfall intensity. Runoff ratios and runoff coefficients are most strongly correlated to ASI, followed by storm size and season. UF2 catchment shows similar trends to HF2 site, however, the relationship between storm size and total flow is weaker, while the relationship between AMCs (represented here by ASI) and runoff ratios is stronger than at HF sites. UF2 site is more sensitive to season and ASI when trying to explain magnitudes of runoff response than is HF2 site. This also seems to be the case for timing-based metrics of recession coefficient and duration.

The Pearson correlation coefficient indicates only the strength of linear relationship between two variables. However, relationship between rainfall-runoff characteristics is often non-linear. Figure 9 examines total stormflow as a function of storm size. For each catchment, there appears to be a storm size threshold above which significant stormflow occurs and this threshold seem to be similar for all five sites. Significant flow occurs only for rainstorms larger than 30 mm. To test how well defined the precipitation threshold is the following method was used to calculate the sum of the squared deviation as a function of storm size:

$$R\ p_t\ =\ (S\ p < p_t\ - S\ p < p_t\ )^2 + \ (S\ p > p_t\ - S\ p > p_t\ )^2 \qquad (4)$$

where p_t is the possible precipitation threshold, p is the storm total precipitation, S is the observed storm total flow for a storm size p, and $R(p_t)$ is the sum of the squared deviations for a threshold at p_t. The calculated threshold is defined as the precipitation value where the sum of the square deviations is minimal. This method was used by Tromp-van Meerveld and McDonnell (2006) to calculate storm size threshold at the hillslope scale. The precipitation

threshold appears to be ~ 32 mm for HF catchments and ~ 30 mm for UF catchments (Figure 10). Although there is evidence of a threshold for all catchments, large variability above this threshold exist (i.e. there is not a clear relationship between total stormflow and storm size above the threshold).

Another factor that determines whether or not significant flow occurs is AMCs (Table 7). There is a strong seasonality in the total stormflow (Figure 11). The seasonal averages of total stormflow varied from 4 mm during growing season to 12.1 mm during non-growing season for UF2 catchment and from 2.3 mm during growing season to 6.3 mm during non-growing season for HF2 catchment Figure 12 shows how total stormflow varies with ASI. For the most part, the soil moisture index (ASI) used here to characterize AMCs needs to exceed 250 mm before any significant runoff occurs. In Table 7 ASI showed stronger correlation with runoff ratios and runoff coefficients than total flow. This can be explained that by normalizing hydrograph volume by precipitation, other factors contributing to stormflow such as AMCs become more noticeable. Although at higher ASIs we see higher total stormflow, there is some complicating variability and there is no clear relationship between TF and ASIs.

Figure 13 shows that consideration of both AMCs (represented here in the form of ASI) and total precipitation amount can clarify a relationship with total flow and determine whether or not significant flow occurs. A very clear threshold is observed in stormflow response when presented as a function of a summed term of storm total precipitation (mm) and ASI (mm). Correlations among other variables such as runoff ratios were also

considered; however, the correlations were not as strong as with total stormflow and the summed term of ASI and total precipitation. Below the threshold, stormflow is not significantly correlated to the sum of antecedent soil moisture and total precipitation. While above the threshold, the relationship between stormflow and this combined index is linear and significantly correlated ($r=.89$, $p<0.0001$ for HF1, $r=0.95$, $p<0.0001$ for HF2, $r=0.91$, $p<0.0001$ for HFW1, $r=0.84$, $p<0.0001$ for UF1, $r=0.92$, $p<0.0001$ for UF2). The threshold for HF2 site is 269 mm, for HF1 is 256 mm, and for HFW1 is 266 mm. Those numbers likely reflect a soil moisture storage threshold below which rain water is mostly retained in the soil and above which rain water is increasingly transferred to the stream. The threshold for UF1 and UF2 sites was 300 mm, indicating a higher storage capacity compared to HF sites before which significant streamflow is generated..

Runoff below these thresholds yields a much smaller percent volume of rainfall. The average runoff ratio at HF2 catchment below threshold is 0.02 compared to the average runoff ratio of 0.17 for the events above the threshold (Table 8). The lag times and event durations are shorter during events below threshold (Table 8). A similar trend is evident at UH2 catchment: average total flow, runoff ratio, lag times, and event duration are significantly higher for events above threshold.

Antecedent wetness indices

To determine how well AMCs are reflected by a range of antecedent wetness indices, the relationship between our integrated 1-m average soil moisture profile (ASI) prior to

rainfall events and additional indices listed in Table 4 (antecedent baseflow, riparian groundwater levels, APs, and APIs) were analyzed. The relationships between average soil moisture and average groundwater levels are relatively linear for both HF2 and UF2 catchments (Figures 14 and 15). The relationships between average soil moisture and average antecedent baseflow are non-linear especially for UF2 catchment (Figure 16). The relationship between average soil moisture and precipitation based indices show the most scatter especially for UF2 catchment (Figures 17 and 18).

DISCUSSION

Storm characteristics

The UF catchments have significantly higher total flow, runoff ratios and peak flow rates than HF sites (Figures 4, 5 and 7). Dunne (1978) showed that high runoff ratios (over 0.25 for catchments less than 1 km^2) suggest dominance of Horton Overland Flow (HOLF), low runoff ratios (0.02-0.21 for small catchments in NC) are indicative of subsurface flow, and a range of 0.02-0.59 (for small catchments in NC and Georgia Piedmont) suggest dominant saturation overland flow component (SOLF). For peak flow rates Dunne (1978) gives a range of 0.76-19.4 cm/hr (catchments less than 1 km^2) for HOLF, 0.01-0.09 cm/hr (small catchments in NC) for subsurface flow, and 0.01-5.0 cm/hr (catchments less than 1 km^2) for catchments with a dominant SOLF component. The higher runoff ratios at UF sites might suggest greater overland flow contributions than at HF sites. HOLF is unlikely to

contribute significantly to the hydrograph at either site. HOLF occurs in the areas where the rainfall intensity exceeds the infiltration capacity of the soil. The maximum observed rainfall rate at the sites for the study period was 51.4 mm/hr. According to National Cooperative Soil Survey, the hydraulic saturated conductivity (K_{sat}) near the surface of the soils at both locations for the most part exceeds maximum rainfall rates at the sites (Table 2). This suggests HOLF would be rare. SOLF could account partially for the higher flow volumes at UF sites. The clay layer impedes infiltration to depth which can result in soil saturation above it. However, the delayed lag times, longer durations and the lack of correspondence with precipitation intensity suggest slower flowpaths than overland flow on saturated areas. (1978) pointed out that recession coefficients were influenced by dominant runoff mechanisms. Low K values for HOLF indicate rapid discharge recession (0.03-0.49), high values for subsurface flow (0.83-0.99) indicate relatively slow discharge decay. Saturation overland flow hydrographs exhibit a wider range of K values (<0.01–0.94). The recession coefficients for all sites are very similar and the average value of 0.98 suggests that the delivery of water is via slower subsurface pathways. One explanation for a larger discharge during wet AMCs at UF sites could be the development of rapid subsurface flow in shallow soil horizon above the low permeability clay layer. Results suggest that this flowpath seems to be activated mainly during wet AMCs. During non-growing season and wet AMCs, average flow rates and runoff ratios at UF sites are four times higher than during dry AMCS (Figure 11). Further interpretation of the runoff generation mechanisms is discussed in more detail in chapter 2.

Relationships between AMCs and storm response

A threshold response in storm runoff generation with either total precipitation or AMCs have been observed in studies with different topography, climate, and geology: Panola Mountain Research Watershed in the southern Piedmont (Tromp-van Meerveld and McDonnell, 2006), steep forested catchment in south central Japan (Gomi et al., 2010), Mont Saint-Hilaire catchment in Quebec, Canada (James and Roulet, 2007). In this study, total stormflow displayed a clear threshold response to both antecedent soil moisture and total precipitation. Total stormflow increased linearly above this threshold. Detty and McGuire (2010) observed similar behavior at a till mantled headwater catchment at Hubbard Brook Experimental Forest, NH. Umstead Farm sites have a higher ASI + precipitation threshold value (300 mm) than Hill Forest sites (256-269 mm). This higher storage capacity at Umstead Farm sites could be due to a lower topographic gradient (average slope at UF sites is 13% and average relief is 95-99 ft compared to slope of 7% and relief of 125-160 ft at HF sites)(Table 3). Detty and McGuire (2010) reported a threshold value of about 316 mm. The sum of soil moisture index and total precipitation could be useful to identify similar relationships at the scale of small catchments (Detty and McGuire 2010). f generatioRunofn mechanisms are difficult to generalize for different basins and different AMCs. A predictable, linear response that arises above threshold may be used to model rainfall-runoff relationships and evaluate land use within headwater catchments.

It has been hypothesized by Tromp van Meerveld and McDonnell in their fill and spill hypothesis that significant stormflow occurs only when bedrock depressions are filled and the subsurface saturated areas become connected. AMCs at both sites influence the activation of catchment runoff sources and delivery flowpaths to the stream. During dry AMCs (runoff below threshold) only a small percent of rainfall volume appears in the stream (average runoff ratio = 0.02 at HF2, average runoff ratio = 0.01 at UF2). This small runoff occurs rapidly (average L_P=27 minutes, average L_c=27 minutes at HF2, average L_P=88 minutes, average L_c=85 minutes at UF2). The runoff volume from small storms on dry AMCs could potentially be explained by flow from the narrow riparian corridor and direct channel interception (Siddle et al., 1995). Riparian areas have the potential to saturate even during small rainfall events and deliver water to stream rapidly. As antecedent wetness increases, flowpaths between the hillslope and riparian zone become connected and the proportion of rainfall that reaches stream increases (average runoff ratio=0.17 at HF2, average runoff ratio=0.4 at UF2). The lag times become longer because subsurface transport from hillslopes contributes to runoff (average L_P=3.4 hours, average L_c=2.4 hours at HF2, average L_P=3.0 hours, average L_c=7.4 hours at UF2). The threshold in runoff response could represent a transition between runoff generated from the near stream zone during below-threshold events and increasing hillslope contributions and activation of preferential pathways during above-threshold events.

Antecedent wetness indices

Precipitation-based antecedent wetness indices showed very poor relationship with soil moisture (ASI) at the UF2 site (Figures 17 and 18). Ali and Roy (2010) showed similar results at a small forested catchment located in Québec, Canada. In their study, soil moisture was not related to cumulative rainfall amounts over seven or ten day periods. At the HF2 site long-term antecedent precipitation (AP_{15} and AP_{30}) represent actual soil moisture better than at the UF2 site (Figure 17). The better relationship between precipitation and soil moisture conditions at HF2 catchments can explain why total stormflow is more sensitive to total precipitation compared to UF2 catchment (Table 7). API index shows a slightly better relationship for both sites because it takes PET into consideration. Antecedent baseflow showed relatively strong non-linear relationships with soil moisture and therefore reflect moisture conditions at the site better than precipitation based indices. Riparian groundwater levels showed the strongest relationship with soil moisture and are useful in quantifying AMCs prior to storms.

CONCLUSION

This study was conducted at five forested catchments in the Piedmont region of North Carolina with the purpose of evaluating rainfall-runoff dynamics of these headwater catchments. The five sites have similar climate and vegetation but different soils derived

from bedrock of Carolina Slate Belt (HF sites) and Triassic Basin (UF sites). It appears that soils influence hydrologic processes and should be considered in planning and management of water resources. The results of this study show that Umstead Farm sites have different storm hydrograph characteristics such as total stormflow, runoff ratios, and lag times than Hill Forest sites. Overland flow or shallow subsurface flow is likely a more important flowpath in Triassic Basin sites than in Carolina Slate Belt sites.

The interaction between soil properties and rainfall characteristics determine which flowpaths are being activated. The examination of relationship between antecedent moisture conditions and storm response shows a clear threshold-based response of stormflow to the sum of antecedent soil index (ASI) and precipitation. This threshold can be seen as a required amount of storage that needs to be reached before saturated areas at the catchment are connected. The threshold-like change in runoff with AMCs (James and Roulet, 2007), storm size (Tromp-van Meerveld and McDonnell, 2006; Gomi et al., 2010) or both (Detty and McGuire, 2010) has been observed at other sites with different climate and geology. The observed linear relationship between storm runoff and sum of antecedent soil index (ASI) and precipitation above threshold can facilitate the prediction of hydrologic response during individual storm events.

CHAPTER 1 TABLES AND FIGURES

Table 1. Average monthly precipitation for Durham, NC (30-year normal totals) (NC Climate Office, 2010)

Month	Jan	Feb	March	April	May	June	July	Aug	Sept	Oct	Nov	Dec
Precipitation (mm)	113	94	119	87	117	102	100	111	111	94	86	87

Table 2. Saturated hydraulic conductivity of the representative soil types at (a) HF sites (Tatum soil series), (b) UF sites (Helena soil series)

a)

Depth, cm	**K_{sat}, mm/hr**
0-20	50.4-151.2
20-30	50.4-151.2
30-99	1.5-5.0
99-117	14.4-50.4
117-203	14.4-50.44

b

Depth, cm	**K_{sat}, mm/hr**
0-15	50.4-151.2
15-25	50.4-151.2
25-97	1.5-5.0
96-127	14.4-151.2
127-203	14.4-151.2

Table 3. Catchments physiographic characteristics

Catchment	**Area (km^2)**	**Mean Slope (%)**	**Catchment Relief (ft)**
HF1	0.124	7.15	125
HF2	0.106	5.54	142
HFW1	0.291	7.39	160
UF1	0.192	5.34	99
UF2	0.283	5.34	95

Table 4. Storm hydrograph characteristics, rainfall characteristics, and measurements of AMCs considered in this study. QF = quickflow, as determined by graphical hydrograph separation; TF= total flow

Storm Hydrograph Characteristics	**AMCs**	**Rainfall Characteristics**
Total flow (mm)	Antecedent baseflow	Storm size (mm)
Runoff ratio (QF/P)	Groundwater level	Maximum intensity (mm/10 min)
Runoff coefficient (TF/P)	AP_3, AP_7, AP_{15} AP_{30}	Average intensity (mm/10 min)
Peak flow (mm/10 min)	API_3, API_7, API_{15} API_{30}	
L_C (hours)	Volumetric soil moisture	
L_P (hours)	ASI	
Recession coefficient	Season	
Duration (days)		

Table 5. Number of storms analyzed for each catchment

Catchment	**Number of storms with continuous flow record and measurable flow**
HF1	95
HF2	106
HFW1	106
UF1	37
UF2	75

Table 6. Statistics on lag times (L_P and L_C) and event durations for each catchment

ID	**n**	**Mean L_P (hrs)**	**Min L_P (hrs)**	**Max L_P (hrs)**	**Mean L_C (hrs)**	**Min L_C (hrs)**	**Max L_C (hrs)**	**Mean Duration (days)**	**Min Duration (days)**	**Max Duration (days)**
HF1	100	2.59	0	24	3.14	0	35.2	1.75	0.13	7.83
HF2	106	1.38	0	12.2	2.57	0	34.5	1.47	0.15	5.85
HFW1	106	2.76	0	87	3.17	0	32.3	1.58	0.17	5.61
UF1	39	3.11	0	23	5.55	0	30.5	2.21	0.07	4.99
UF2	75	4.12	0	24.5	5.88	0	32.8	2.21	0.24	6.17

Table 7. Pearson correlation between storm characteristics, rainfall characteristics, and AMCs for a) HF2 catchment, b) UF2 catchment

a)

	Total flow	Runoff Ratio (QF/P)	Runoff coefficient (TF/P)	Peak flow	L_P	L_C	Recession coefficient	Duration
Storm size	0.83	0.59	0.46	0.75	0.09	0.49	0.01	0.75
Max rainfall intensity	-0.03	-0.08	-0.21	0.25	-0.07	-0.10	-0.53	-0.08
Mean rainfall intensity	-0.08	-0.10	-0.21	0.20	-0.05	-0.14	-0.51	-0.20
Season	0.28	0.42	0.52	0.02	0.13	0.36	0.18	0.38
ASI	0.47	0.66	0.78	0.38	0.30	0.19	0.30	0.49

b)

	Total flow	Runoff Ratio (QF/P)	Runoff coefficient (TF/P)	Peak flow	L_P	L_C	Recession coefficient	Duration
Storm size	0.69	0.33	0.25	0.65	0.11	0.30	-0.16	0.42
Max rainfall intensity	-0.06	-0.20	-0.27	0.22	0.03	-0.18	-0.54	-0.24
Mean rainfall intensity	-0.22	-0.34	-0.39	-0.04	-0.14	-0.37	-0.61	-0.47
Season	0.36	0.52	0.56	0.21	-0.04	0.28	0.58	0.51
ASI	0.53	0.81	0.85	0.47	-0.05	0.29	0.85	0.65

Table 8. Catchments response to events below and above thresholds in ASI + total precipitation.

	Avg stormflow at HF2 (mm)	Avg stormflow at UF2 (mm)	Avg runoff ratio at HF2	Avg runoff ratio at UF2	Avg L_P at HF2 (hours)	Avg L_P at UF2 (hours)	Avg L_C at HF2 (hours)	Avg L_C at UF2 (hours)	Avg duration at HF2 (days)	Avg duration at UF2 (days)
Below threshold	0.69	0.47	0.02	0.01	0.42	1.1	0.45	1.42	0.75	0.66
Above threshold	11.39	17.41	0.17	0.4	2.79	1.34	3.45	7.4	2.44	3.3

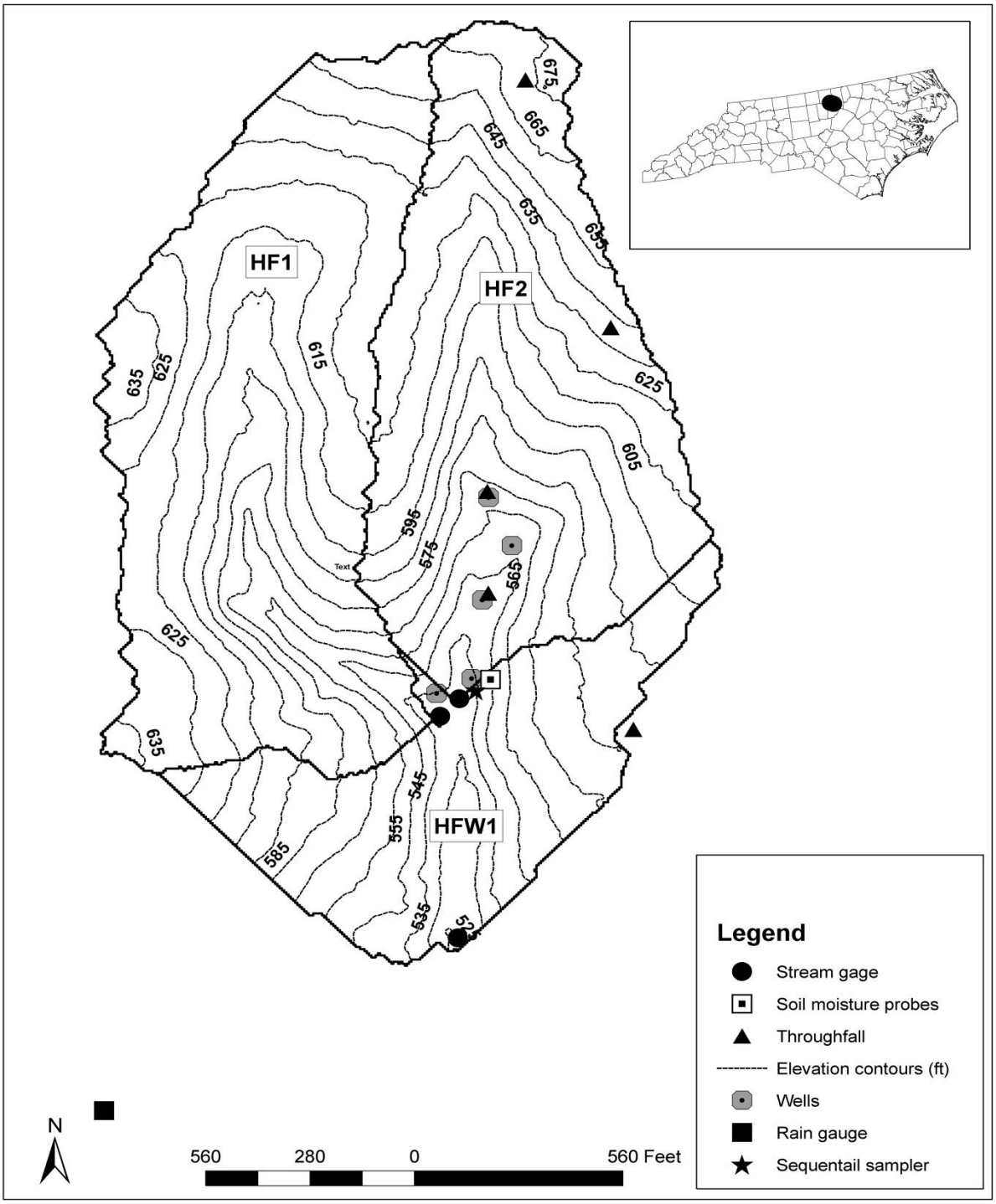

Figure 1. Hill Forest study catchments (HFW1, HF1, HF2) and the location of field equipment

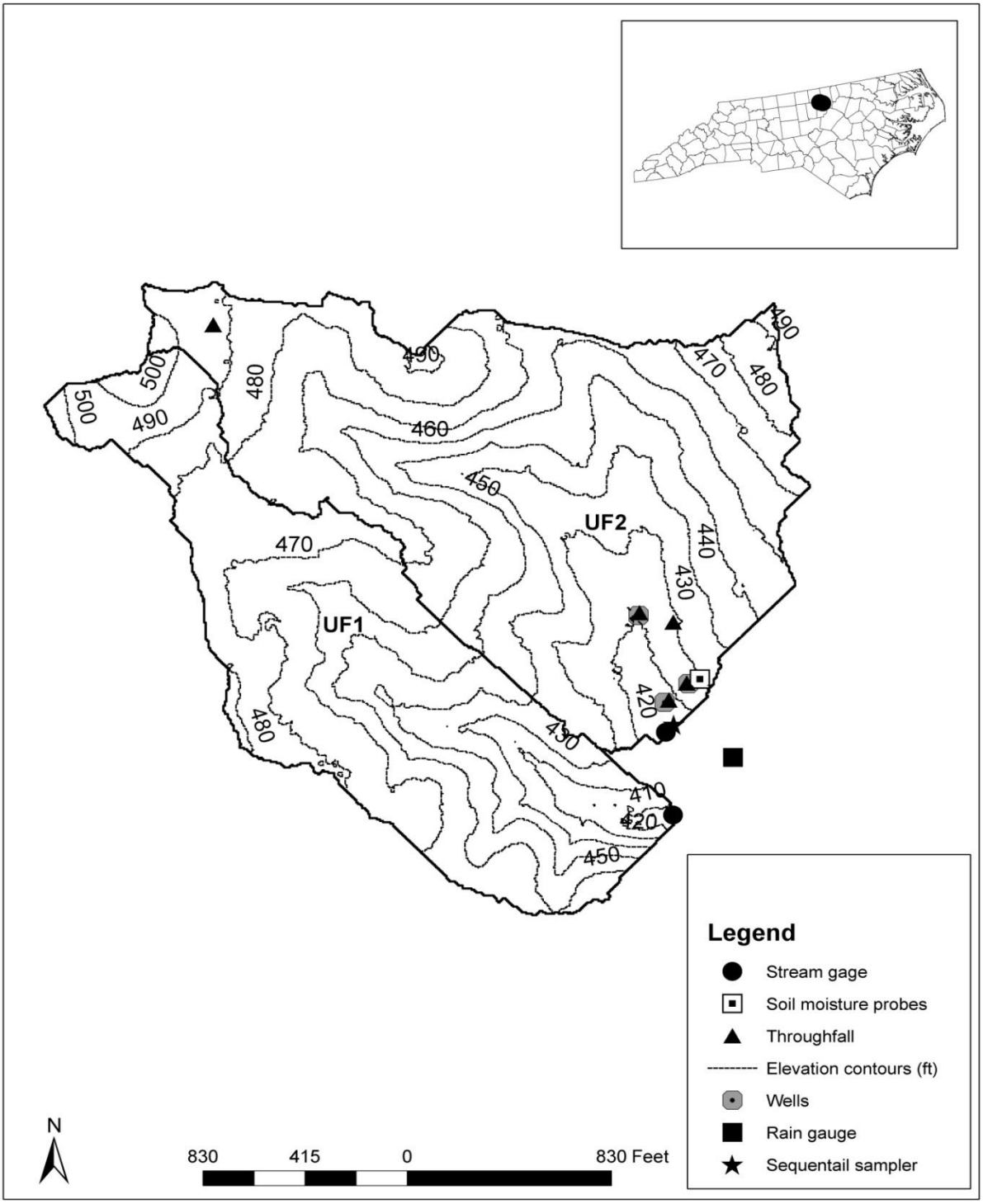

Figure 2. Umstead Farm study catchments (UF1, UF2) and the location of field equipment

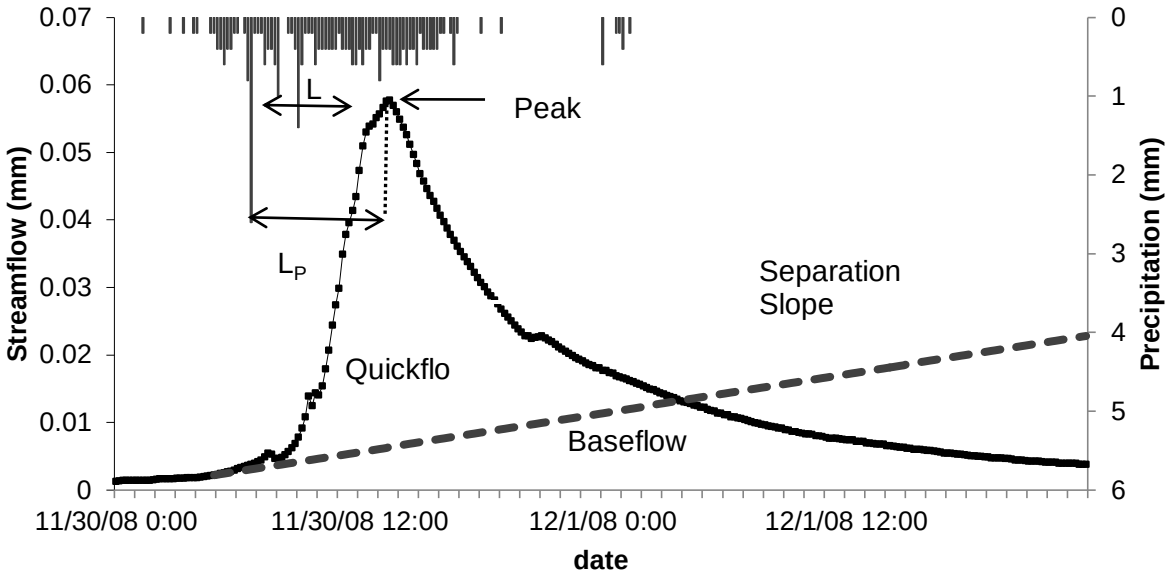

Figure 3. Example of storm hydrograph characteristics at HF2 catchment

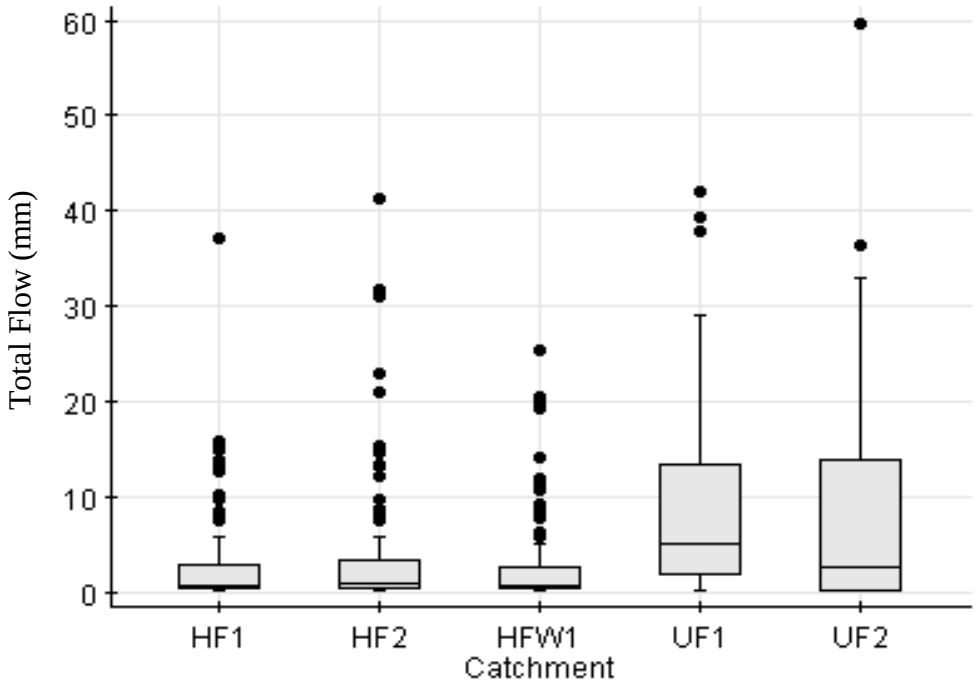

Figure 4. Box plot of total flow for five headwater catchments in Slate Belt ecoregion (HF1, HF2, HFW1) and Triassic Basin ecoregion (UF1, UF2)

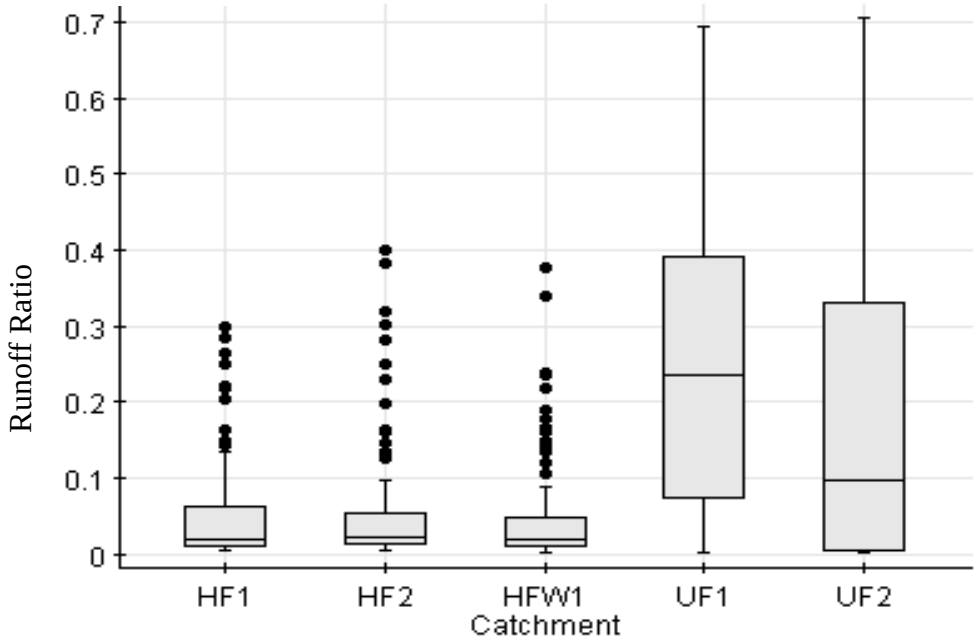

Figure 5. Box plot of runoff ratios (QF/P) for five headwater catchments in Slate Belt ecoregion (HF1, HF2, HFW1) and Triassic Basin ecoregion (UF1, UF2)

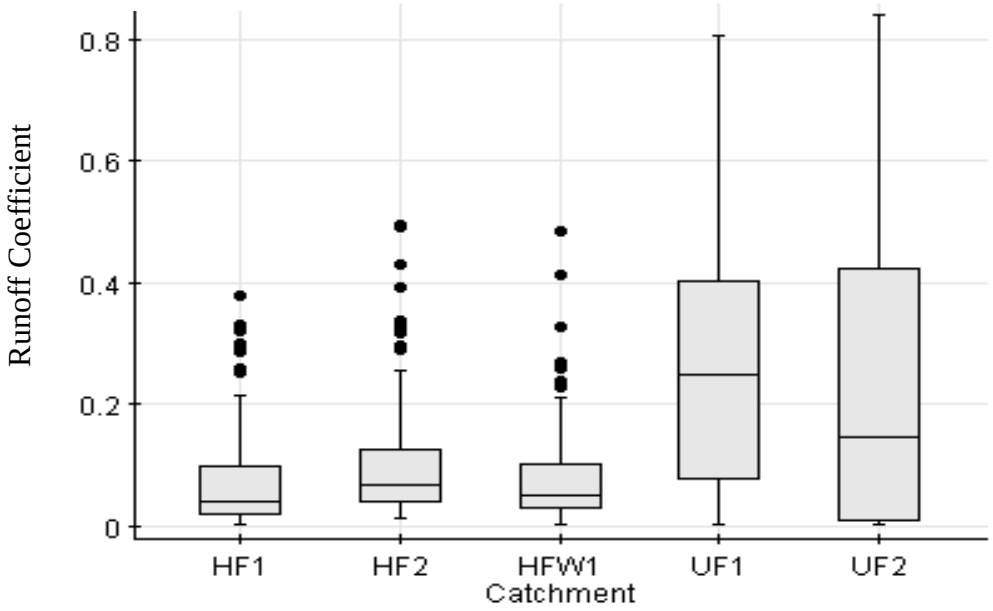

Figure 6. Box plot of runoff coefficients (TF/P) for five headwater catchments in Slate Belt ecoregion (HF1, HF2, HFW1) and Triassic Basin ecoregion (UF1, UF2)

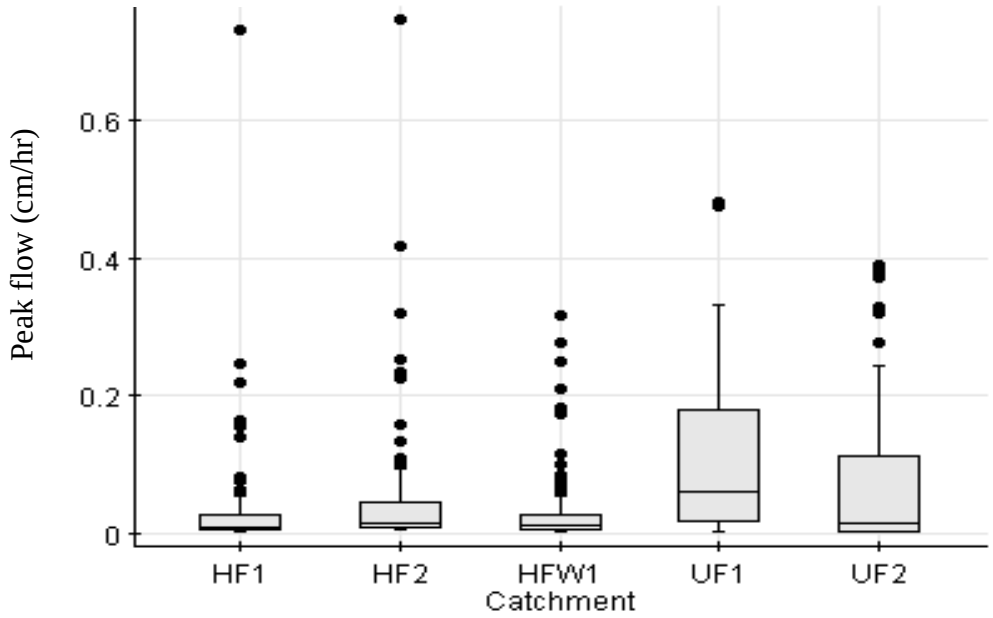

Figure 7. Peak flow in cm/hr for five headwater catchments in Slate Belt ecoregion (HF1, HF2, HFW1) and Triassic Basin ecoregion (UF1, UF2)

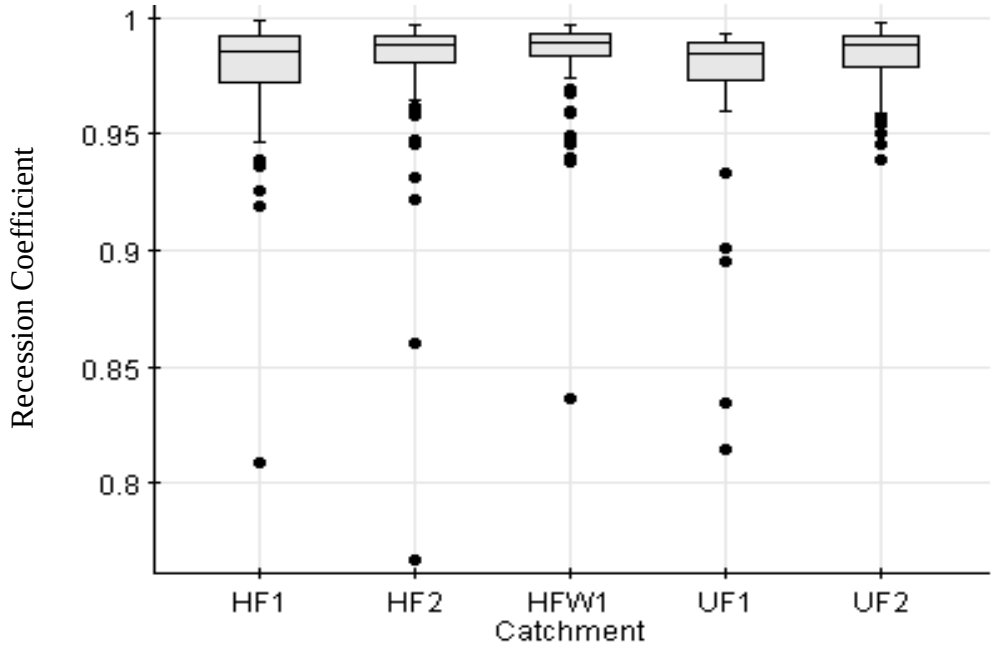

Figure 8. Box plot of recession coefficients in Slate Belt ecoregion (HF1, HF2, HFW1) and Triassic Basin ecoregion (UF1, UF2)

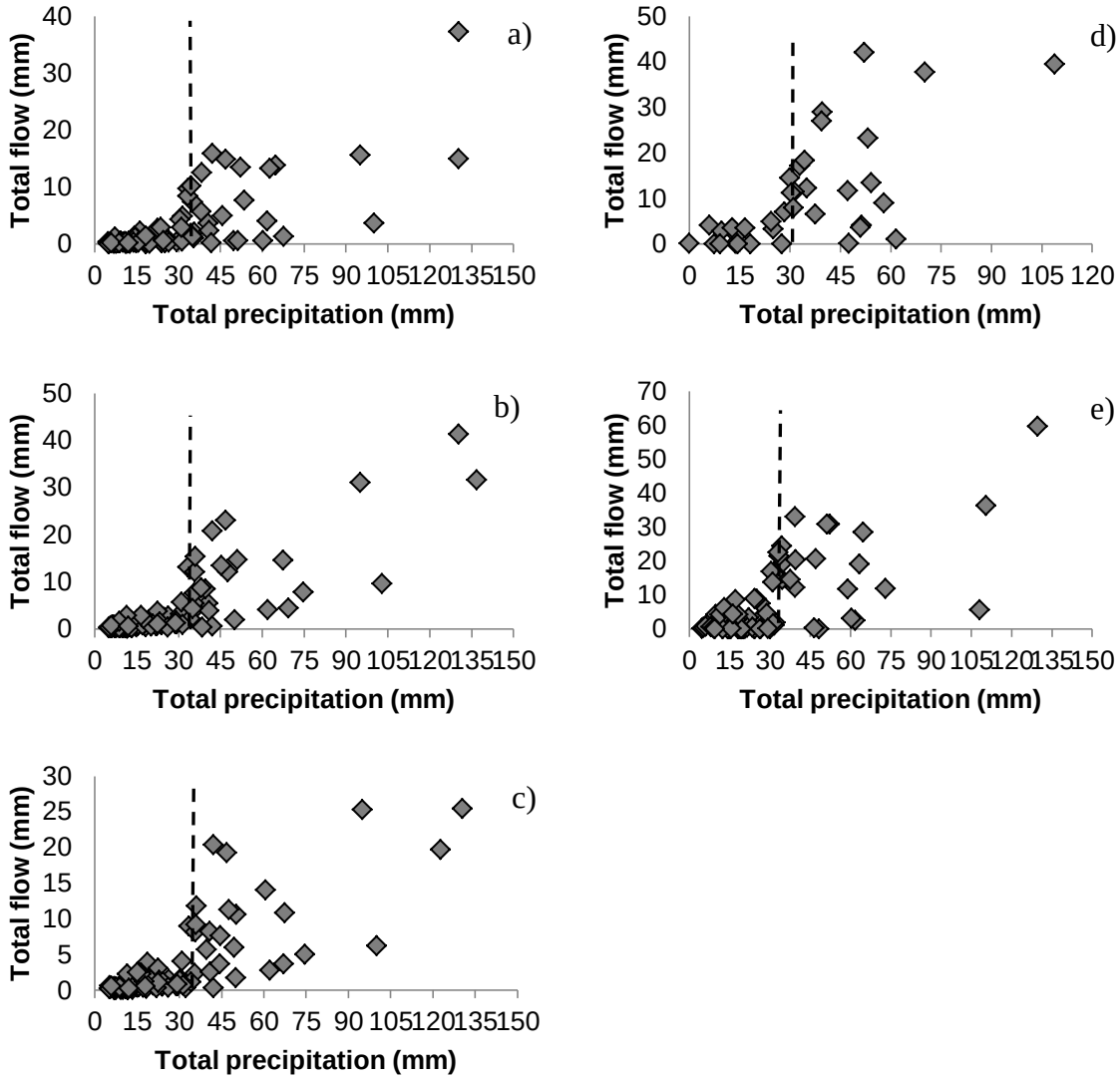

Figure 9. Total flow as a function of storm size for (a) HF1, (b) HF2, (c) HFW1, (d) UF1, (e) UF2 catchments. Dashed vertical line represents precipitation threshold

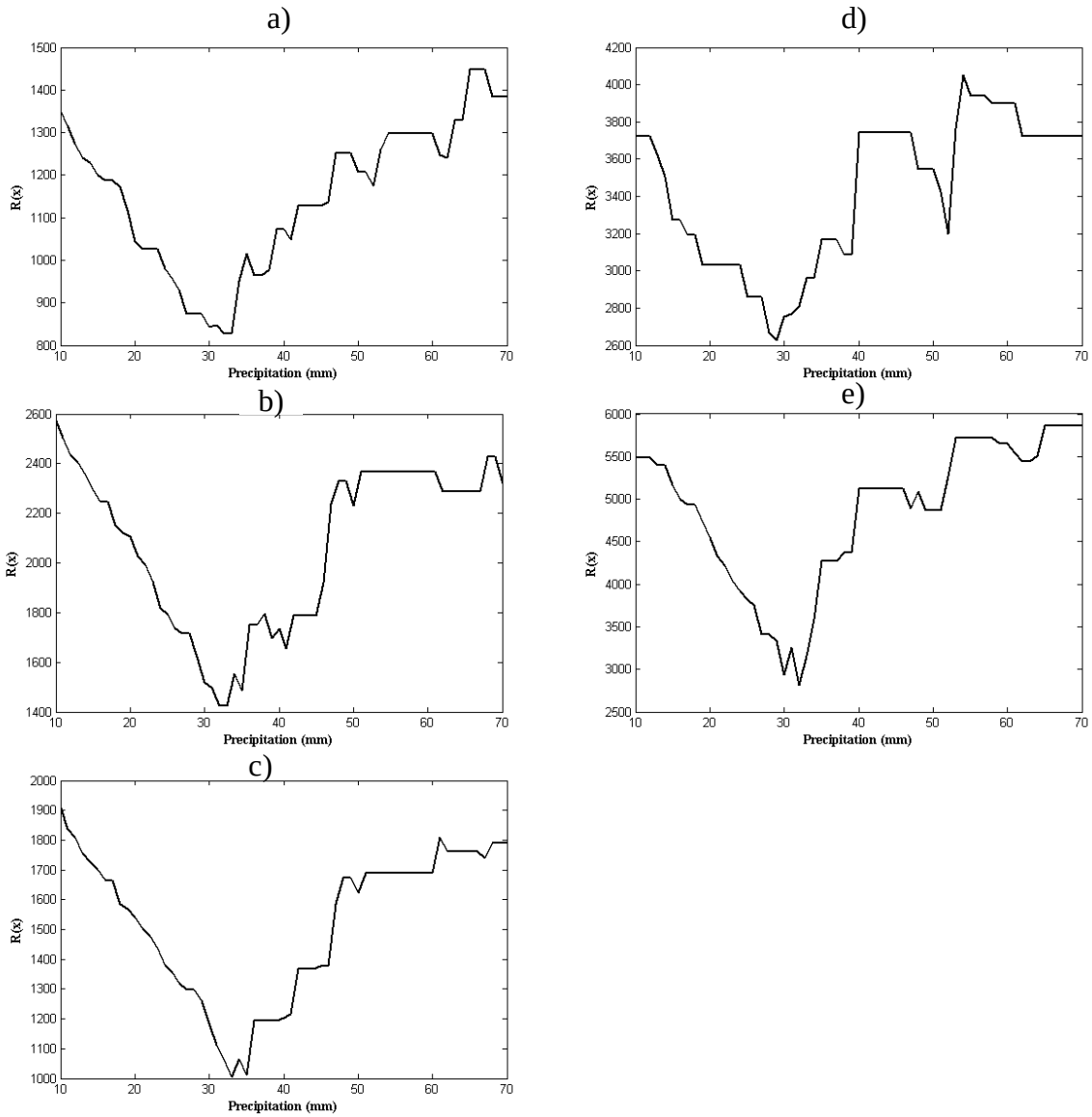

Figure 10. Evaluation of precipitation threshold. The sum of the squared deviations R(x) (mm^2) as a function of storm size for (a) HF1, (b) HF2, (c) HFW1, (d) UF1, (e) UF2 catchments

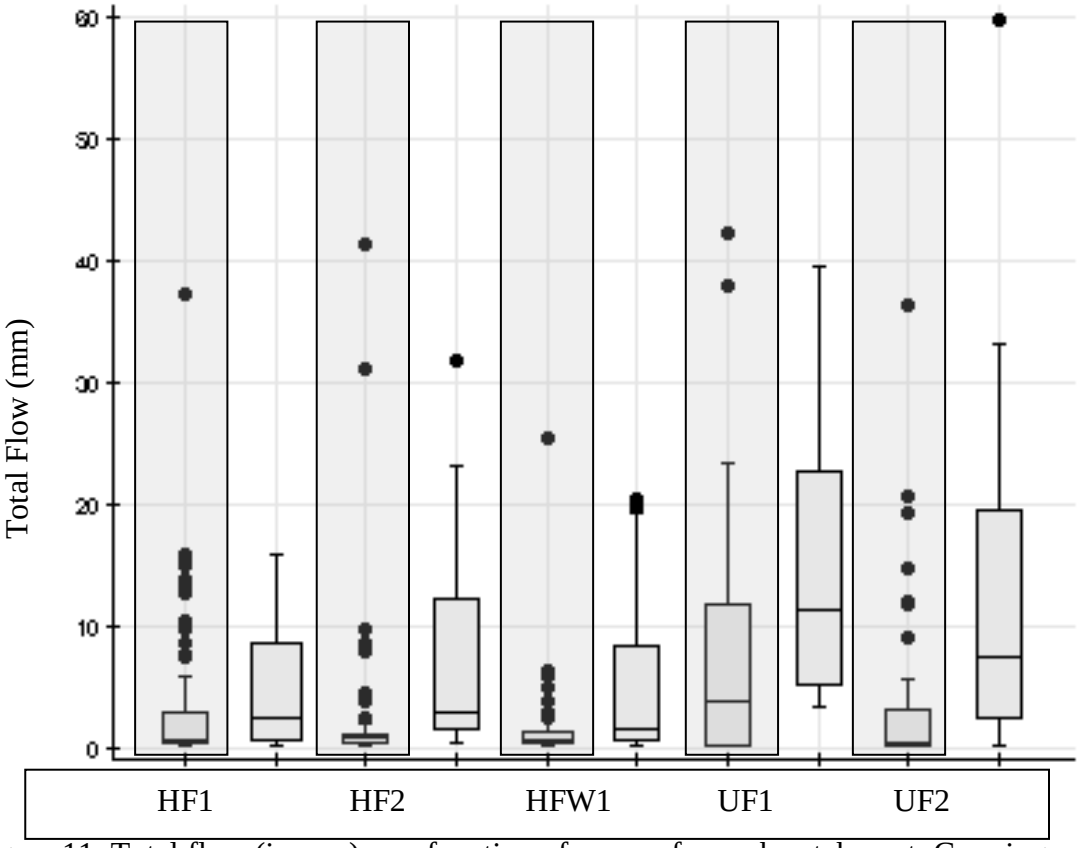

Figure 11. Total flow (in mm) as a function of season for each catchment. Growing season is in white; non-growing season is shaded.

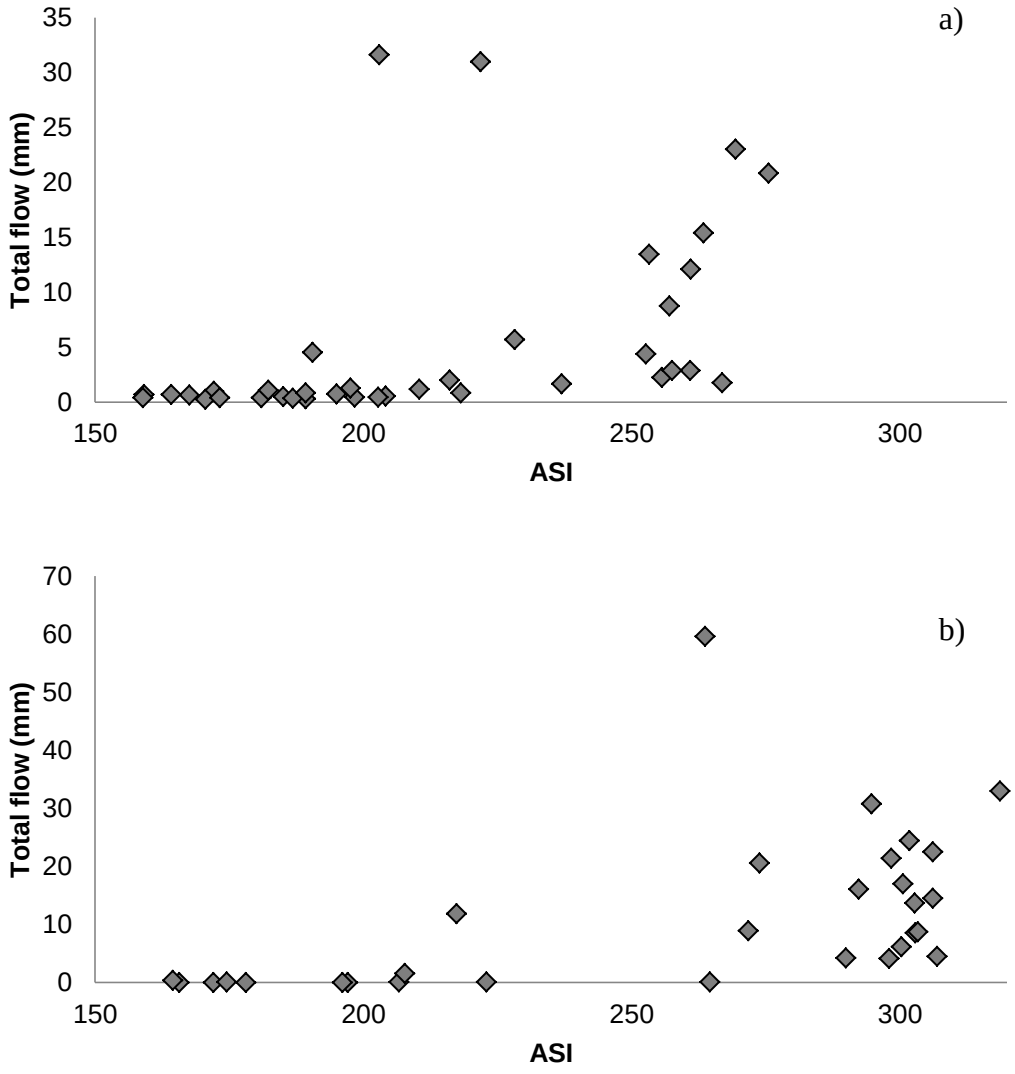

Figure 12. Total flow as a function of AMCs for (a) HF2 and (b) UF2 catchments

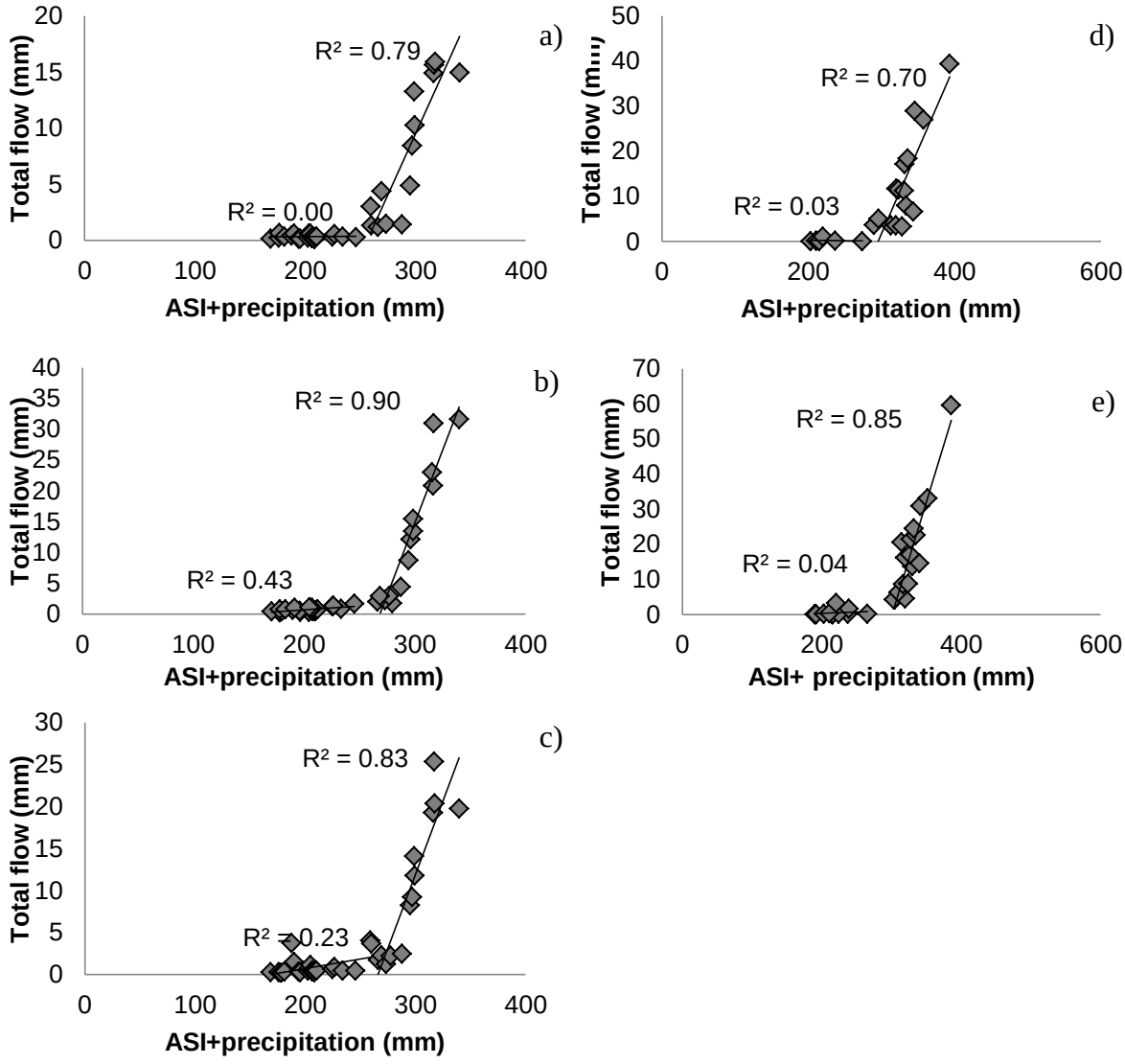

Figure 13. Threshold relationship between the combined term of ASI+ precipitation (mm) and total flow (mm) for (a) HF1, (b) HF2, (c) HFW1, (d) UF1, (e) UF2 catchments.

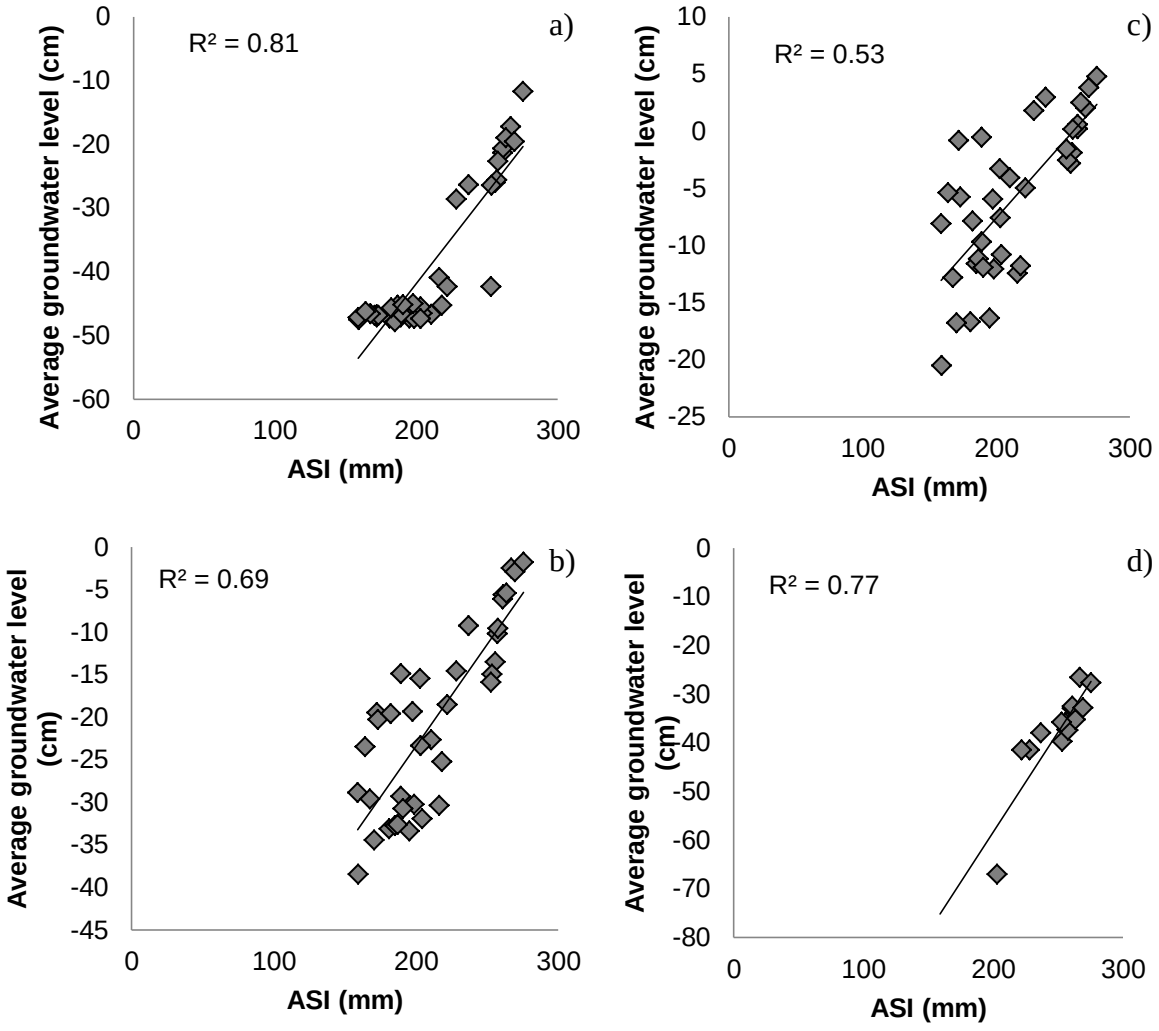

Figure 14. Relationship between Antecedent Soil Index (ASI) and groundwater levels at HF2 site, (a) well 1, (b) well 2, (c) well 3, (d) well 4

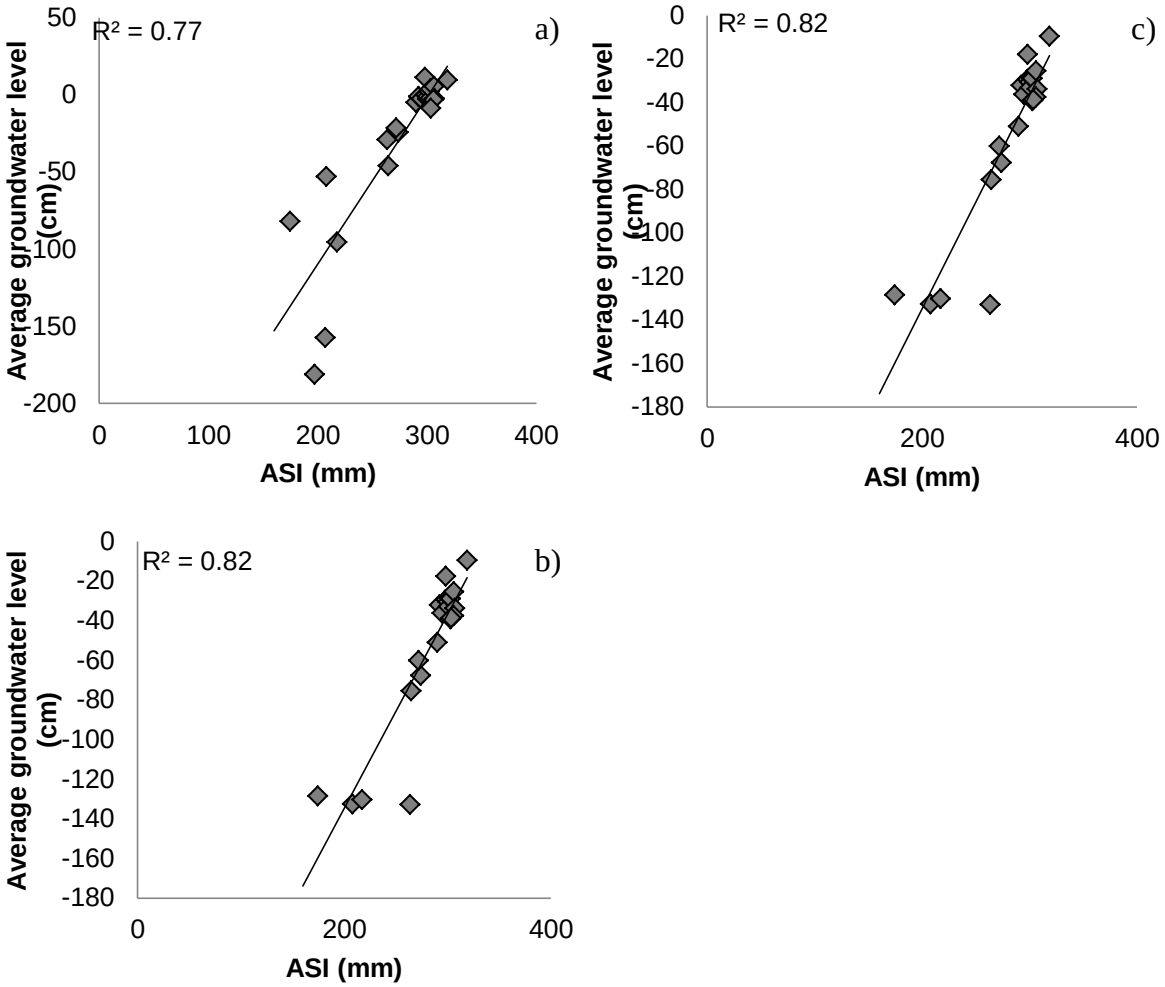

Figure 15. Relationship between Antecedent Soil Index (ASI) and groundwater levels at UF2 site, (a) well 1, (b) well 2, (c) well 3

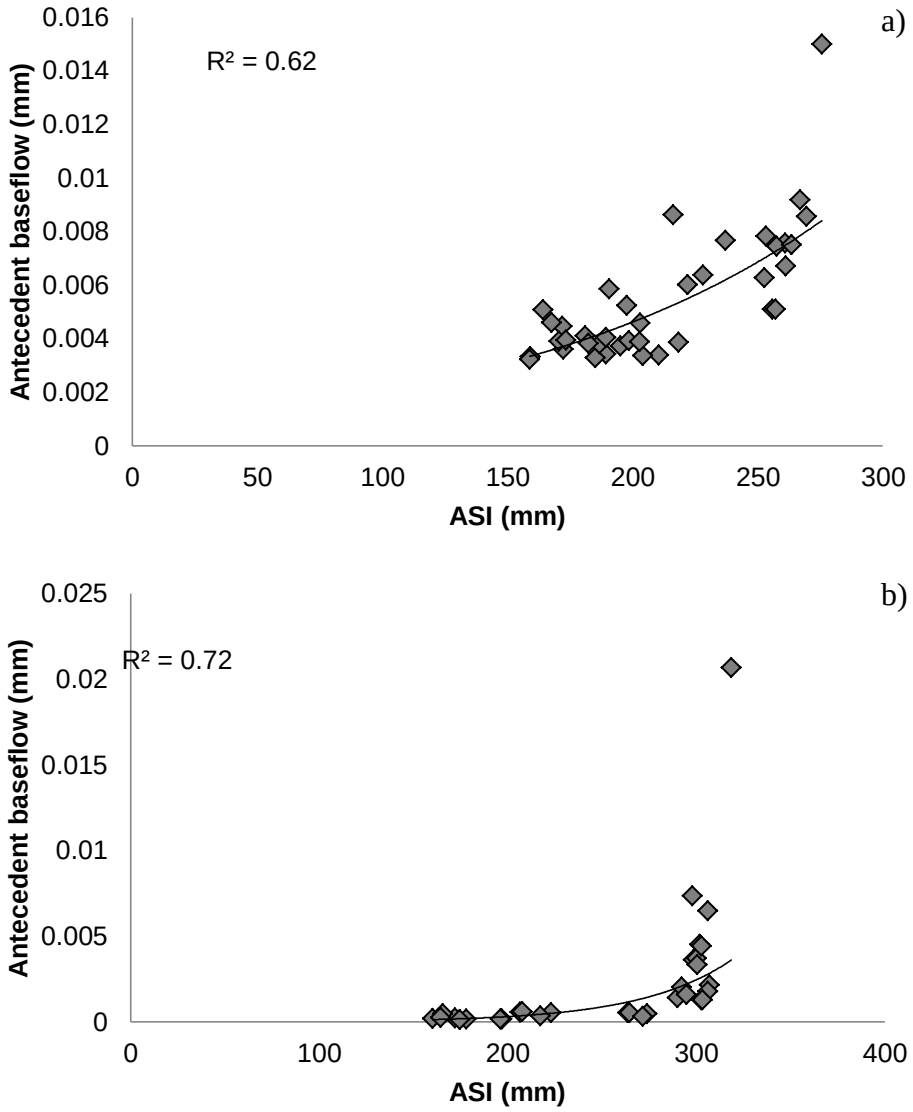

Figure 16. Nonlinear relationship between Antecedent Soil Index (ASI) and antecedent baseflow at (a) HF2 catchment, (b) UF2 catchment

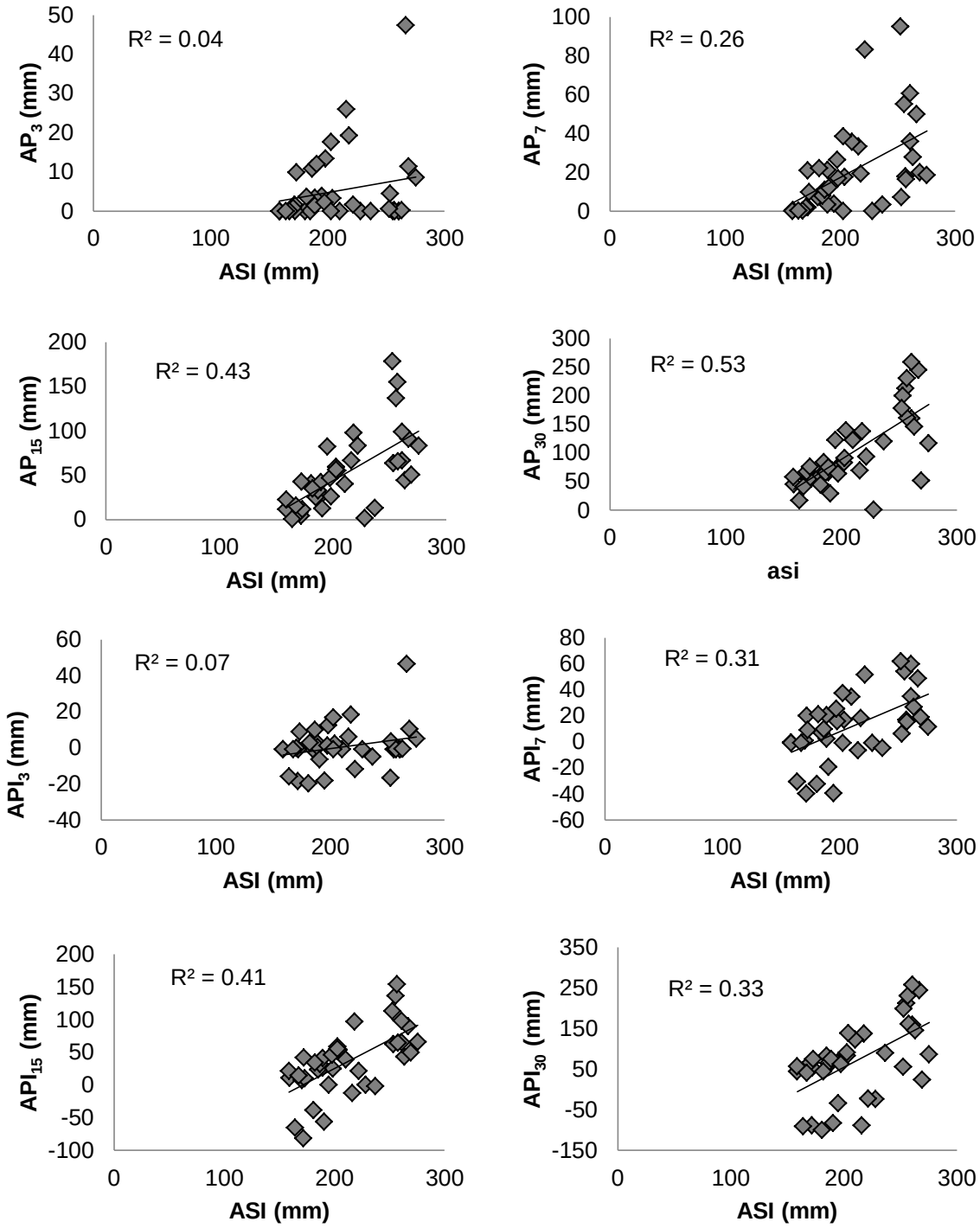

Figure 17. Relationship between Antecedent Soil Index (ASI) and precipitation based antecedent wetness indices at HF2 site

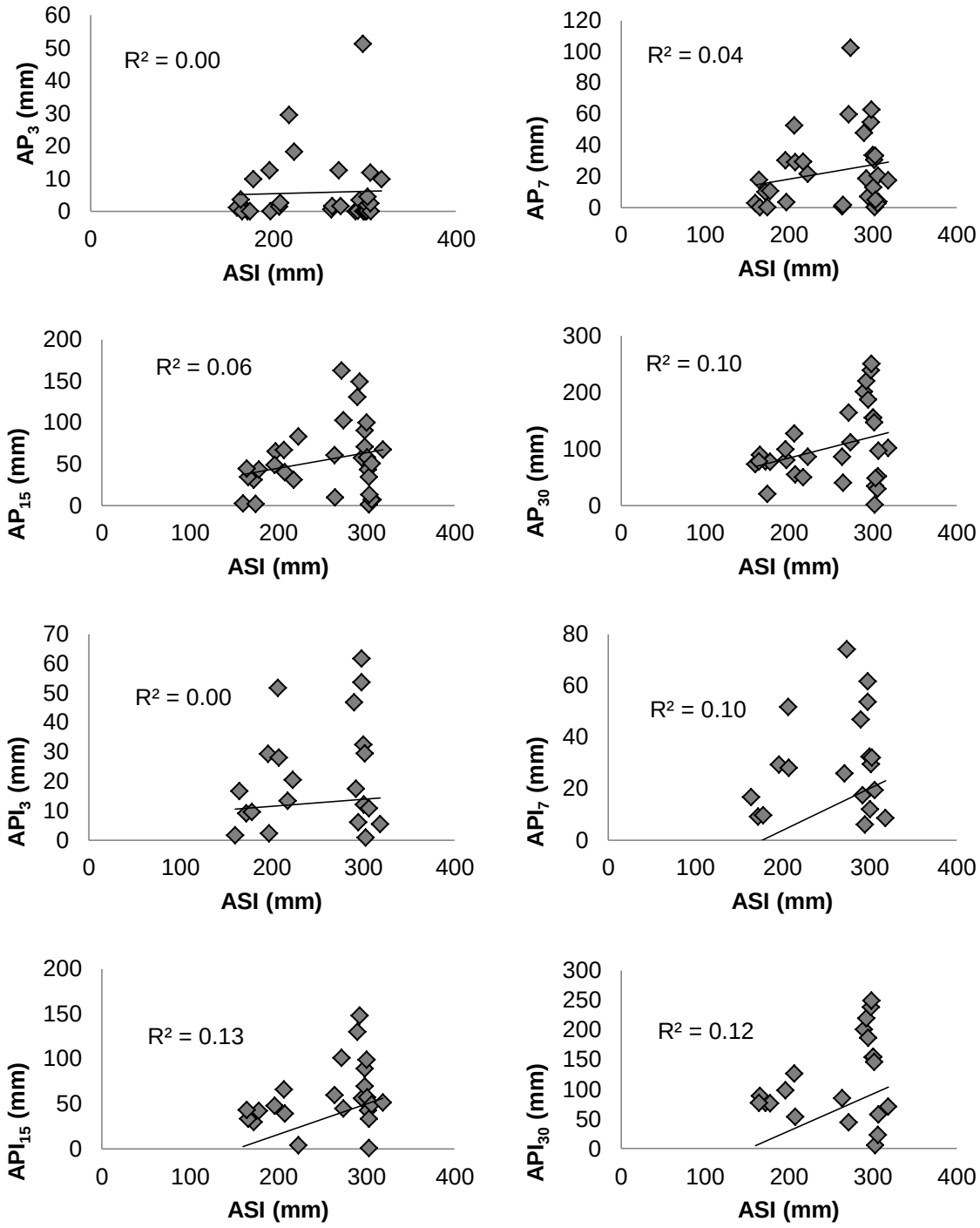

Figure 18. Relationship between Antecedent Soil Index (ASI) and precipitation based antecedent wetness indices at UF2 site

CHAPTER 2

INTRODUCTION

Stable Isotopes of Water

Isotopes are atoms of the same element that have the same numbers of protons and electrons but different numbers of neutrons. Oxygen has three stable isotopes, ^{16}O, ^{17}O, and ^{18}O; hydrogen has two stable isotopes, ^{1}H and ^{2}H (deuterium). Differences in the number of neutrons result in the differences in masses between isotopes. For example, all isotopes of oxygen have 8 electrons and 8 protons; however, an oxygen atom with a mass of 18 (denoted ^{18}O) has 2 more neutrons than oxygen-16 (^{16}O) and is heavier (Kendall and McDonnell, 1998). The stable isotopic compositions of oxygen and hydrogen are normally reported as δ values in parts per thousand (denoted as ‰) enrichments or depletions relative to a standard of known composition:

$$\delta \ in \ ‰ \ = \ \frac{R_X}{R_s} - 1 \ * 1000 \qquad (1)$$

where R is the ratio of heavy to light isotope, R_x and R_s are the ratios in sample and standard, respectively (Kendall and McDonnell, 1998).

The ratios of stable isotopes in water may change or fractionate in nature due to evaporation, condensation and biological processes. As a result of fractionation, waters develops unique isotopic compositions and produces a natural labeling effect within the global water cycle that has been applied to study a wide range of hydrological and climatic

processes at the local and regional scales (Gibson et al, 2005). Global atmospheric moisture arises from the ocean surface and undergoes rain-out of heavy isotopes during transport (Gibson et al, 2005). These effects produce a general shift towards lower heavy isotope content from coastal to inland areas and with increasing latitude (Gibson et al, 2005). $\delta^{18}O$ and $\delta^{2}H$ values of monthly precipitation commonly plot in strongly linear clusters close to the meteoric water line (MWL), and best-fit local MWLs drawn through these clusters can provide isotopic input functions for local hydrological studies (Gibson et al, 2005).Subsequently, it is important to determine whether the different components of water (groundwater, baseflow, runoff) reflects that of local precipitation.

Hydrologic studies have shown that seasonal difference in precipitation can be used to study recharge and runoff processes. A recent example illustrating the seasonal changes in precipitation and groundwater discharge isotope signatures is the study by Lee and Kim (2007) in the North Han River basin in Korea. They found a difference in isotopic signature between winter and summer precipitation and this signal can provide a basis for interpretation of groundwater recharge. Rose (1996) investigated temporal environmental isotopic variation in the Falling Creek watershed located near the southern margin of the Piedmont province of Georgia. $\delta^{18}O$ values within baseflow varied seasonally ($-5.8‰ < \delta^{18}O < -3.5‰$), consistent with established trends (Kendall and Coplen, 2001). $\delta^{18}O$ values decreased from -3.5‰ to -5.8‰ during non-growing season and the time of maximum net water influx; the diluted runoff suggested that a significant component of runoff came from shallow subsurface and from the near steam zone. During growing season when

evapotranspiration is high, more geochemically evolved (heavier) water indicated that baseflow was generated along deeper flowpaths. Rose (1996) applied a mixing model which indicated that event water makes less than 10% of the shallow subsurface storm runoff for individual storm events. The study by Wenner et al. (1991) investigated the stable isotopic composition of rainfall, water from unsaturated zone and saturated zone, and baseflow in a Piedmont watershed. The observations of isotopic signatures of rainfall, baseflow, groundwater, and soil water were consistent with the hypothesis that the recharge by rainfall occurs only in winter. Very little summer rainfall moved through the soil due to high evapotranspiration.

Isotope Hydrograph Separation

The storm hydrograph characteristics such as peak flow rates, lag times, and runoff ratios can give a first impression of relevant runoff generation mechanism. For example, the calculation of runoff ratios for single events can give a first idea of the hydrologic behavior of a catchment under different AMCs conditions and storm characteristics. Although the storm hydrograph is the primary source of information about hydrological behavior, this information is very limited. The storm hydrograph does not provide information on the origin and flowpaths of water. Isotope hydrograph separation (IHS) in combination with hydrometric or hydrochemical measurements is often used to identify the origin, timing, and pathways of surface and subsurface runoff. IHS is a two-component mixing model that uses a mass balance approach to separate stormflow into pre-event and event water on the basis of

stable isotope ratios (Sklash and Farvolden, 1979). The principle of IHS is based on a contrast in the isotopic composition of groundwater and rainfall of a given storm. The groundwater in the basin has an isotopic composition that reflects the long-term average input while an individual rain event can have a distinct signature.

The large majority of the studies in small forested catchments have established that that pre-event water dominates (>60%) stormflow hydrographs (Gibson et al, 2005). However, the development of perched water table can result in high event water contribution. Laudon et al. (2007) used IHS in combination with hydrometric measurements to investigate how catchment scale and landscape characteristics affect runoff generation in boreal streams at Vindeln Experimental Forests in Sweden with glacial till soils in the upper portion and sorted sediments consisting mainly of sand and silt in the lower portion. Laudon et al. (2007) found large differences in hydrological flowpaths between forested catchments and wetland dominated catchments. The proportion of event-water was over 50% in wetland catchments, while forested catchments were dominated by pre-event water (77-84%). They concluded that in forested catchments the majority of rain and melt water infiltrates into the soil and mobilizes pre-event water stored in the hillslopes. In contrast, in wetland catchments an overland flow and shallow subsurface flowpaths contribute strongly to runoff. The shallow subsurface flowpath is probably caused by a continuous soil frost layer that prevents water from infiltrating deeper. In our study, the Triassic Basin (UF) sites have a tendency to promote development of shallow perched water due to shallow clay layer. Therefore, we may

expect higher event water contributions at these sites during storm events to coincide with high runoff ratios discussed in Chapter 1.

Greater understanding of controls that soil wetness plays in runoff generation processes is important for our ability to monitor and model basin hydrochemistry (Buttle et al, 2001). IHS studies suggest that AMCs play an important role in the partitioning of event and pre-event water (James and Roulet, 2009). For example, Buttle et al (2001) using Cl^- and Br^- concentrations for hydrograph separation observed an initial increase in bedrock runoff with the increase of antecedent soil wetness which then declined at large antecedent soil wetness. Chemical end-member-mixing and isotopic tracing approaches revealed that rapid lateral flow in the shallow subsurface may be a dominant mechanism during high intensity summer rainstorms (Brown et al, 1999). Brown et al. (1999) investigated the role of event-water in summer stormflow in seven nested headwater catchments and showed that event-water contributed 49% to 62 % in the 7 catchments. Experimental studies have shown that during dry conditions, most of the stormflow is generated from channel interception and riparian saturated overland flow (Sidle et al. 2000). A high event-water contribution could also be explained by the development of perched saturation in shallow soil horizon due to differences in saturated hydraulic conductivity between the top organic layer and the mineral soil beneath it. James and Roulet (2009) investigated runoff generation under different antecedent moisture conditions in small forested nested catchments ranging in size from 7 to 147 ha. For large storms under dry AMCs some of the smallest catchments generated a high percent of new water. A high contribution of event water can be explained by development of

perched water and generation of shallow-subsurface stormflow, in addition to depleted groundwater stores. During wet AMCs, hillslopes become linked to the channel system, preferential flow systems expand and subsurface flow contributes significantly to the stormflow (Sidle et al. 2000). Thus, in our study we expect the event water contribution to differ depending on the AMCs. Under wet AMCs greater hydrologic connectivity should lead to a more uniform response while dry AMCs should result in greater variability in new water contribution across storms. Monitoring soil moisture and shallow groundwater levels at different parts of the catchment can help establish which parts of the catchment (e.g. hillslope and riparian zones) contribute to the storm hydrograph.

Hydrograph Separation Using Electrical Conductivity and δD versus $\delta^{18}O$

Although stable isotopes have been recognized as a preferred method for hydrograph separation, electrical conductivity of water has been used as a tracer for separation (Pellerin et al., 2008). The benefits of electrical conductivity (EC) measurements are that they are simple, inexpensive, and can provide data when storms do not meet the criteria for IHS (e.g. baseflow and precipitation stable isotope signatures are not sufficiently different). In their study, Pellerin et al. (2008) used EC to infer the contribution of surface runoff in an urban watershed. A comparison of IHS for two storms indicated that total contributions of new water were similar using three natural tracers (EC, Si, and δD). They reported large differences between antecedent streamflow concentrations and precipitation because in urban watersheds groundwater EC values are commonly elevated by non-point source pollution.

However, studies in forested watersheds using EC as a tracer have presented contradictory results. For example, Laudon and Slaymaker (1997) conducted hydrograph separation in two nested alpine basins in the Coast Mountains of British Columbia and concluded that using EC for hydrograph separation underestimated the pre-event water contributions to stormflow in the upper portion of the basin. Their results can be explained by the changes in chemical composition of water as a result of interaction with soil and bedrock. Pilgrim et al. (1979) investigated the effect of contact time of water with watersheds soils on the specific conductance of runoff water and suggested that high conductivity was not only caused by an increased groundwater discharge, but also by solute load obtained during contact with the soil surface. If the stormflow at UF sites moves partially as overland flow, the effects of solute load on the ability of EC to be an effective tracer might be more of a potentially issue at UF compared to HF sites.

Lyon et al. (2009) investigated differences in hydrograph separation for runoff event using δD versus $\delta^{18}O$. They showed that the choice of isotope may influence hydrograph separation especially when using one sample collected in space and time as representative of all rainfall in the catchment. The largest difference of 33% in the event water estimation using δD versus $\delta^{18}O$ was reported by Lyon et al. (2009) with the bulk representation of rainfall. This was largely due to the independent variations of δD and $\delta^{18}O$ values in sampled precipitation as measured by different rain gauges. The $\delta^{18}O$ composition at one of the rain gauges was similar to that of the pre-event water sample. The deviation of precipitation signatures about the meteoric water line can come from secondary evaporation

of raindrops below the cloud base, precipitation that originally evaporated from different source waters, mixing of water from different climates, and mixing with an evaporated body of water (Lyon et al. 2009). The result of this is that precipitation signatures collected across a catchment can have independent variations of δD and $\delta^{18}O$. Lyon et al. (2009) commented that the use of both stable isotopes has the potential to identify the unrealistic conclusion reached solely using $\delta^{18}O$ to separate the event hydrograph.

RESEARCH QUESTIONS

This Chapter will characterize δD and $\delta^{18}O$ stable isotopic signatures of baseflow and rainfall across seasons at the five HF and UF catchments. Individual storm events will be analyzed to quantify event and pre-even water contributions to streamflow generation across the sites. The following specific research questions will be addressed in Chapter 2:

- Are there seasonal variations in δD and $\delta^{18}O$ stable isotope ratios in baseflow and rainfall for the HF and UF catchments? Based on previous studies conducted in the Piedmont (e.g. Wenner et al., 1991; Rose, 1996) we might expect to see $\delta^{18}O$ values to decrease (becomes less heavy during the non-growing season due to increasing net water recharge) by ~ 2-3 per mil.
- What is the percent of event-water contribution to stream runoff from each catchment for storm events occurring on a range of antecedent moisture conditions?

- Is there difference in new/old water delivery across sites? We may expect higher event water contributions at the UF sites compared to the HF sites during storm events to coincide with high runoff ratios discussed in Chapter 1.
- Is there difference in new/old water delivery above/below ASI + precipitation threshold?
- Is there difference in hydrograph separation using δD, $\delta^{18}O$ and EC?

METHODS

Sampling for Stable Isotopes and EC

Baseflow and storm sampling for stable isotopes was performed from October 2008 to May 2010. Baseflow from five catchments (HF1, HF2, HFW1, UF1, UF2) was collected approximately every 2 weeks by grab sampling during non-storm periods. Stormflow from the five catchments (gauging stations shown in Figures 1 and 2) was sampled by automated samplers during rain events. Automated samplers were programmed to trigger by the change in flow to fill a total of 12 bottles per storm event. Change in flow rate was 0.04 cfs for HF1 and HF2 catchments and 0.07 cfs for HFW1, UF1, and UF2 catchments. The first six samples were collected at 10 minutes intervals and the last six samples were collected at 1 hour (Hill Forest catchments) and 1.5 hours (Umstead Farm catchment) intervals. Near stream groundwater samples were collected once a month from three shallow groundwater wells at HF2 and UF2 catchments. Water samples were collected in 20 mL vials and rinsed

with stream water prior to sample collection. From February, 2009 onwards samples were filtered using 0.45 μm syringe filters.

One bulk rainfall and five bulk throughfall gauges were used to collect precipitation at both HF2 and UF2 catchments (locations shown in Figures 1 and 2). Good agreement in storm event volumes delivered was found between the five bulk throughfall gauges and the tipping bucket rain gauge located at the lower station; the relationship between rainfall collected in the open by the tipping bucket and throughfall gauges is linear for all gauges (Figure 19). Depending on individual throughfall gauges, measured throughfall ranged from 78% to 100% of open rainfall measured with tipping bucket for HF catchments and from 90% to 99% for UF catchments (Figure 19). To address the potential of changing isotope signatures during rainfall, one sequential rain sampler was installed in both HF2 and UF2 catchments (Figures 1 and 2) and monitored from August 2009 to May 2010. Sequential samplers were built using a funnel connected to individual 250 ml sample bottles, representing 3.0 mm increments, calculated by dividing the bottle volume by the sectional area of the funnel. Each bottle was filled before rain flowed to the next bottle in sequence. An air vent prevented siphoning from bottle to bottle (Figure 20). Laboratory testing of each sequential sampler was performed prior to field installation using colored water to ensure no mixing as bottles were sequentially filled. The amount of rainfall collected by sequential samplers tended to be less than the observed rainfall because the connection from funnel to the bottles often got plugged by debris, even with a screen in place on the collecting funnel. Some storms did not have sequential samples for entire duration of the storm due to funnel

clogging. All water samples were stored in 20 mL vials with cone shape cap to prevent head space. Vials were sealed with parafilm and stored in cool shaded area to prevent any fractionation prior to analysis.

During the field collection period 23 storms were sampled to evaluate stable isotope signatures. Six of the storms (baseflow, stormflow, and rainfall) were sampled for electrical conductivity as an alternative tracer using a VWR Electrical Conductivity Meter. For each storm, precipitation, baseflow prior the storm and streamflow from peak hydrograph were sent for preliminary analysis to the Stable Isotope Facility at UC Davis to evaluate potential for IHS. The Stable Isotope Facility provides analysis of δD and $\delta^{18}O$ ratios in liquid water samples using a Water Isotope Analyzer V2 (Los Gatos Research, Inc., Mountain View, CA, USA). The internal check performed by Stable Isotope Facility at UC Davis revealed that standard deviation ranged from 0.04 to 0.16 for $\delta^{18}O$ and from 0.18 to 0.74 for δD. Ten percent of the samples were duplicated and provided a mean repeatability of isotope composition. Standard deviation in new water composition due to spatial variability was within 8.2 ‰ for δD and within 1.0 ‰ for $\delta^{18}O$. Spatial variability in old water composition was within 2.2 ‰ for δD and within 0.5 ‰ for $\delta^{18}O$.

The uncertainty associated with the computed mixing fractions can be evaluated using the technique described by Genereux (1998):

$$W_{fn} = \left[\left(\frac{f_o}{C_o - C_n} W_{co} \right)^2 + \left(\frac{f_n}{C_o - C_n} W_{cn} \right)^2 + \left(\frac{1}{C_o - C_n} W_{cs} \right)^2 \right]^{1/2} \quad (2)$$

where C refers to the isotopic signatures and subscripts o, n, and s are old, new and streamwater respectively. Instantaneous new water runoff (Xn) is the product of instantaneous total runoff (Q) and the fraction of new water (f):

$$X_n = Q f_n \quad (3)$$

Where uncertainty in new water runoff (W_{xn}) is estimated by:

$$W_{xn} = X_n \left(\frac{W_Q}{Q} \right)^2 + \left(\frac{W_{fn}}{f_n} \right)^{2\ 1/2} \quad (4)$$

Uncertainty in total new water dlivered during the stom is estimate by summing the errors for each instantaneous measurement during the storm hydrograph.

Isotope Hydrograph Separation

The respective contributions of pre-event and event water components to streamflow can be calculated using the mixing model based on a steady-state form of a mass balance equation for water and a conservative tracer:

$$Q_{on} = Q_s \left[\frac{C_s - C_o}{C_n - C_o} \right] \quad (4)$$

where Q_s is streamflow, Q_o and Q_n are contributions from old and new water; C_s, C_o, and C_n are stable isotope concentrations in streamflow, old, and new water (Sklash and Farvolden, 1979). Use of equations (1) rests on several assumptions (Buttle 1998): there is a significant difference between the isotopic content of the different components (new and old water); the isotope signature of event water is constant in space and time, or any variations

can be accounted for; contributions of additional components (e.g. soil water) must be negligible, or the isotopic content must be similar to that of another component (e.g. old water); contributions to streamflow from surface storage are negligible.

Isotope hydrograph separations were carried using three types of new water concentrations: constant weighted mean, incremental volume-weighted mean and incremental intensity mean. In this study, a constant volume-weighted mean value for throughfall bulk samples has been computed as:

$$\delta D = \sum_{i=1}^{n} P_i \delta_i / \sum_{i=1}^{n} P_i \quad (5)$$

where P_i and δ_i denote fractionally collected precipitation depth and δ value, respectively. To address the within-storm isotopic variability, an incremented mean value for the storm rainfall has been computed when several rainfall samples have been collected by the sequential sampler during storm. In this way, rain that has not yet fallen is excluded from the estimates:

$$\delta D = \sum_{i=1}^{n} A_i \delta_i / \sum_{i=1}^{n} A_i \quad (6)$$

where A_i is the incremental amount of input, δi is the corresponding tracer concentration of inputs.

Another method, the incremental intensity mean, includes rainfall intensity:

$$\delta D = \sum_{i=1}^{n} I_i \delta_i / \sum_{i=1}^{n} I_i \quad (7)$$

where, I_i is the average mm/15 minutes rainfall intensity during the sampling increment and δ_i is the corresponding tracer concentration (McDonnell et al, 1990).

RESULTS

Characterization of Stable Isotope Signatures

Figure 21 shows δD versus $\delta^{18}O$ for baseflow, bulk rainfall and groundwater wells. The Global Meteoric Water Line (GMWL) and Local Meteoric Water Line (LMWL) are included for reference. The GMWL shows the relationship between in rain, snow, rivers, and lakes from all over the world (Craig 1961). The LMWL was estimated from samples of local precipitation collected at GNIP station in Cape Hatteras, NC (IAEA). The LMWL for precipitation is described by the equation $\delta^{2}H=6.1\delta^{18}O+4.3$.

Figures 22 and 23 show the range of δD and $\delta^{18}O$ values for different types of water samples. The mean baseflow isotopic signatures for the three HF sites are very similar to each other. For example, the mean $\delta^{18}O$ signature in baseflow is -6.0‰, -6.2‰, and -6.1‰ for HF1, HF2, and HFW1 sites (Table 9). The mean δD signature in baseflow at HF1, HF2, and HFW1 is -32.8‰, -34.1‰, and -33.7‰ respectively (Table 10). The water sampled from three shallow groundwater wells at HF2 catchment shows no significant differences from baseflow (mean $\delta^{18}O$ signature of 6.1‰). The $\delta^{18}O$ signature of the spring located approximately 100 feet above HF2 flume is also very similar to baseflow: 6.2‰ versus 6.3‰. The mean of the $\delta^{18}O$ in UF1 and UF2 baseflow is -5.7‰ for both catchments. The $\delta^{18}O$ signature at three shallow groundwater wells at UF2 catchment ranged from -5.2‰ to -5.8‰. For these catchments we observed very little difference in $\delta^{18}O$ or δD values within

baseflow during growing and non-growing seasons (Table 11). There is a large variability in event rainfall isotopic signatures (Tables 9 and 10). However, the weighted averages of $\delta^{18}O$ and δD values within precipitation at HF and UF sites, -5.7‰ and -31.2‰, respectively, are similar to baseflows for the study period (-5.7‰ and -31.2‰).

Characterization of Electrical Conductivity

The EC of baseflow for HF1, HF2, and HFW1 sites was 45.4 µs/cm, 47.3 µs/cm, and 46.0 µs/cm respectively. The EC at UF1 (mean of 95.1 µs/cm) and UF2 (mean of 123.3 µs/cm) watersheds was significantly higher than at HF sites and displayed a more varied EC signal (Table 12). The EC of baseflow during growing season is higher than during non-growing, especially for UF catchments (Table 13). Rain typically showed a low EC due to its lack of contact with mineral soil. The mean rainfall EC concentrations were 13.2 µs/cm at HF sites and 11.0 µs/cm at UF sites (Table 12).

Isotope Hydrograph Separation

Out of the 23 storms for which stable isotope sampling was performed, four storms had good coverage of storm hydrograph and met the first assumption of IHS of a significant difference between isotopic signature of precipitation and baseflow (Table 14). For storms 3, 4, and 6, event water exhibited a heavier (less negative) δD and $\delta^{18}O$ signature than baseflow resulting in dilution of stream water during the storm. For storm 5 event water exhibited a lighter (more negative) δD and $\delta^{18}O$ than baseflow. Six additional storms that did not

separate with stable isotopes were analyzed using EC. As some catchments did not have data during these storms, IHS was performed on a total of 9 catchment-storm pairs. The ten storms differ in terms of rainfall maximum intensity, total precipitation, and AMCs. Table 15 shows where these individual storms map with respect to the rainfall characteristics, AMCs, ASI + precipitation threshold (identified in Figure 13), and tracer sampling availability and site coverage. The rainfall, storm hydrograph, and associated $\delta O^{18}$and δ D concentrations are presented by storm in Figures 24-31.

Table 16 summarizes results of the IHS for all 26 catchment-storm pairs. New water contributions ranged from 22% to 47% for HF1, 24% to 48% for HF2, and 22% to 52% for HFW1. Event water contributed a larger percent at UF catchments (43% -55% of streamflow at UF1 and 45%-75% at UF2).

Comparison of hydrograph separation using δD, δ^{18}O and EC is used here to evaluate the variability in IHS one can get using a variety of tracers. In all but one case, IHS using δD gave a smaller percent of event water contribution than δ^{18}O. Differences ranged from 1% to 8% in the event water estimate when comparing separation using δD or δ^{18}O (Table 16). Storm 3 was sampled for EC as well as δD and δ^{18}O. Figure 32 illustrates the differences in separation using all three tracers. The percent of new water contribution at HF2 and HF1 sites for this event is within 1-3 % of each other using δ^{18}O, δD, and EC (Table 16). Based on the results from storm 3, EC can be used as a tracer for HF catchments.

Differences in hydrograph separations using the bulk representation of rainfall and two mean approaches are shown in Table 17. Predictions using bulk rainfall, incremented

mean, and incremental intensity mean agree closely. The difference ranges from 0% to 5% in the event water estimate when comparing separation using bulk rainfall and two mean methods.

DISCUSSION

Characterization of Stable Isotope Signatures and Electrical Conductivity

In this study, there is no clear trend in isotopic signatures between winter and summer precipitation (Figure 33). Rose (1996) found that precipitation isotopic parameters varied randomly rather than in seasonal manner in the Falling Creek watershed in the southeastern Piedmont province of Georgia. The isotopic composition of rainfall was also quite variable (weighted monthly averages ranged from -1.2‰ to -7.1‰) in the small Piedmont watershed in Wenner et al. (1991) study.

The non-storm baseflow sampling showed $\delta^{18}O$ and δD values to be relatively constant through the data collection period (Tables 9 and 10). The mean δD and $\delta^{18}O$ values of groundwater are about -33±1‰ and -6.1±0.1‰ at HF sites and -31±0.5‰ and -5.7±0.2‰ at UF sites. The ^{18}O and D values obtained from shallow groundwater wells closely matched the baseflow (Tables 9 and 10). These values are also comparable to average precipitation (-31.1‰ and -5.7‰) and are consistent with established trends (mean $\delta^{18}O$ values from -4‰ to -8 ‰ for Piedmont and mean δD values from -20‰ to -40‰) (Kendall and Coplen, 2001). Although there is variability within the baseflow (1.4 -1.7 per mil difference in $\delta^{18}O$ and 4.7-7.4 per mil difference in δD at HF sites; 2.4-3.3 per mil difference in $\delta^{18}O$ and 13.8-14.0 per

mil difference in δD at UF sites), it shows no consistent seasonal trend. In the study by Rose (1996) located in the Falling Creek watershed in the southeastern Piedmont province of Georgia, baseflow became isotopically lighter by 2-3‰ during the non-growing season. However, Falling Creek is a much larger system (187 km^2), compared to 0.12-0.29 km^2catchments in our study. Wenner et al. (1991) found that the $\delta^{18}O$ of groundwater and baseflow in the perennial stream remained isotopically uniform (approximately -5.7‰) over the year at a 0.23 km^2 forested watershed in the Georgia Piedmont. In their study, the sampling of water from tension lysimeters showed that soil water was isotopically similar to waters in the saturated zone during the winter months but different during summer. They concluded that most groundwater recharge occurred during winter (wet) periods because any significant contribution of summer rainfall to groundwater should produce more variable isotopic signature in the saturated zone.

The EC of baseflow for HF sites was lower than at UF sites (mean EC of 46±1.3 μs/cm at HF sites, 95.1 μs/cm at UF1 and 123.3 μs/cm at UF2.) The differences in soils of UF sites and longer contact due to lower slopes and relief are most likely responsible for high EC concentrations. The EC of baseflow during growing season is higher than during non-growing, especially for UF catchments (Table 13). The mean rainfall EC concentrations were 13.2 μs/cm at HF sites and 11.0 μs/cm at UF sites (Table 12).Increasing concentrations suggest that mean residence time of streamflow is increasing during dryer summers as groundwater storage is depleted.

Isotope Hydrograph Separation

The percent of new water delivery observed at three HF catchments ranged from 22% to 52% and from 43% to 75% at two UF catchments (Table 16). No trends in the percent of new water delivery were observed for dry versus wet AMCs or above versus below the ASI + precipitation threshold. However, all five catchments had the larger range of new water delivery for the storms below ASI + precipitation threshold (25-39% above threshold and 29-52% below at HF catchments, 45-66% above and 43-75% below at UF catchments). All five catchments had the highest event water contribution for the storms below ASI + precipitation threshold as well (storm 3 for HF catchments and storm for 2 UF catchments). A linear regression for HF catchments suggests that for the events above ASI + precipitation threshold the total volume of rainfall influence the percent of new water delivered to the stream (R^2=0.97) while for the events below threshold the maximum rainfall intensity is more important in partitioning the water (R^2=0.78).

Brown et al (1999) and James and Roulet (2009) observed high event water contributions during dry conditions. They concluded that rapid shallow flow component is a major component of runoff generation during high intensity summer storms under dry AMCs. Another important component during dry AMCs is overland flow from riparian zone. To further explain the event water contributions, hydrometric measurements such as shallow groundwater well response and soil moisture response are examined in Figures 34 through 37.

Figure 34 illustrates the storm during dry AMCs and below ASI + precipitation threshold (storm 3, 26 mm) at HF catchments. Shallow groundwater wells in the riparian zone (wells 1, 2, and 3) responded rapidly (within 0.5 hours) to rainfall at HF catchments. Well 4 which is above the perennial reach of the stream channel remained dry. The groundwater in the riparian wells 2 and 3 came very close to the surface suggesting overland flow is possible there. During this event a small volume of runoff occurred rapidly, there is a lag time of 0.5 hours between center of mass of rainfall and the peak flow. The soil moisture and shallow groundwater tables lagged behind the peak stormflow. The rain event of 26 mm resulted in 0.32, 0.39, and 0.37 mm of total flow at HF1, HF2, and HFW1 catchments respectively and runoff ratio of 0.01 for all three catchments. The small stormflow volume and runoff ratio suggest that there is a lot of storage available for incoming water on the hillslopes. During these dry AMCs, the wetting front has not percolated to the depth of 90 cm, which remains unsaturated through the entire event. The low runoff ratio derived from this storm with dry AMCs is likely due to overland flow or shallow subsurface flow from the riparian zone which is prone to saturation and rapid response. For the HF catchments, almost half of streamflow during this storm is new water (45-52%).

Figure 35 demonstrates the response of UF catchments to the same event. The rain event of 18.2 mm resulted in 0.08 and 0.03 mm of total flow at UF1 and UF2 catchments respectively and runoff ratio of 0.002 and 0.001. Well 2 which is the most upstream riparian well in the UF2 catchment responded the most to this rain event. At this well no perched water table was observed for the duration of the study. Soil moisture observations reveal that

wetting front has not percolated to the depth of 50 and 90 cm, which remain unsaturated through the entire event. A high event-water contribution (55% at UF1 and 75% at UF2 catchments) could be explained by the development of perched saturation in shallow soil horizon due to differences in saturated hydraulic conductivity between the top organic layer and the impeding clay layer.

Hydrograph separation results indicate that event water contributes a larger percent to stormflow at UF catchments than at HF catchments for both events occurring above and below threshold (Table 16). Figure 36 demonstrates the response of HF catchments to storm 7 on wet AMCs and where ASI+ precipitation is above threshold. The total precipitation of 44.6 mm produced 5.02 mm of total flow at HF1 catchment , 7.61 mm of total flow at HFW1 catchment and runoff ratio of 0.06 and 0.08. All four wells showed significant increase in maximum groundwater levels and the response was fairly synchronized. Water table in riparian wells 1, 2, and 3 came to or close to ground surface; well 4 was active during this event. The soil moisture at all four depths on the hillslope responded to the rain event which serves as evidence that hillslopes are more connected by the fact that they are showing saturation and response at a range of depths. It can be inferred that hillslope contributions is greater for this event in contrast to a previously discussed storm (3) because soil moisture (except 90 cm depth) and groundwater tables peaked before stormflow and started to release water once the threshold of ASI+ precipitation is exceeded. For this event the pre-event water was the major contributor to stormflow (65% at HF2 and 75% at HFW1 catchments). Sidle et al. (2000) revealed that hillslope areas tend to respond differently depending on AMCs in

the steep forested headwater catchment in Japan. During dry AMCs, saturated overland flow from riparian zones was a major contributor to stormflow, while during wet AMCs subsurface flow from hillslopes dominated the hydrograph.

The response of UF catchments to storm 7 on wet AMCs and ASI+ precipitation above threshold is shown in Figure 37. The rainfall of 31 mm produced 8.03 mm and 13.72 mm of total flow at UF1 and UF2 catchments respectively resulting in runoff ratio of 0.26 and 0.39l; the runoff ratios are approximately 4 times larger at UF sites than at HF sites for the same event. The maximum water table in riparian well 1 was above ground surface. The soil moisture at 25, 50 and 90 cm has not increased during the rain event and the maximum water table elevation at well 3 located near the soil moisture probes rose to 7 cm below the ground indicating that soil at 25, 50 and 90 cm was at or near saturation, while at HF2 site only soil moisture at the depth of 80 cm remains saturated (Figures 36 and 37). This suggests that UF2 has a larger saturated area during non-growing season and these saturated areas are connected by subsurface flow. One explanation for large increase in stormflow during wet AMCs at UF sites is the development of overland flow and rapid subsurface flow in shallow soil horizon above the low permeability clay layer. UF catchments are more prone to perching water tables above the expanding clay layer illustrated in Figure 37 by soil moisture probe response at 12 cm. The development of both overland flow and shallow subsurface flow is promoted by transmissivity feedback. The transmissivity feedback concept refers to the condition in which saturation develops from a lower boundary upwards and enters soil of higher hydraulic conductivity (Kendall et al, 1999). When the water table rises above the clay

layer it enters soil profile with higher hydraulic conductivity, which increases stormflow rates. Both overland flow and shallow subsurface flow can contribute strong new water components.

CONCLUSION

Results from this study showed that new/old water delivery is a complex process due to level of interaction between soil properties, antecedent moisture conditions, and storm size and intensity. Analysis of summer storms indicate that event water is a significant component (with examples of up to half or more of streamflow being new water) of summer storm hydrographs for both sites (Table 16). The event water contribution was highest during dry AMCs and was a strong function of maximum rainfall intensity. The partitioning of event/pre-event water had a smaller variability during wet AMCs than during dry conditions at HF sites and total rainfall volume influenced the most the percent of new water delivered to the stream. Comparing the bulk rainfall to the temporally variable representation of event rainfall, the hydrograph separations using stable isotopes are fairly similar (Table 17). The influence of isotope selection on the percent of new water contribution (δD vs. δ^{18}O) was more pronounced (the difference of 1%-12%) (Table 16). The hydrograph separation indicates that event water contributes a larger percent to stormflow at UF catchments than at HF catchments for both events occurring above and below threshold which is consistent with higher runoff ratios discussed in Chapter 1. The number of storms for which stable isotope analysis is available provides a limited study on the range of new water delivery across

different AMCs and rainfall characteristics. More information on rainfall, soil, groundwater and stream chemistry, is required to identify runoff generation mechanisms and flowpaths.

CHAPTER 2 TABLES AND FIGURES

Table 9. Summary statistics of $\delta^{18}O$ for different water types (all values in units of permil (‰) except for n)

Water type	n	Mean	Variance	Std. Dev.	Std. Err.	Median	Range	Min	Max
Precipitation HF	29	-5.10	11.33	3.37	0.62	-4.12	13.35	-13.43	-0.08
HF2 Spring	17	-6.25	0.07	0.27	0.07	-6.25	1.06	-6.82	-5.76
Baseflow HF1	32	-6.00	0.10	0.32	0.06	-5.92	1.42	-6.57	-5.15
Baseflow HF2	34	-6.18	0.10	0.32	0.05	-6.21	1.68	-6.81	-5.13
Baseflow HFW1	30	-6.10	0.07	0.27	0.05	-6.13	1.49	-6.74	-5.25
Wells HF2	8	-6.09	0.25	0.50	0.18	-6.29	1.54	-6.56	-5.02
Precipitation UF	27	-4.84	9.07	3.01	0.58	-4.70	12.19	-11.49	0.70
Baseflow UF1	29	-5.66	0.48	0.69	0.13	-5.69	3.30	-6.99	-3.69
Baseflow UF2	31	-5.69	0.36	0.60	0.11	-5.50	2.45	-7.27	-4.82
Wells UF2	7	-5.54	0.28	0.52	0.20	-5.58	1.63	-6.09	-4.46

Table 10. Summary statistics of δD for different water types (all values in units of permil (‰) except for n)

Column	n	Mean	Variance	Std. Dev.	Std. Err.	Median	Range	Min	Max
Precipitation HF	29	-26.90	697.41	26.41	4.90	-17.40	100.40	-93.50	6.90
HF2 Spring	17	-34.58	2.16	1.47	0.36	-35.10	5.82	-36.54	-30.72
Baseflow HF1	32	-32.77	1.74	1.32	0.23	-32.50	5.20	-35.00	-29.80
Baseflow HF2	34	-34.09	1.56	1.25	0.21	-34.20	7.45	-36.85	-29.40
Baseflow HFW1	30	-33.75	1.19	1.09	0.20	-33.70	4.68	-35.50	-30.83
Wells HF2	8	-32.20	8.95	2.99	1.06	-32.45	8.50	-35.40	-26.90
Precipitation UF	27	-24.50	538.88	23.21	4.47	-20.60	92.80	-83.60	9.20
Baseflow UF1	29	-30.78	10.19	3.19	0.59	-30.70	13.80	-38.40	-24.60
Baseflow UF2	31	-30.94	11.40	3.38	0.61	-30.45	14.00	-39.20	-25.20
Wells UF2	7	-30.53	3.50	1.87	0.71	-30.00	5.10	-32.70	-27.60

Table 11. Mean baseflow $\delta^{18}O$ and δD values for growing and non-growing seasons

	Catchment									
	HF1		HF2		HFW1		UF1		UF2	
Season	$\delta^{18}O$	δD	$\delta^{18}O$	δD	$\delta^{18}O$	δD	$\delta^{18}O$	δD	$\delta^{18}O$	δD
Growing	-6.01	-32.64	-6.25	-34.22	-6.18	-33.85	-5.51	-30.22	-5.54	-30.21
Non-growing	-5.99	-32.92	-6.13	-33.99	-6.03	-33.67	-5.8	-31.29	-5.83	-31.63

Table 12. Summary statistics of EC for different water types (all values in units of µs/cm, except for n)

Column	**n**	**Mean**	**Variance**	**Std. Dev.**	**Std. Err.**	**Median**	**Range**	**Min**	**Max**
Precipitation HF	20	13.2	54.2	7.4	1.6	11.1	31.1	6.3	37.4
Baseflow HF1	21	45.4	67.6	8.2	1.8	44.8	32.5	32.0	64.5
Baseflow HF2	22	47.3	14.8	3.8	0.8	46.9	15.3	40.0	55.3
Baseflow HFW1	13	46.0	33.9	5.8	1.6	46.3	23.4	36.8	60.2
Precipitation UF	15	11.0	18.0	4.2	1.1	11.2	13.2	4.3	17.5
Baseflow UF1	22	95.1	1111.2	33.3	7.1	89.7	117.8	44.1	161.9
Baseflow UF2	21	123.3	2553.3	50.5	11.0	116.8	150.6	49.3	199.9

Table 13. Mean baseflow EC values for growing and non-growing seasons

	Catchment				
	HF1	HF2	HFW1	UF1	UF2
Season					
Growing	49.9	49.0	49.1	114.8	155.8
Non-growing	38.1	44.3	40.9	60.7	70.4

Table 14. δD and $\delta^{18}O$ isotopic compositions (per mil) of new and old waters

Storm number		3	4	5	6
Date		7/17/09	7/30/09	9/7/09	9/16/09
New Water	δD	-15.3	-15.9	-84.3	-11.3
	$\delta^{18}O$	-3.6	-3.2	-11.8	-3.0
Spatial Std. Deviation	δD	2.2	2	8.2	1.7
	$\delta^{18}O$	0.4	0.2	1.0	0.6
Old Water	δD	-33.8	-33.5	-32.7	-32.1
	$\delta^{18}O$	-6.1	-6.1	-5.9	6.2
Spatial Std. Deviation	δD	0.6	1.0	2.2	1.4
	$\delta^{18}O$	0.2	0.2	0.5	0.2
New-Old Difference	δD	18.5	17.6	51.6	20.8
	$\delta^{18}O$	2.5	2.9	5.9	3.2

Table 15. Storm characteristics, AMCs and threshold status for 10 storms. Shading highlights storms for which ASI + precipitation index is above catchment thresholds indicated in Figure 13

	Storm number	**1**	**2**	**3**	**4**	**5**	**6**	**7**	**8**	**9**	**10**
	Date	3/15/09	7/5/09	7/17/09	7/30/09	9/7/09	9/16/09	1/17/10	3/13/10	3/28/10	5/15/10
	Julian day	74	186	198	211	250	260	17	72	88	136
HF	Total rain (mm)	50.2	31.4	26	15.4	21.8	8.8	31	18	44.6	12
	Max rain intensity (mm/15 minute)	1.6	6.6	20.4	6.8	3	0.8	1.8	3.8	8.6	2
	AMCs (ASI in mm)	231 (wet)	172 (dry)	181 (dry)	195 (dry)	159 (dry)	187 (dry)	228 (wet)	223 (wet)	259 (wet)	191 (dry)
	ASI+precip (mm)	305	203	207	210	181	196	259	241	303	176
	Threshold status	above	below	below	below	below	below	above	below	above	below
HF1	Tracer	EC	EC	EC, δD, $\delta^{18}O$	δD, $\delta^{18}O$					EC	
HF2		EC	EC	EC, δD, $\delta^{18}O$	δD, $\delta^{18}O$	δD, $\delta^{18}O$	δD, $\delta^{18}O$	EC			
HFW1					δD, $\delta^{18}O$	δD, $\delta^{18}O$		EC		EC	
UF	Total rain (mm)	52.2	60.4	18.2		26.4		31	37.6	25.2	29.2
	Max rain intensity (mm/15 min)	2	18	5.2		3.6		2.2	4	3.6	9.6
	AMCs (ASI in mm)	337	160	197		166		303	306	303	174
	ASI+precip (mm)	390 (wet)	220 (dry)	215 (dry)		192 (dry)		334 (wet)	344 (wet)	329 (wet)	204 (dry)
	Threshold status	above	below	below		below		above	above	above	below
UF1	Tracer		EC						EC	EC	EC
UF2		EC	EC							EC	EC

Table 16. Percent new water estimated by IHS using $\delta^{18}O$, δD and EC for a total of 26 storm-catchment pairs. Shading highlights storms for which ASI + precipitation index is above catchment thresholds

Storm number	Date	Tracer	HF1	HF2	HFW1	UF1	UF2	Threshold status
1	3/15/09	EC	35	39	37		50	above
2	7/5/09	EC	36	34		55	75	below
3	7/17/09	$\delta^{18}O$ δD EC	47±27 46±23 48	45± 39 48±28 47	52±28 45±26			below
4	7/30/09	$\delta^{18}O$ δD	30±19 22±16	36 ±15 33±15	23±16 22±12			below
5	9/7/09	$\delta^{18}O$ δD		39±22 35±19	33±21 31±17			below
6	9/16/09	$\delta^{18}O$ δD		29±19 24±6				below
7	1/17/10	EC		35	25			above
8	3/13/10	EC				45		above
9	3/28/10	EC	35		37	50	66	above
10	5/15/10	EC				43	45	below

Table 17. Percent of event water component estimated using bulk rainfall, incremental mean, and incremental intensity mean methods

Storm number	Date	Method	HF1		HF2		HFW1	
			O^{18}	D	O^{18}	D	O^{18}	D
3	7/17/2009	Bulk	47	46	45	48	52	45
		Incr mean	45	45	43	47	49	44
		Incr intensity						
4	7/30/2009	bulk	30	22	36	33	23	22
		incr mean	29	21	35	32	22	22
		incr intensity	30	23	36	33	23	23
5	9/7/2009	bulk			39	34	33	30
		incr mean			36	32	30	28
		incr intensity			33	29	28	25
6	9/16/2009	bulk			29	22		
		incr mean			31	24		
		incr intensity			33	24		

a) b)

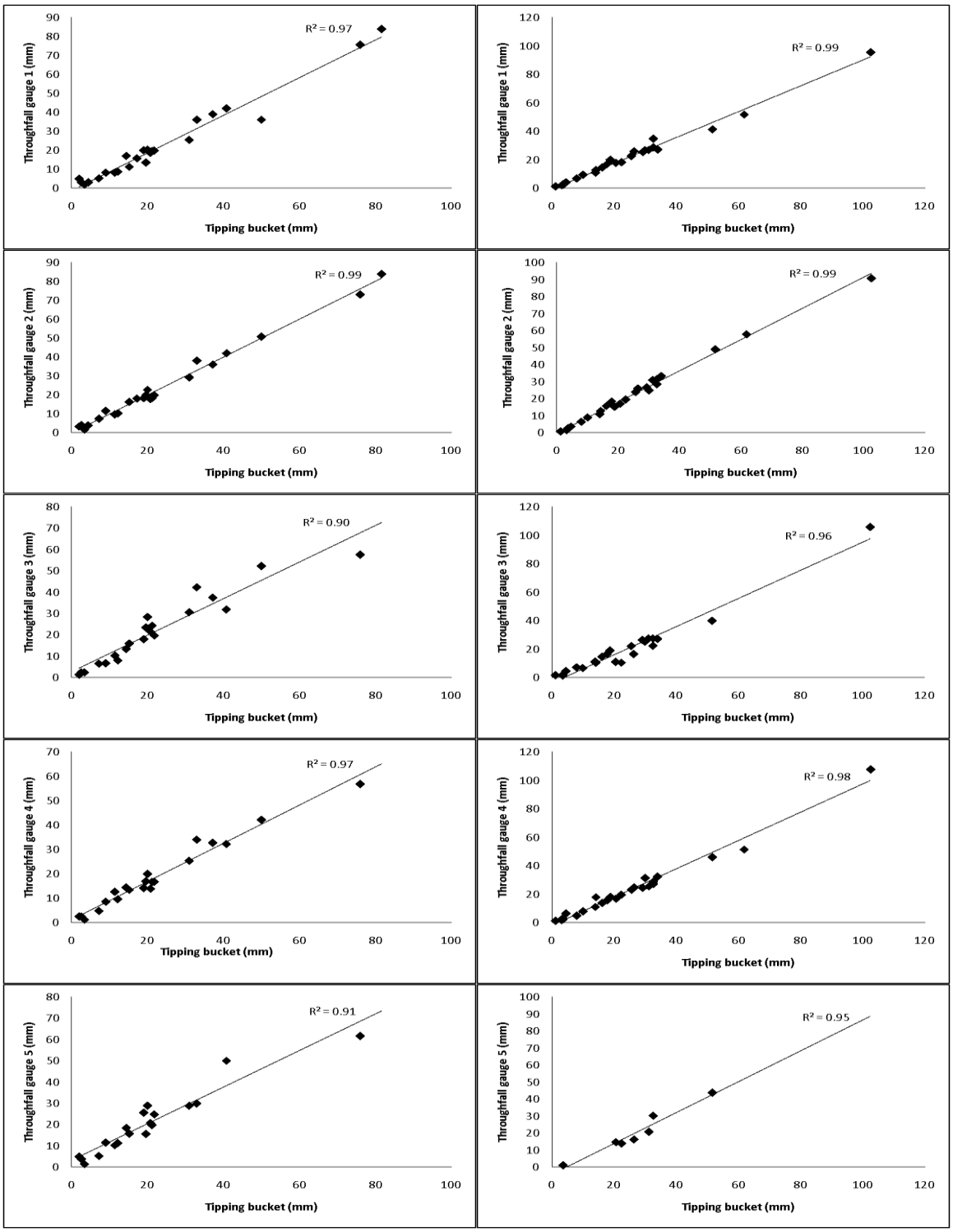

Figure 19. The relationship between rainfall collected by the tipping bucket and throughfall gauges at HF2 site (a) and UF2 site (b)

Figure 20. Sequential rain sampler built and laboratory tested prior to field installation by Y. Kuntukova.

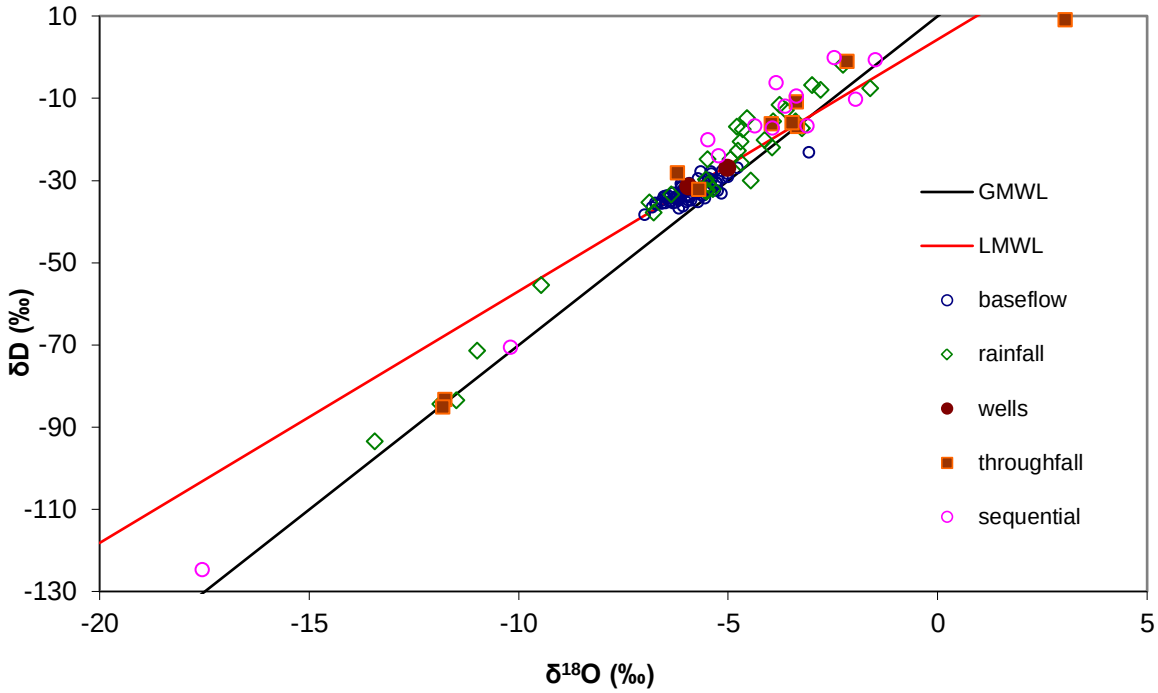

Figure 21. Stable isotope signatures ($\delta^{18}O$ vs. δD) for all water types and sites

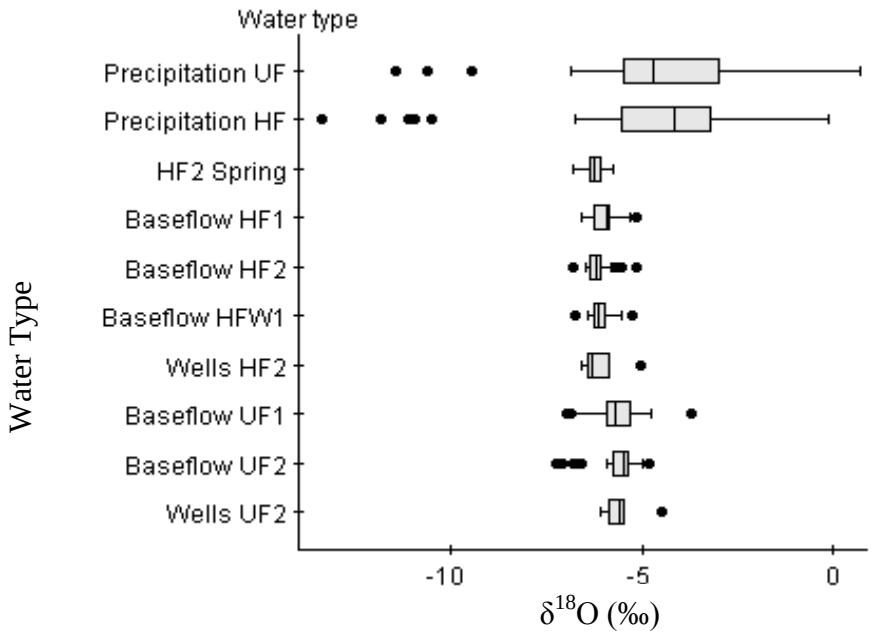

Figure 22. Box-and-whisker plot showing the range of $\delta^{18}O$ values for different water types

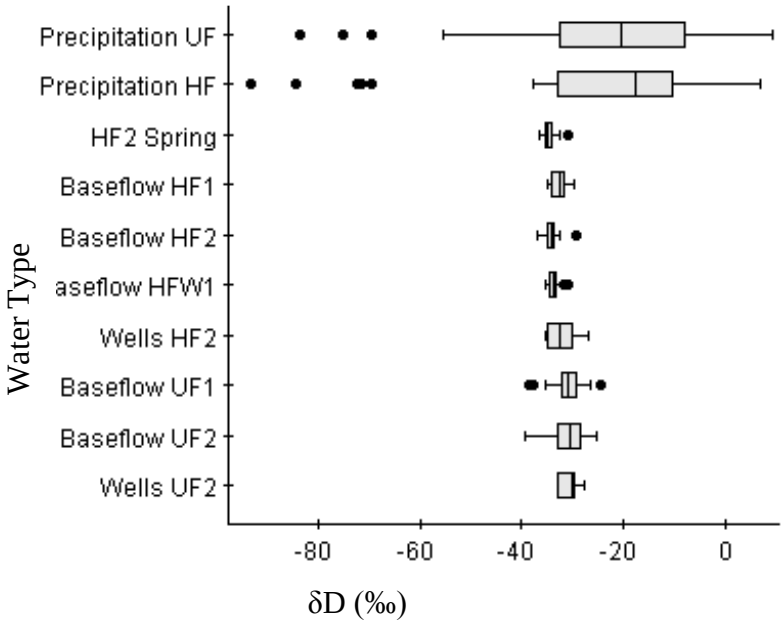

Figure 23. Box-and-whisker plot showing the range of δD values for different water types

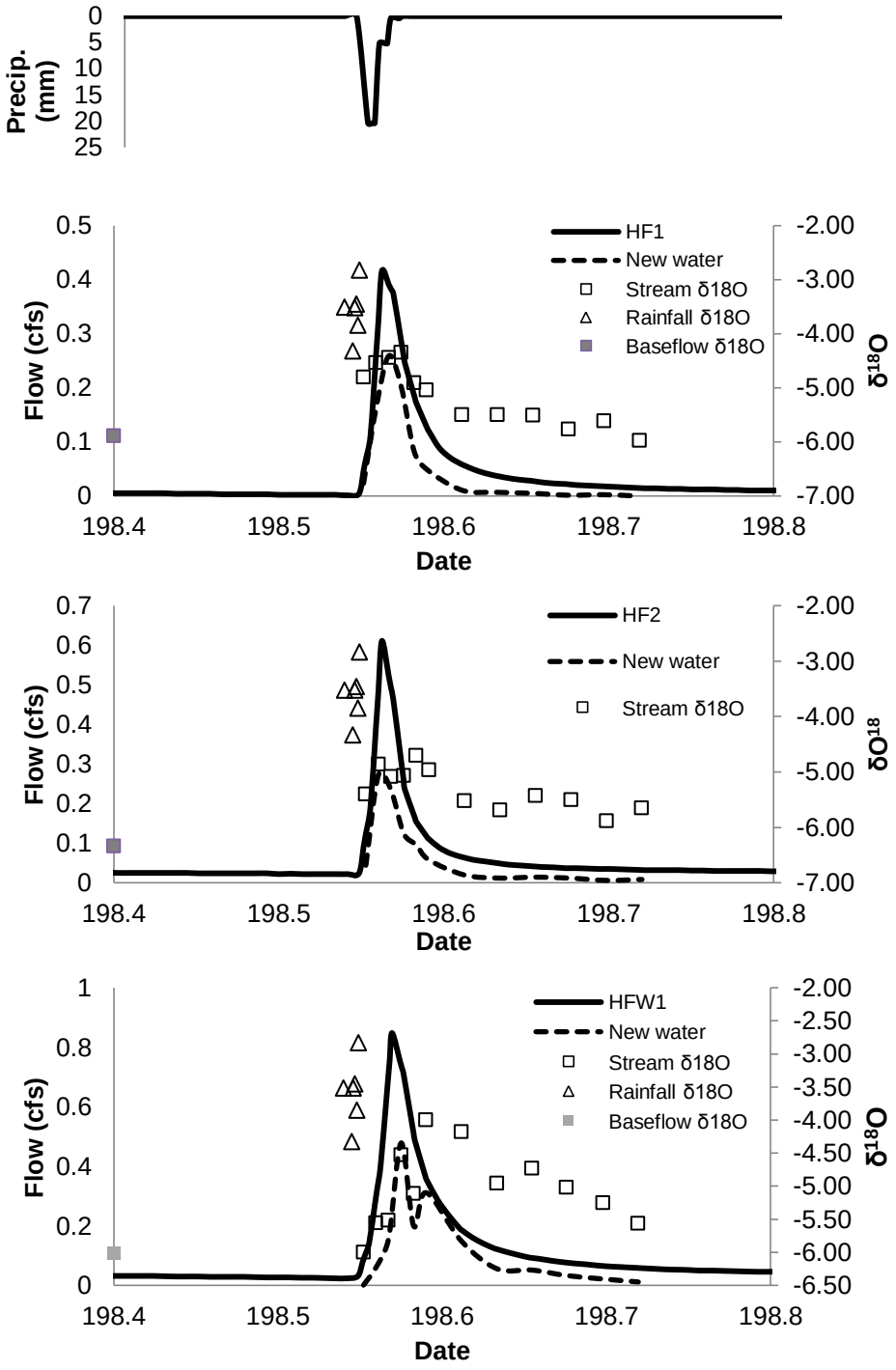

Figure 24. Rainfall, stormflow, and associated $\delta^{18}O$ concentrations for storm 3 (7/17/2009)

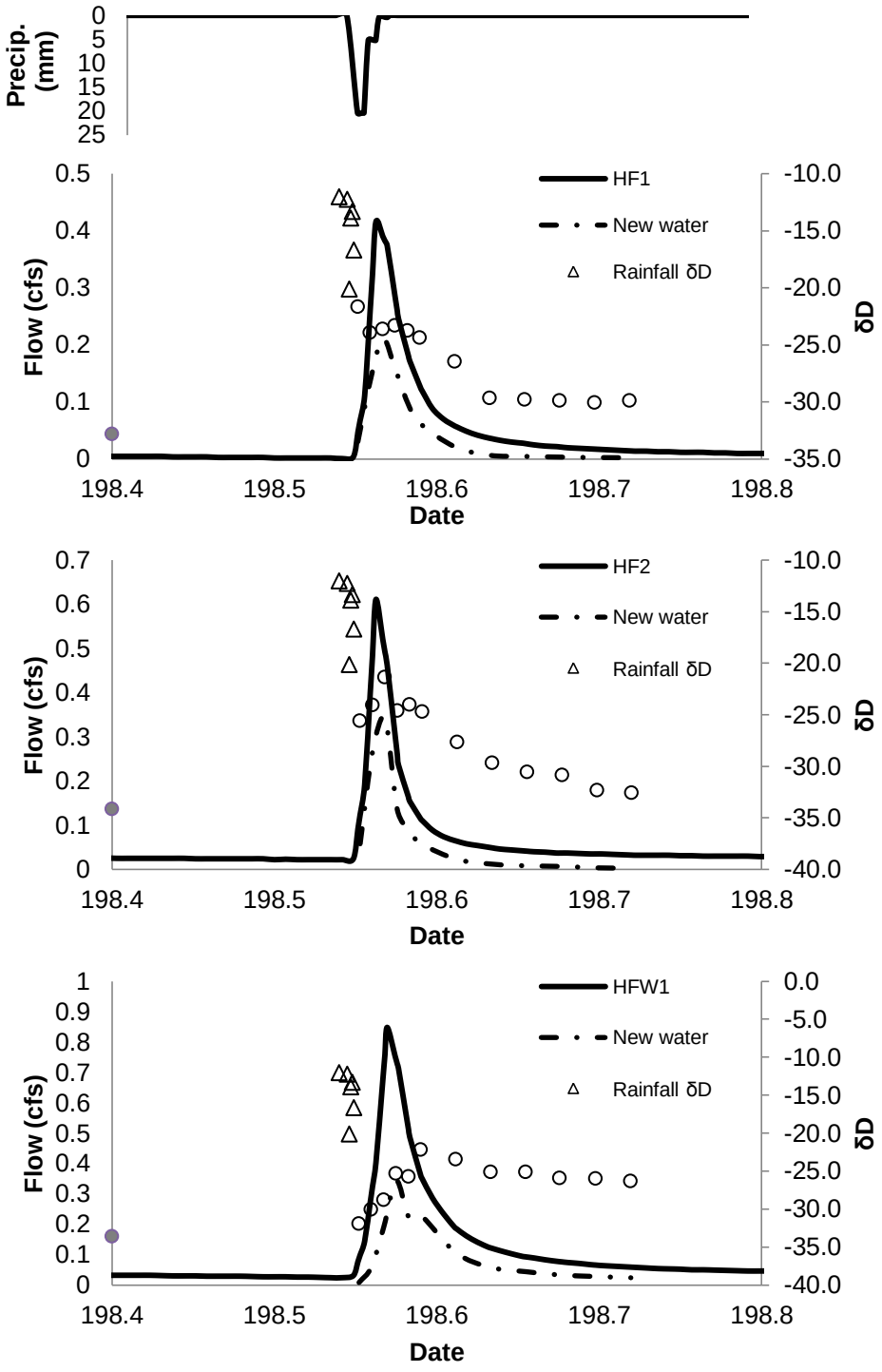

Figure 25. Rainfall, stormflow, and associated δD concentrations for storm 3 (7/17/2009)

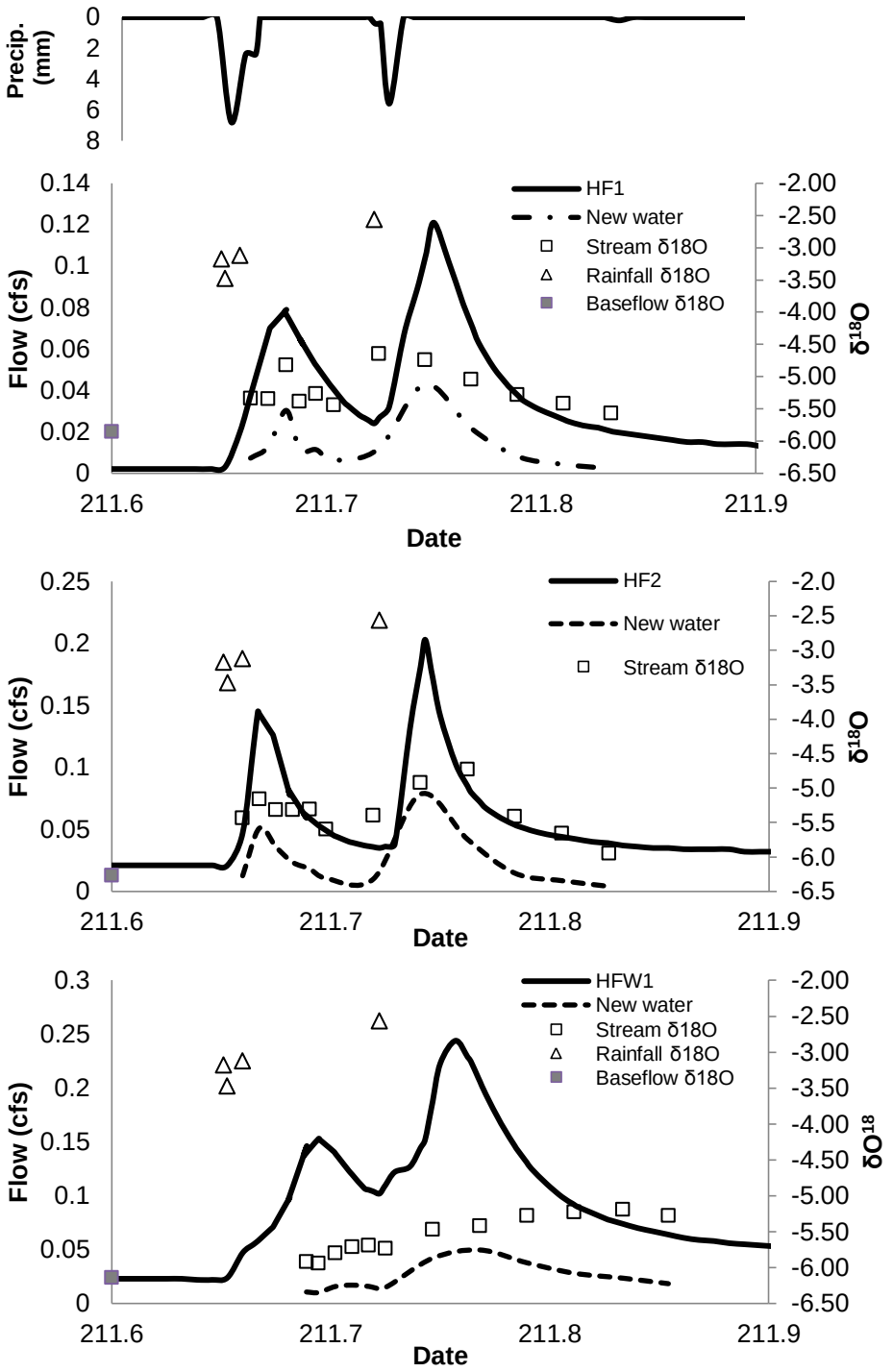

Figure 26. Rainfall, stormflow, and associated $\delta^{18}O$ concentrations for storm 4 (7/30/2009)

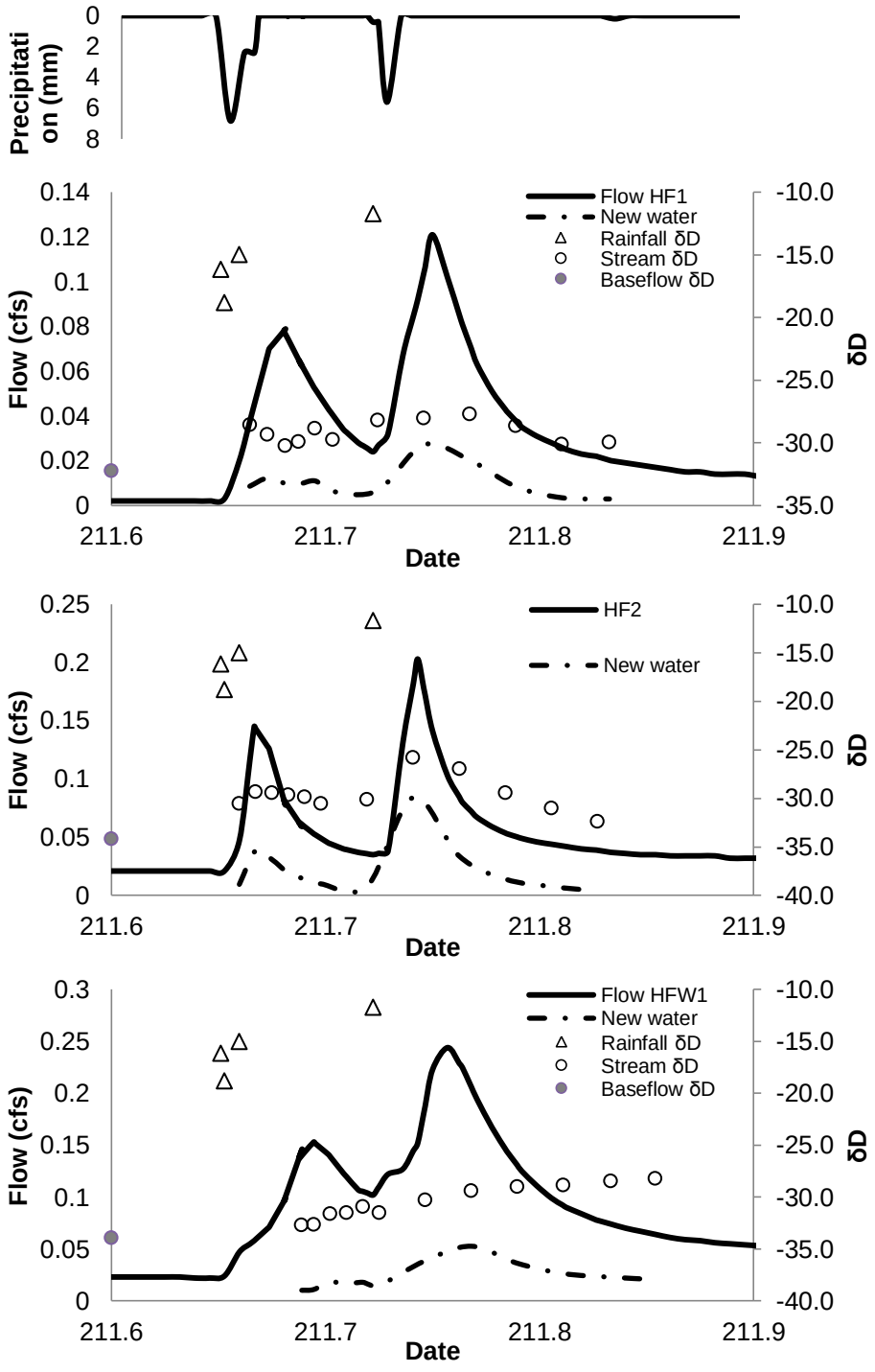

Figure 27. Rainfall, stormflow, and associated δD concentrations for storm 4 (7/30/2009)

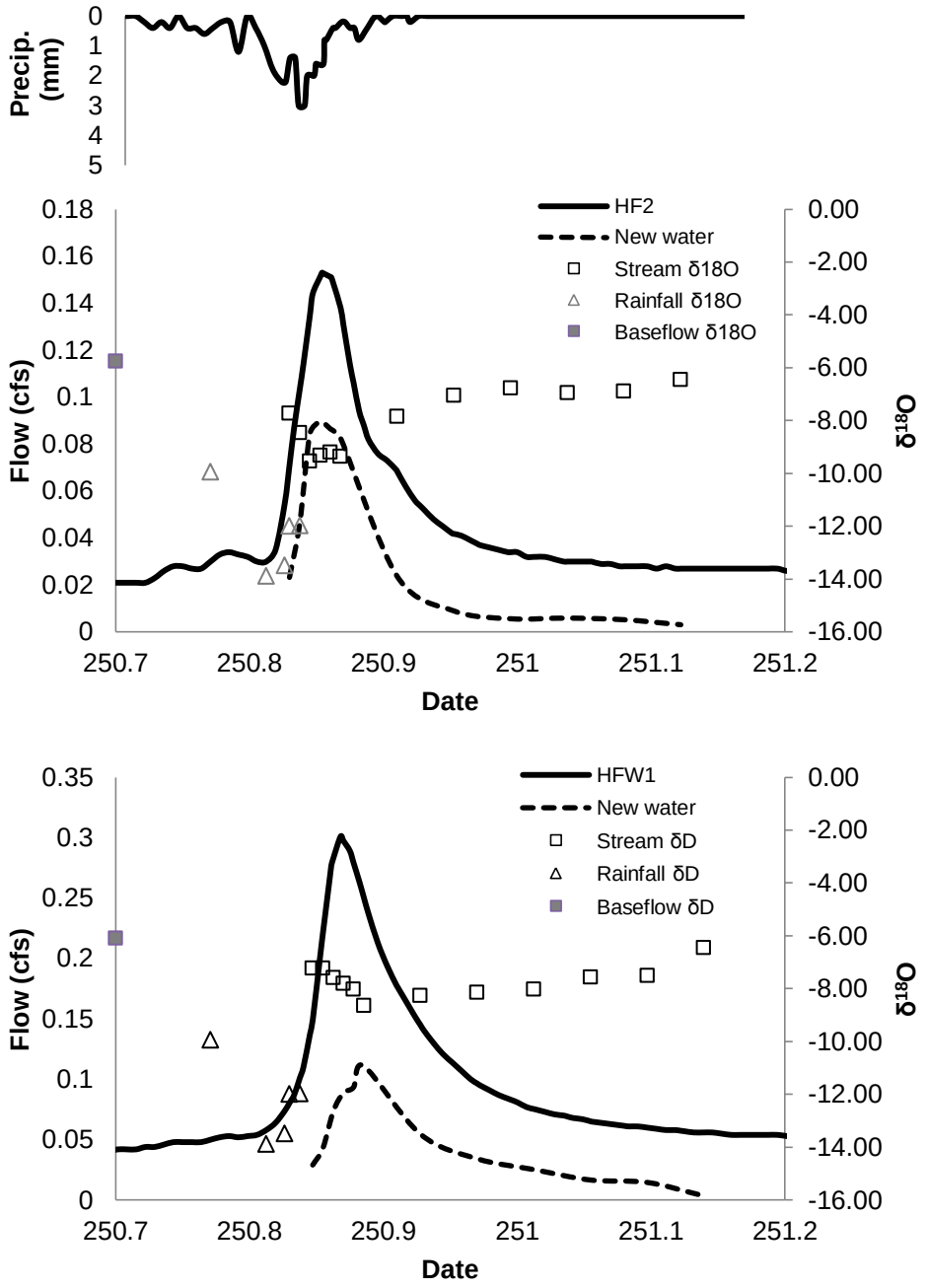

Figure 28. Rainfall, stormflow, and associated $\delta^{18}O$ concentrations for storm 5 (9/7/2009)

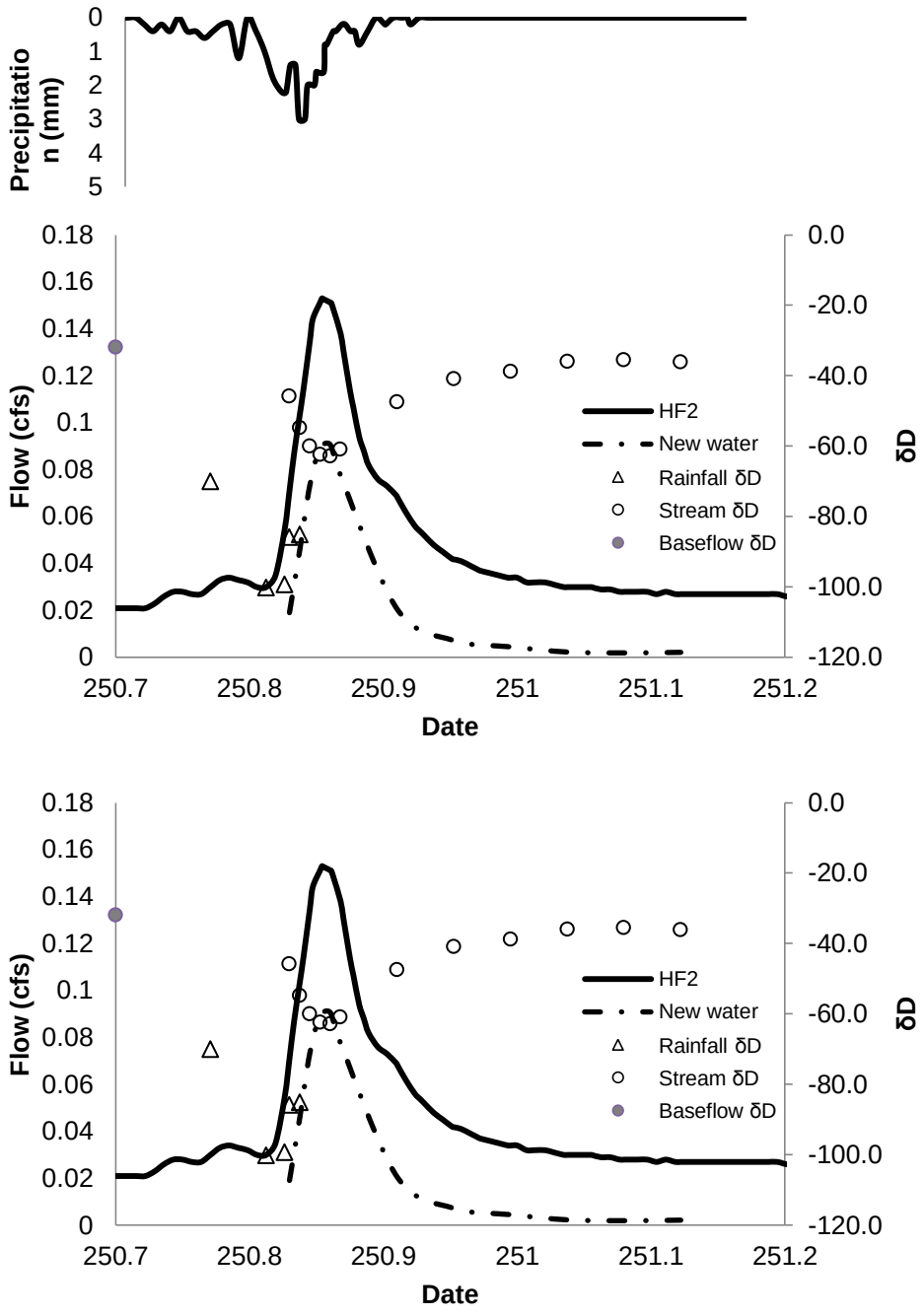

Figure 29. Rainfall, stormflow, and associated δD concentrations for storm 5 (9/7/2009)

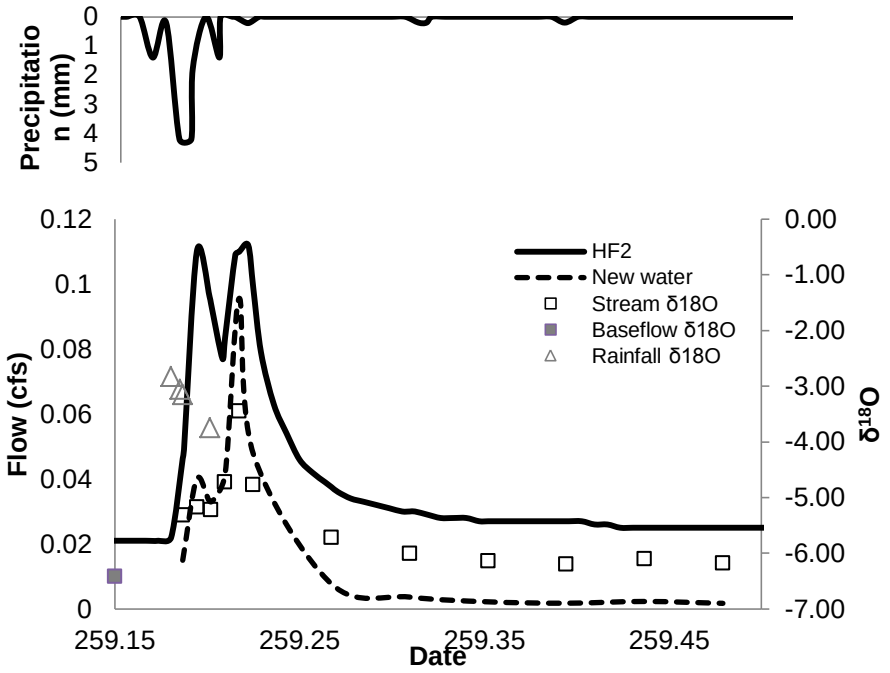

Figure 30. Rainfall, stormflow, and associated $\delta^{18}O$ signatures for storm 6 (9/16/2009)

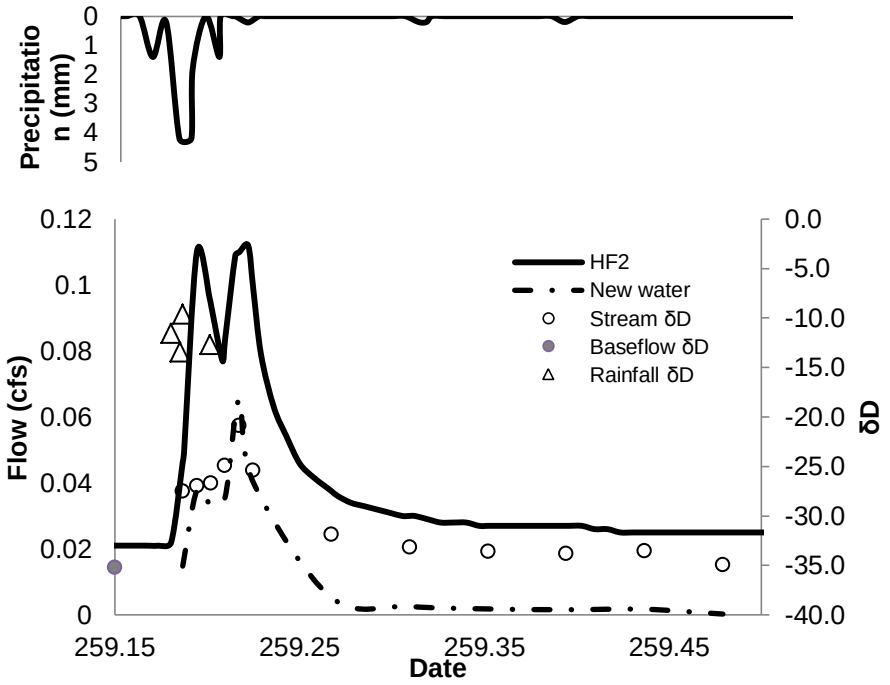

Figure 31. Rainfall, stormflow, and associated δD signatures for storm 6 (9/16/2009)

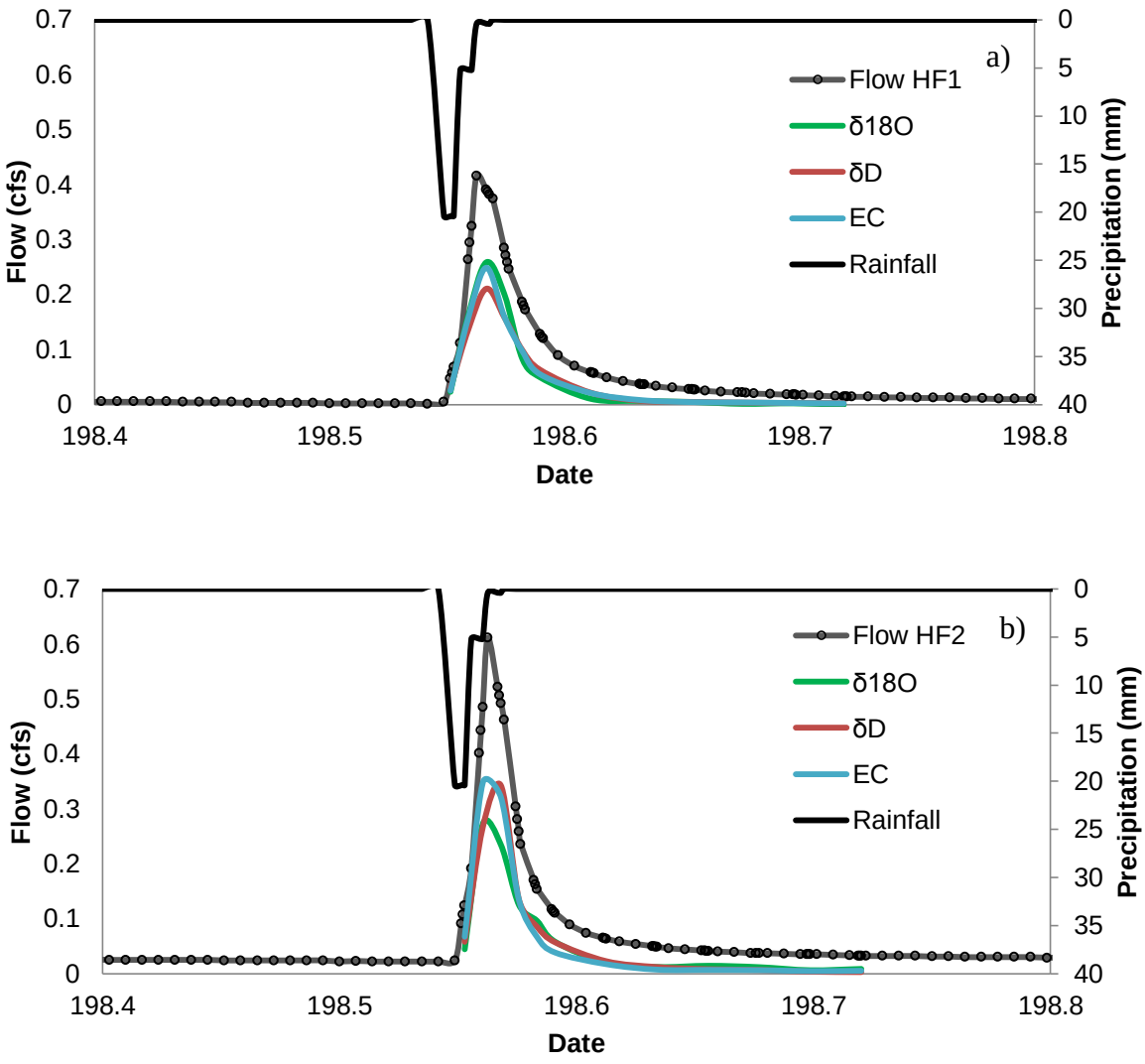

Figure 32. Differences in two-component hydrograph separation (new water contributions to streamflow) using $\delta^{18}O$, δD, and EC for storm 3 (7/17/2009) at HF1 catchment (a) and HF2 catchment (b)

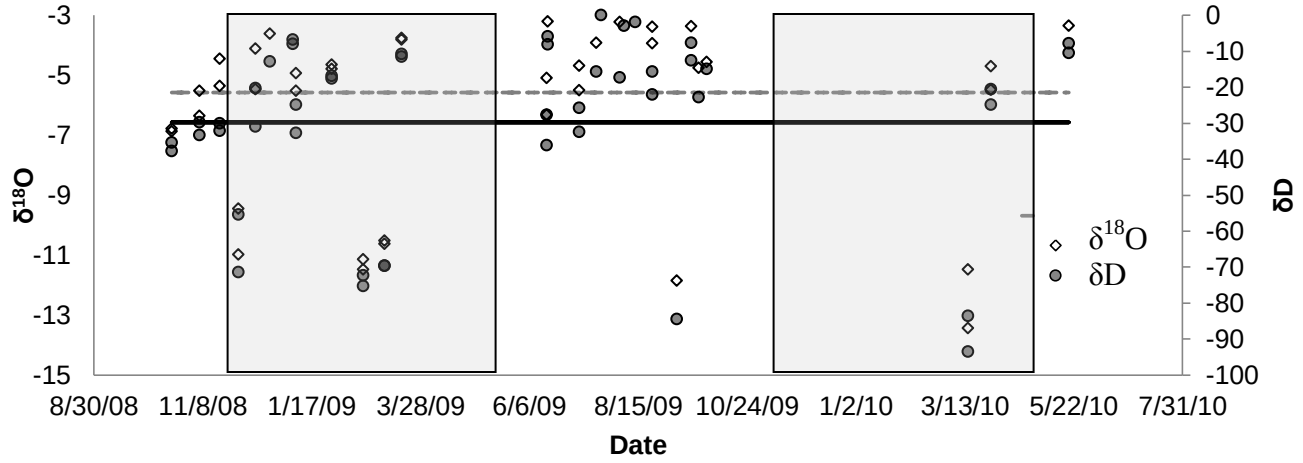

Figure 33. Time series of $\delta^{18}O$ and δD values for precipitation for the study period. The solid line is average δD signature; the dashed line is average $\delta^{18}O$ signature. Growing period is shaded

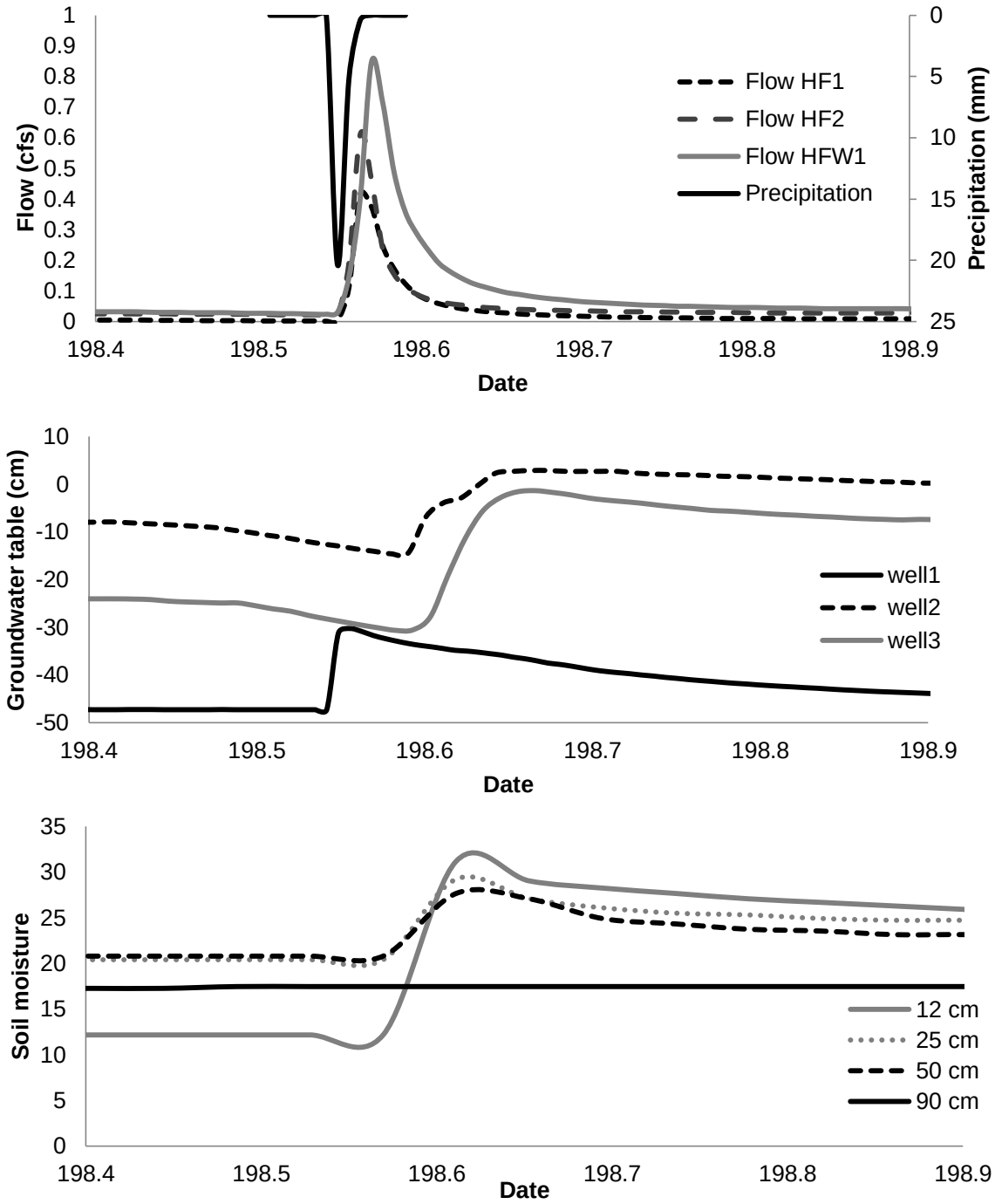

Figure 34. Runoff, groundwater wells and soil moisture response of HF catchments to an event 3 (7/17/2009)

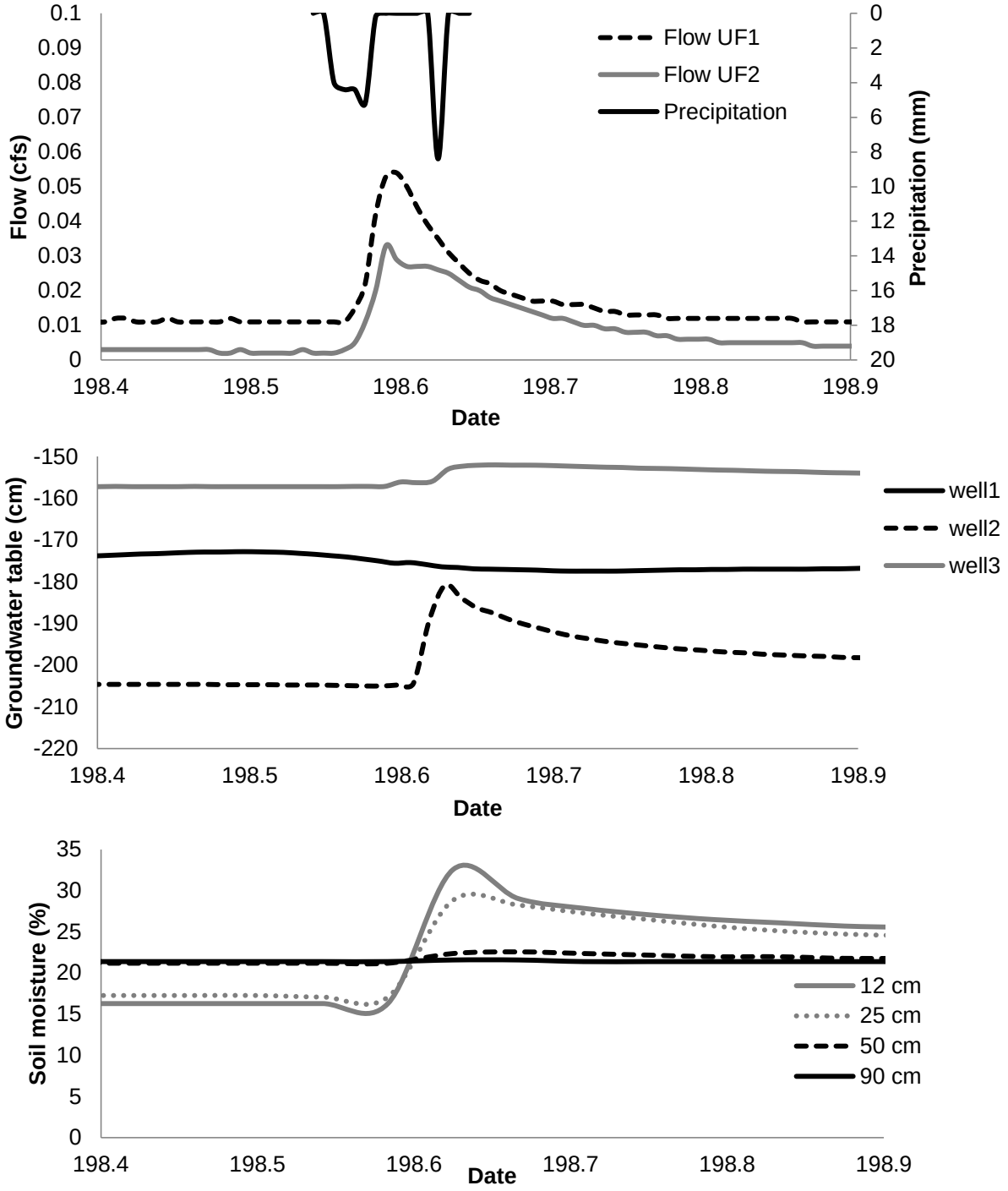

Figure 35. Runoff, groundwater wells and soil moisture response of UF catchments to an event 3 (7/17/2009)

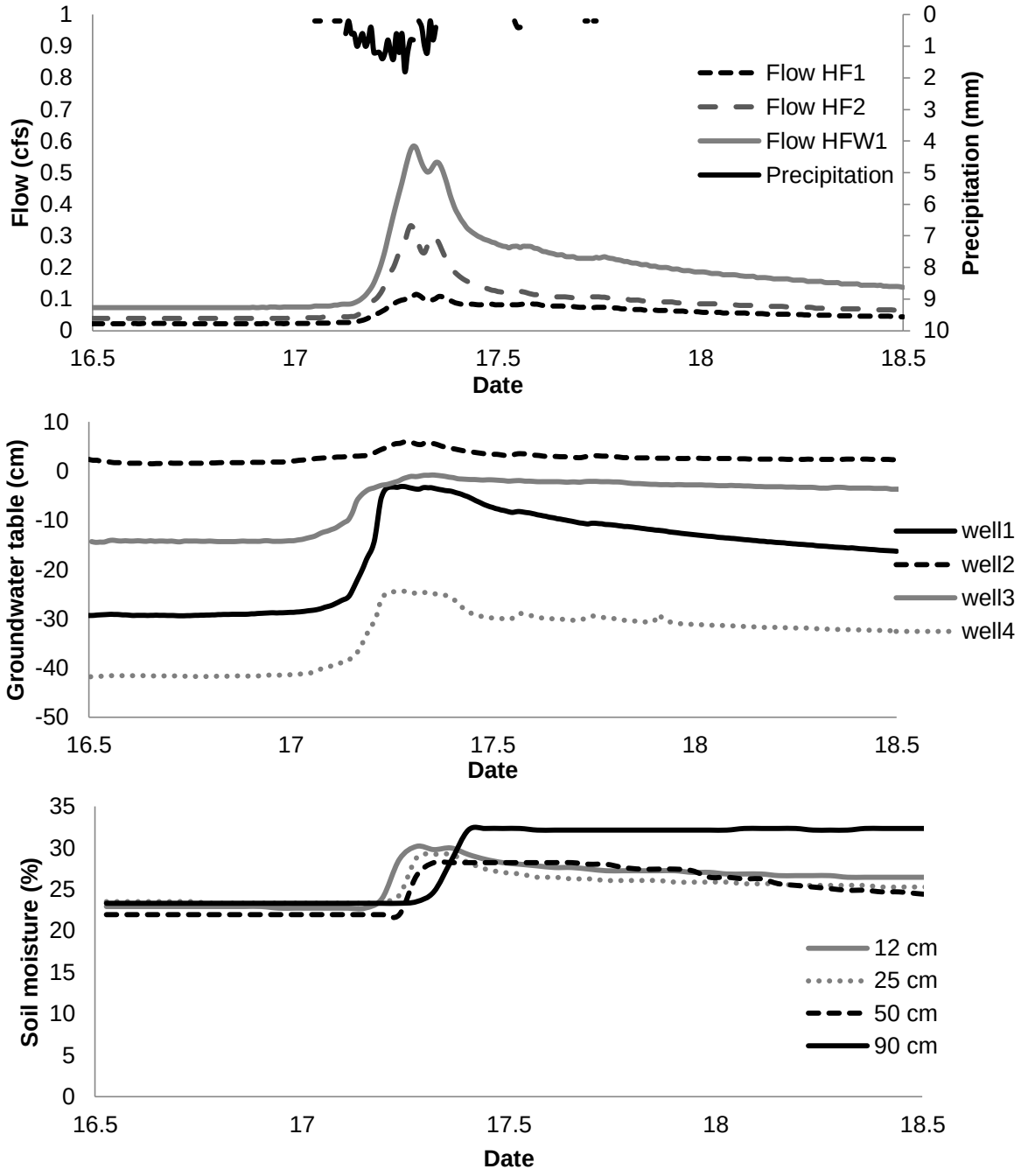

Figure 36. Runoff, groundwater wells and soil moisture response of HF catchments to an event 7 (1/17/2010)

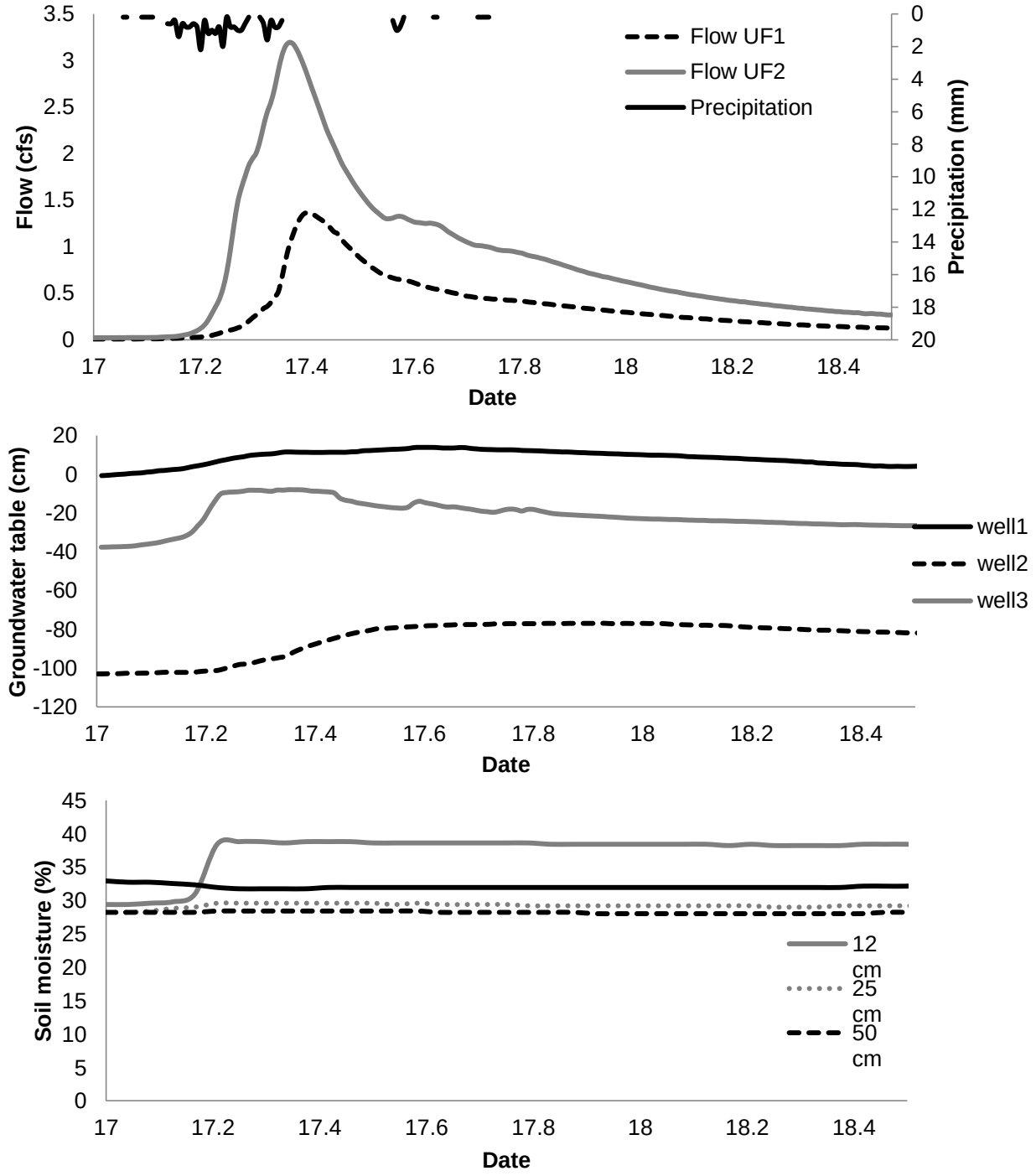

Figure 37. Runoff, groundwater wells and soil moisture response of UF catchments to an event 7 (1/17/2010)

REFERENCES

Abdul, A.S. and R.W. Gillham. (1989). Field studies of the effects of the capillary fringe on streamflow generation. *Journal of Hydrology,* 112: 1-18.

Allen R.G., Smith M., Perrier A., Pereira L.S. (1994). An update for the definition of reference evapotranspiration. *ICID Bulletin* 43: 1–34.

Ali G. A. and A. G. Roy (2010). A case study on the use of appropriate surrogates for antecedent moisture conditions (AMCs) *Hydrol. Earth Syst. Sci. Discuss*., 7, 3329–3363.

Beven, K. J., Rainfall-Runoff Modelling: The Primer, John Wiley, Hoboken, N. J., 2000.

Bishop K., Buffam, I., Erlandsson, M., Fölster, J., Laudon, H., Seibert J. and J. Temnerud.(2008). Aqua Incognita: the unknown headwaters. *Hydrological Processes,* 22: 1239–1242.

Bishop K. (1991). Episodic increases in stream acidity, catchment flow pathways and hydrograph separations. Dissertation, University of Cambridge, Department of Geography, Cambridge, UK

Boggs, J.L., Sun, G., Summer, W., McNulty, S.G., Swartley, W and Treasure, E. (2008). 2008 AWRA Summer Specialty Conference

Brown V., McDonnell J., Burns D. and C. Kendall. (1999). The role of event water, a rapid shallow flow component, and catchment size in summer stormflow. *Journal of Hydrology*, 217(3-4), 171.

Buttle, J.M. (1994). Isotope hydrograph separations and rapid delivery of pre-event water from drainage basins. *Progress in Physical Geography,* 18(1), 16.

Buttle J. (2006). Mapping first-order controls on streamflow from drainage basins: the T3 template. *Hydrological Processes*, 20: 3415–3422.

Buttle, J. M., S. W. Lister, and A. R. Hill, (2001). Controls on runoff components on a forested slope and implications for N transport, *Hydrological Processes*, 15, 1065–1070.

Buttle, J. M. (1998). Fundamentals of small catchment hydrology. In Isotope Tracers in Catchment Hydrology, C. Kendall and J.J. McDonnel, 1–49. Amsterdam: Elsevier

Cleland, D.T.; Freeouf, J.A.; Keys, J.E., Jr.; Nowacki, G.J.; Carpenter, C; McNab, W.H. (2007). Ecological Subregions: Sections and Subsections of the Conterminous United States [1:3,500,000] [CD-ROM]. Sloan, A.M., cartog. Gen. Tech. Report WO-76. Washington, DC: U.S. Department of Agriculture, Forest Service.

Craig H. (1961). Isotopic variations in meteoric waters. *Science* 133:1702–1703.

Detty JM, McGuire KJ. (2010). Threshold changes in storm runoff generation at a till mantled headwater catchment. *Water Resources Research,* 46, W07525.

Dreps C. (2010). Water Storage Dynamics and Water Balances of Two Piedmont North Carolina Headwater Catchments. Master Thesis, North Carolina State University, Department of Forestry and Environmental Resources, Raleigh, NC.

Dunne, T. (1978). Field studies of hillslope flow processes.In Kirkby, M.J., editor, *Hillslope hydrology*. Chichester: Wiley, 227-93.

Freeze, R.A.,(1972). Role of subsurface flow in generating surface runoff;2. Upstream source areas. *Water Resources Research,* 8: 1272–1283.

Genereux, D. 1998. Quantifying uncertainty in tracer-based hydrograph separations. *Water Resources Research,* vol. 34, no. 4, 915–919

Gibson, J., Edwards T, Birks S., St Amour N., Buhay W., McEachern P., Wolfe B. and D. Peters. (2005) Progress in isotope tracer hydrology in Canada. *Hydrological Processes.* 19**,** 303–327.

Gomi T, Asano Y, Uchida T, Onda Y, Miyata S, Sidle RC, Kosugi K, Mizugaki S, Fukuyama T, Fukushima T. (2010). Evaluation of storm runoff pathways in steep nested catchments draining a Japanese Cypress forest in central Japan: a geochemical approaches *Hydrological Processes*, 24: 550–566.

Haga, H., Y. Matsumoto, J. Matsutani, M. Fujita, K. Nishida, and Y. Sakamoto (2005), Flow paths, rainfall properties, and antecedent soil moisture controlling lags to peak discharge in a granitic unchanneled catchment *Water Resources Research.*, *41*, W12410.

Hewlett, J.D., Hibbert, A.R., (1967). Factors affecting the response of small watersheds to precipitation in humid areas, In: Sopper, W.E., Lull, H.W. (Eds.), International Symposium on Forest Hydrology, pp. 275–271.

IAEA. http://www-naweb.iaea.org/napc/ih/IHS_resources_gnip.html (accessed on November, 2009).

James, A. L., and N. T. Roulet (2007), Investigating hydrologic connectivity and its association with threshold change in runoff response in a temperate forested watershed, *Hydrological Processes*, *21*(25), 3391-3408.

James AL, Roulet NT. *(*2009). Antecedent moisture conditions and catchment morphology as controls on spatial patterns of runoff generation in small forest catchments. Journal of Hydrology 377*:* 351–366.

Kendall C, McDonnell JJ (eds). (1998). *Isotope Tracers in Catchment Hydrology*. Elsevier Science Publishers: Amsterdam; 839 pp.

Kendall C. and T. Coplen. (2001). Distribution of oxygen-18 and deuterium in river waters across the United States. *Hydrological Processes.* 15, 1363–1393.

Kendall KA, Shanley JB, McDonnell JJ. *(*1999). A hydrometric and geochemical approach to test the transmissivity feedback hypothesis during snowmelt. *Journal of Hydrology* 219*:* 188–205.

Laudon H, Sjöblom V, Buffam I, Seibert J, Mörth CM. *(*2007). The role of catchment scale and landscape characteristics for runoff generation of boreal streams. *Journal of Hydrology* 344*:* 198–209.

Laudon H, Slaymaker O. (1997). Hydrograph separation using stable isotopes, silica and electrical conductivity: an alpine example. *Journal of Hydrology* 201: 82–101.

Lischeid G. (2008). Combining Hydrometric and Hydrochemical Data Sets for Investigating Runoff Generation Processes: Tautologies, Inconsistencies and Possible Explanations. *Geography Compass*, 2/1: 255–280.

Lee, K. and Y. Kim. (2007). Determining the seasonality of groundwater recharge using water isotopes: A case study from the upper North Han River basin, Korea. *Environmental Geology*, *52*(5), 853.

Lowe W.H. and G.E. Likens. (2005). Moving headwater streams to the head of the class, *Bioscience*, 55: 196–197.

Lyon SW, Desilets SLE, Troch PA. (2009). A tale of two isotopes: differences in hydrograph separation for a runoff event when using delta D versus delta O-18. *Hydrological Processes* 23: 2095–2101.

Mallin M.A., K.E. Williams, E.C. Esham and R.P. Lowe. (2000) Effect of human development on bacteriological water quality in coastal watersheds. Ecological Applications **10**, pp. 1047–1056.

Meyer, J. L. and J. B. Wallace. (2001). Lost Linkages and Lotic Ecology: Rediscovering Small Streams. In *Ecology: Achievement and Challenge*. M.C. Press and N.J. Huntly. Oxford, MA,Blackwell Scientific Publications: 295-317.

McDonnell, J. (1990). A rationale for old water discharge through macropores in a steep, humid catchment. *Water Resources Research, 26*(11), 2821.

Monteith, S.S., Buttle, J.M., Hazlett, P.W., Beall, F.D., Semkin, R.G. and D.S. Jeffries (2006). Paired-basin comparison of hydrologic response in harvested and undisturbed hardwood forests during snowmelt in central Ontario: II. streamflow sources and groundwater residence times. *Hydrological Processes, 20*(5), 1117.

National Cooperative Soil Survey
http://www.soils.usda.gov/partnerships/ncss/ (accessed on 20 August 2010).

Natural Resources Conservation Service
www.nrcs.usda.gov/ (accessed on 4 December 2009).

North Carolina Floodplain Mapping Program
http://www.ncfloodmaps.com/ (accessed on 24 November 2009).

Onda Y, Tsujimura M, Fujihara J, Ito J. 2006. Runoff generation mechanisms in high-relief mountainous watersheds with different underlying geology. *Journal of Hydrology* 331: 659-673.

Pellerin, B. A.; Wollheim, W. M.; Feng, X. H.; Vorosmarty, C. J. (2008) The Application of

Electrical Conductivity as a Tracer for Hydrograph Separation in Urban Catchments. *Hydrological Processes*, 22 (12), 1810–1818.

Pilgrim D.H., D.D. Huff and T.D. Steele, Use of specific conductance and contact time relations for separating flow components. *Water Resources Research.* **15** 2 (1979), pp. 329–339

Rose, S. (1996). Temporal environmental isotopic variation within the Falling Creek (Georgia) watershed: Implications for contributions to streamflow. *Journal of Hydrology*, *174*(3-4), 243.

Sidle, R. C., Y. Tsuboyama, S. Noguchi, I. Hosoda, M. Fujieda, and T. Shimizu (2000). Stormflow generation in steep forested headwaters: A linked hydrogeomorphic paradigm, *Hydrological Processes*, 14: 369– 385.

Sidle, R.C., Tsuboyama, Y., Noguchi, S., Hosoda, I., Fujieda, M. and T. Shimizu. (1995). Seasonal hydrologic response at a various spatial scales in a small forested catchment, Hitachi Ohta, Japan. *Journal of Hydrology*, 168(1-4), 227.

Sklash, M. G., and R. N. Farvolden (1979), The role of groundwater in storm runoff, *Journal of Hydrology*, *43*: 45-65.

Slattery M. Gares P. and J. Phillips.(2006). Multiple modes of storm runoff generation in a North Carolina coastal plain watershed. *Hydrological Processes*, 20: 2953–2969.

State Climate Office of North Carolina. http://www.nc-climate.ncsu.edu/climate/ncclimate.html (accessed on 12 November, 2009

Tromp-van Meerveld, H.J. and J.J. McDonnell. (2006). Threshold relations in subsurface stormflow: 1. A 147-storm analysis of the Panola hillslope. *Water Resources Research*, *42*(2), W02410.

US EPA Landscape Characterization Branch www.epa.gov/esd/land-sci/lcb/default.htm (accessed on 10 December 2009).

Wenner, D.B., Ketcham, P.D. and J.F. Dowd. (1991). Stable isotopic composition of waters in a small Piedmont watershed. In: Taylor Jr., H.P., O'Neil, J.R. and Kaplan, I.R. Editors, 1991. *Stable Isotope Geochemistry: A Tribute to Samuel Epstein* The Geochemical Society, pp. 195–203 Special Publication No. 3